Interreg CENTRAL EUROPE

Co-funded by the European Union

TRANSGEO

Feasibility study for the pilot site Groß Schönebeck (North German Basin)

TRANSGEO Deliverable 2.3.8

Version 1

October 2025

Interreg CENTRAL EUROPE
Co-funded by the European Union
TRANSGEO

D 2.3.8 Feasibility study for the pilot site Groß Schönebeck (North German Basin)

Corresponding author			
Lingkan Finna Christi	GFZ Helmholtz Center for Geosciences	christi@gfz.de	Germany
Contributors			
Hannes Hofmann Günter Zimmermann	GFZ Helmholtz Center for Geosciences	hannes.hofmann@gfz.de guenter.zimmermann@gfz.de	Germany
Katrin Sieron	State Office for Mining, Geology, and Raw Material of Brandenburg (LBGR)	katrin.sieron@lbgr.brandenburg.de	Germany
Tomislav Kurevija Marija Macenić	University of Zagreb – Faculty of Mining, Geology and Petroleum Engineering (UNIZG – RGNF)	tomislav.kurevija@rgn.unizg.hr marija.macenic@rgn.unizg.hr	Croatia

Table of content

0. Executive Summary

Located approximately 40 km north of Berlin within the North German Basin, the Groß Schönebeck site benefits from more than two decades of geothermal research and subsurface data collection. The site's principal deep well, E GrSk 3/90, was originally drilled in 1990 for gas exploration targeting the Rotliegend reservoir. Although insufficient hydrocarbons were found, the well revealed a bottom-hole temperature of 149 °C at 4240 m TVD, positioning Groß Schönebeck as one of the most promising deep geothermal test sites in Northern Germany. Selected from over 50 abandoned wells, E GrSk 3/90 and the later Gt GrSk 4/05 well have since formed the core of an internationally recognized research platform for advancing geothermal energy technologies.

This study evaluates three pathways for continuing the development of geothermal energy at Groß Schönebeck: **Enhanced Geothermal Systems (EGS)**, **Deep Borehole Heat Exchanger (DBHE)** systems, and **medium-depth hydrothermal resources**.

For an **EGS-based approach**, the study proposes converting Gt GrSk 4/05 (A2) into an injection well via a side-track from the 13.375″ casing at approximately 2116–2200 m MD. This is supported by recent accessibility tests and available surface area that minimizes civil works. However, clogging observed in the casing requires mechanical integrity verification and a completion strategy that avoids carbon steel. While EGS remains a high-potential option for accessing the Rotliegend, uncertainty remains regarding fracture sustainability, multi-fracture stimulation efficiency, scaling and clogging risks, and long-term thermal performance. Due to these unresolved technical uncertainties, a reliable economic assessment cannot yet be provided, and further research and demonstration are necessary.

The **DBHE concept** offers a nearer-term deployment pathway with lower geological risk. The exceptional bottom-hole temperatures and existing well depth make the site highly suitable for closed-loop heat extraction. Simulations show that using vacuum-insulated tubing and inlet temperatures between 10–25 °C can produce outlet temperatures of 49–67°C over 30 years, yielding 500–750 kW of thermal power at flow rates up to ~26 m^3h^{-1}. To ensure reliability and cost-effectiveness, further evaluation of insulation performance, thermal conductivity of formation materials, and long-term well integrity are required. This approach is particularly attractive where district heating demand is established or nearby consumers exist, conditions that Groß Schönebeck already meets.

A third pathway focuses on **medium-depth hydrothermal development** in Muschelkalk and Buntsandstein formations situated around the local salt structure. The project proposes reservoir characterization, development of a hydrothermal doublet tailored for salt-dome settings, and optimized material and process designs to withstand hypersaline conditions. Crucially, the **existing deep wells can be repurposed as monitoring infrastructure**, enabling seismic and pressure monitoring, and fiber-optic-based reservoir surveillance, significantly reducing exploration risk and increasing investor confidence. Planned activities include reprocessing of 3D seismic data, VSP surveys, core drilling, fluid testing, and controlled production tests to establish sustainable flow potential.

Strategic outlook: Groß Schönebeck is uniquely positioned to drive the next phase of geothermal innovation in Germany:

- **Deep, high-temperature wells already exist**, reducing capital cost and development time.
- **District heating networks can be built**, enabling rapid market integration.
- **The site provides a controlled research and demonstration environment, facilitating scalable solutions.**
- **Multiple technology pathways allow adaptive investment**, from early DBHE heat supply to future EGS expansion.

With targeted funding, Groß Schönebeck can advance from research to demonstration and ultimately to **regional deployment**, contributing reliable, renewable baseload energy while supporting Germany's heat transition and climate objectives.

The TRANSGEO project (https://www.interreg-central.eu/projects/transgeo/) is co-funded by the European Regional Development Fund through the Interreg Central Europe program. The overall objective of TRANSGEO is to investigate the potential to transform abandoned hydrocarbon wells into new sources of green geothermal energy. To reach this goal, the TRANSGEO team is providing new tools and knowledge to support communities and industries in the energy transition and to break down economic and technical barriers to well reuse. This deliverable report reflects the views of the authors.

1. Introduction

The Groß Schönebeck project was started with an idea of developing geothermal energy extraction technology by converting a former gas exploration well, E GrSk 3/90 into an underground research laboratory. This site in the North German Basin (NGB), a region known for its gas exploration activities in northern Europe, was chosen for the development of EGS technology because of the widespread presence of the low-permeability Rotliegend formation with sufficiently high temperatures for geothermal power generation. Geothermal power generation becomes attractive at temperatures above 100°C and flow rates of 35 L/s to 150 L/s (Agemar et al., 2014). Such temperatures are typically found at depths of 3000-4000 m across the North German Basin, as shown in **Figure 1.1**. However, natural permeability sufficient to support high flow rates is limited at this depth range, unless it is artificially enhanced.

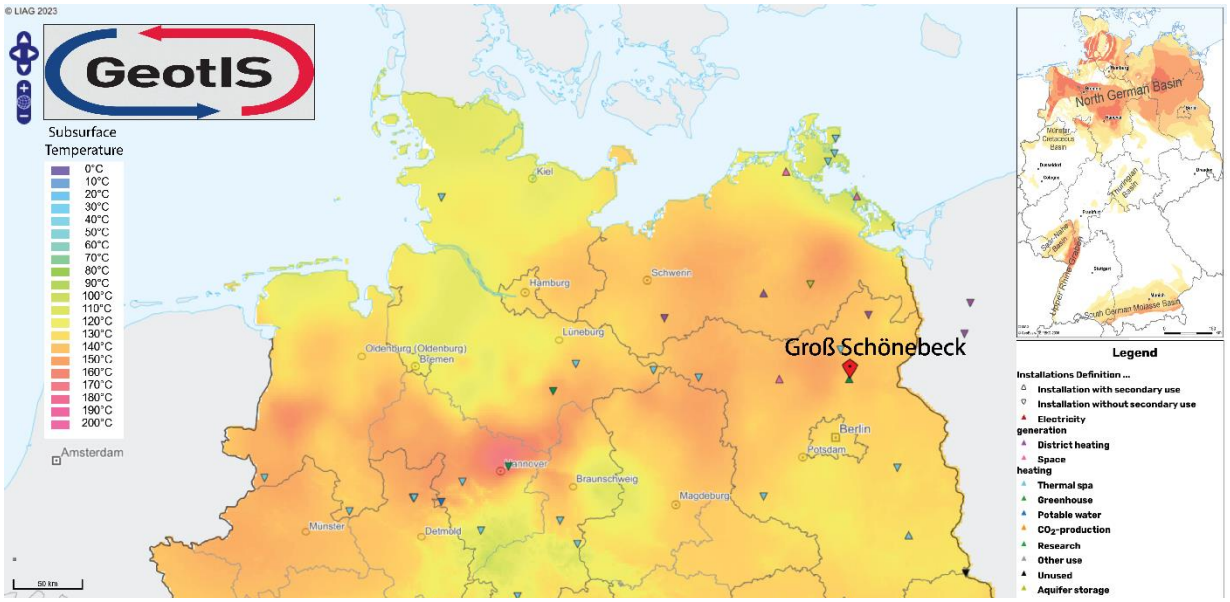

Figure 1.1: Temperature distribution at a depth of 4000 m below the surface in the northern part of Germany within the North German Basin (Agemar et al., 2014).

The selection of the E GrSk 3/90 well marked the development of the Groß Schönebeck geothermal research platform. The well was originally drilled in 1990 to target a Rotliegend gas reservoir at a depth of more than 4 km. It was drilled almost vertically and cored in the 4040 - 4270 m measured depth (MD) interval. The well was abandoned immediately after drilling due to insufficient gas shows (Legarth et al., 2003). Later in 2000, the well was selected from 50 plugged and abandoned deep former oil and gas exploration wells in north-eastern Germany as a candidate for reuse as a geothermal research well. This was based on the observed bottom-hole temperature of 149°C at 4240 m true vertical depth (TVD) and the large regional extent of the Rotliegend formation as a potential geothermal reservoir (Huenges et al., 2002) as shown in **Figure 1.2**. Since then, the well site has been developed as an *in-situ* subsurface laboratory owned and operated by the GFZ. Following the reopening and deepening of the borehole in 2001, extensive multidisciplinary research into geothermal development has been carried out in this field.

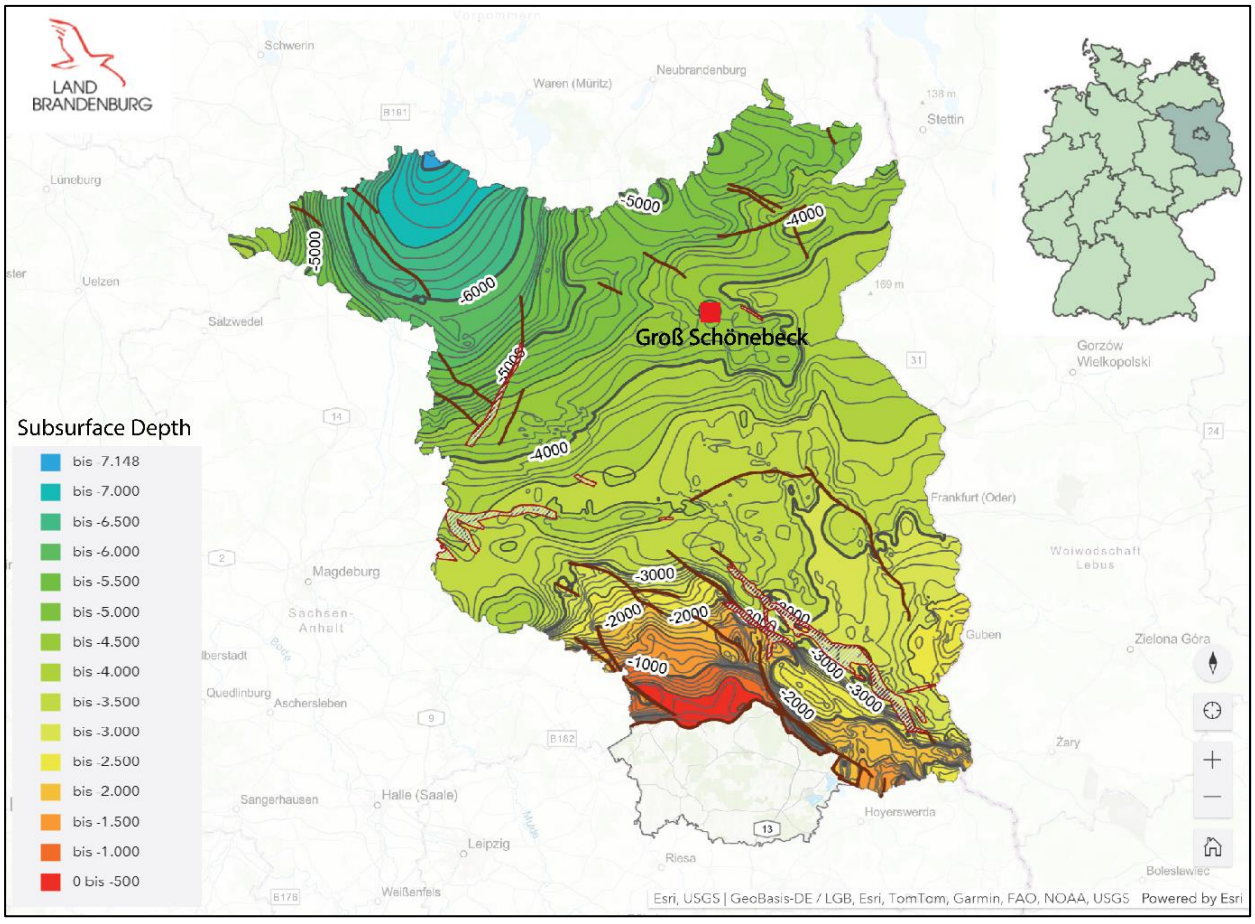

Figure 1.2: Top of Rotliegend depth based on seismic interpretation in Berlin-Brandenburg area (*LGBR*, 2024). Source: https://gst.brandenburg.de. (Accessed November, 2024).

2. Geographic location and analysis of spatial planning documentation

2.1 Location

The location of the Groß Schönebeck is shown in **Figure 2.1**. Coordinates, well site area, and address are provided in **Table 2.1**.

Figure 2.1: Geographical location of the Groß Schönebeck EGS site. Source:https://www.google.com/maps/place/16244+SchorfheideGro%C3%9F+Sch%C3%B6nebeck/@52.9326553,13.4190752,25634m/. (Accessed August 29, 2025).

Coordinates of wells	E GrSk 3/90 (Northing: 5862487.86; Easting: 405948.4) Gt GrSk 4/05 (A2) (Northing; 5862461.17; Easting: 405944.6) Reference coordinate: UTM-WGS84, Zone 33
Address	Eichhorster Chaussee 99 16244 Schorfheide / Ortsteil Groß Schönebeck
State	Brandenburg
Country	Germany

Table 2.1: Coordinates of the Groß Schönebeck location (Reinsch et al., 2015) and address.

2.2 Transport connectivity

Groß Schönebeck is located approximately 45 km from Berlin, as shown in **Figure 2.2**. The site is easily accessible via Eichhorster Straße, which is accessible by car from the main railway stations, the airport and the regional highway. The site is also accessible from two main railway stations: Groß Schönebeck station and Eberswalde station. The site itself can only be reached by private car or by public bus, with the nearest bus stop 1 km away.

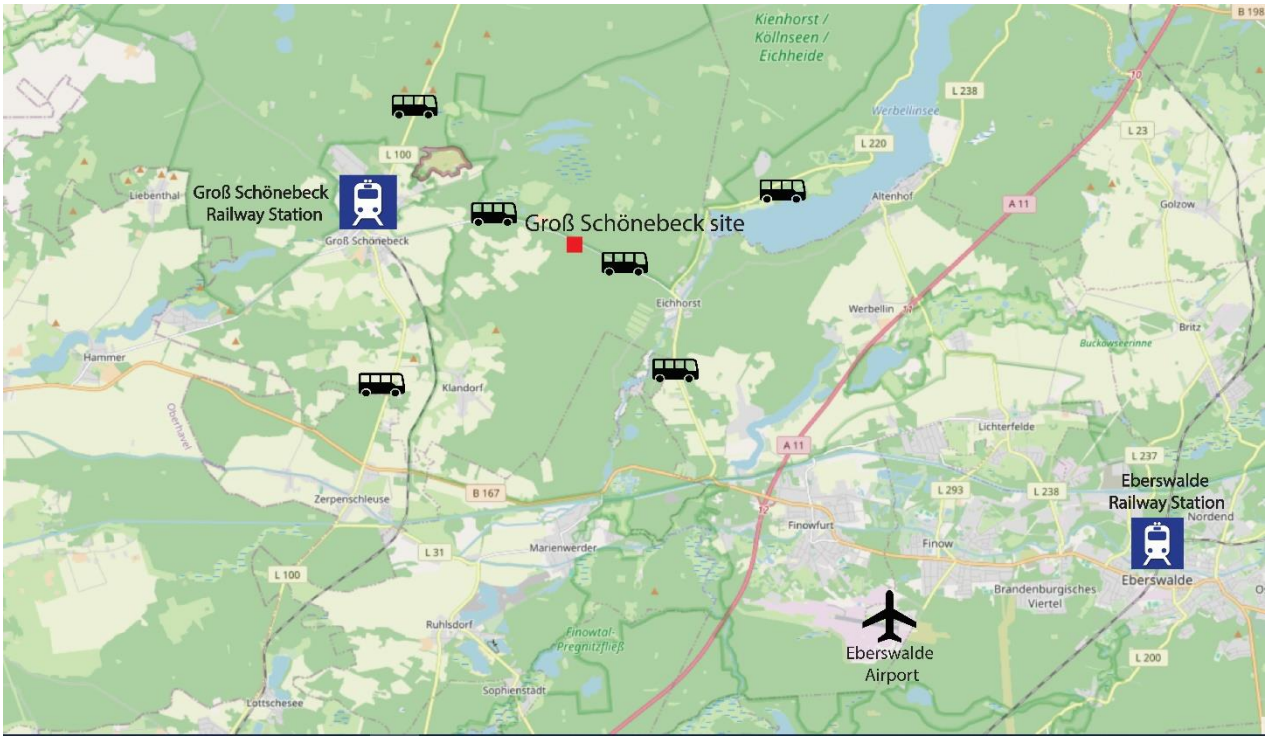

Figure 2.2: Figure of transport connectivity of the site relatively to the main roads, main railway stations and closest airport. Source: https://www.openstreetmap.de/karte/#. (Accessed August 29, 2025).

2.3 Demographic aspects

Groß Schönebeck is one of the villages that meets the requirement of a pluralistic society based on evaluation of Rural Roadmap in 2018 (Europäische ARGE Landentwicklung und Dorferneuerung, 2018). Together with four smaller settlements, Groß Schönebeck forms part of the larger municipality of Schorfheide, which was created in 2003. Groß Schönebeck itself has only 1,740 inhabitants out of a total population of 10,000 inhabitants in Schorfheide municipality as shown in **Figure 2.3.** Over the last two centuries, Groß Schönebeck has become a hunting ground, used more and more intensively by the various state authorities - the Prussian emperors, the Nazi rulers and finally the leaders of the GDR - to the point of hunting.

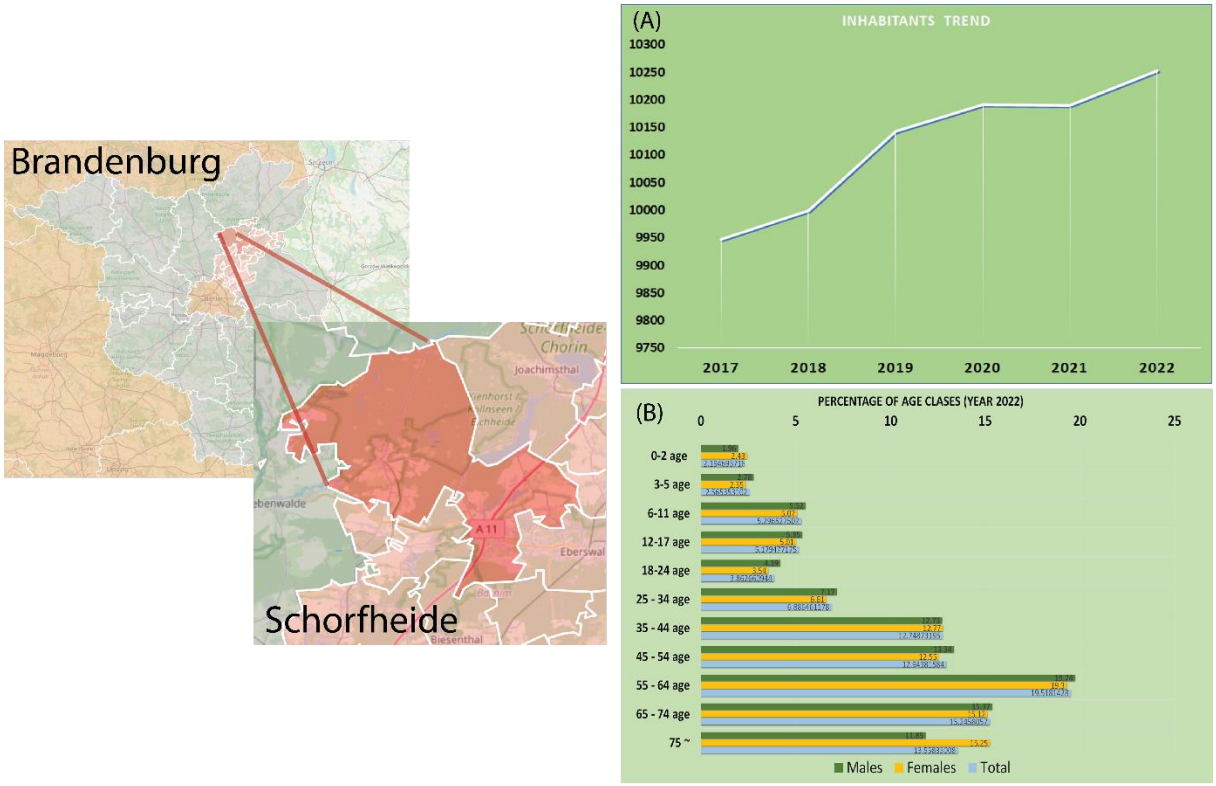

Figure 2.3: Demographic aspects of Schorfheide: (A) Total inhabitants over the years (2017 – 2022); (B) Percentage of age classes of the inhabitants. Source: https://ugeo.urbistat.com. (Accessed August 29, 2025).

2.4 Power grid

The power lines around the Groß Schönebeck site are shown in **Figure 2.4** which was taken from Open Infrastructure Map (2024). The site lies between two power lines. One, less than 10 kV power line, is connecting the centre of Groß Schönebeck to the power source. This network is located 4.5 km away from the site. The other, a 100 kV power line, is located to the east, towards the Eichhorst area, about 13 km from the site. The site is located within a radius of 13 - 15 km of several power generation plants, such as Klosterfelde Wind Farm (20.85 MW), Finowtower 1 (24.24) & 2 (60.39 MW) Solar Park, Eberswalde Hokawe Biomass Power Plant (21 MW), Deponie Ostend Eberswalde Solar Park, Templin - Groß Dölln Solar Park (128.42 MW).

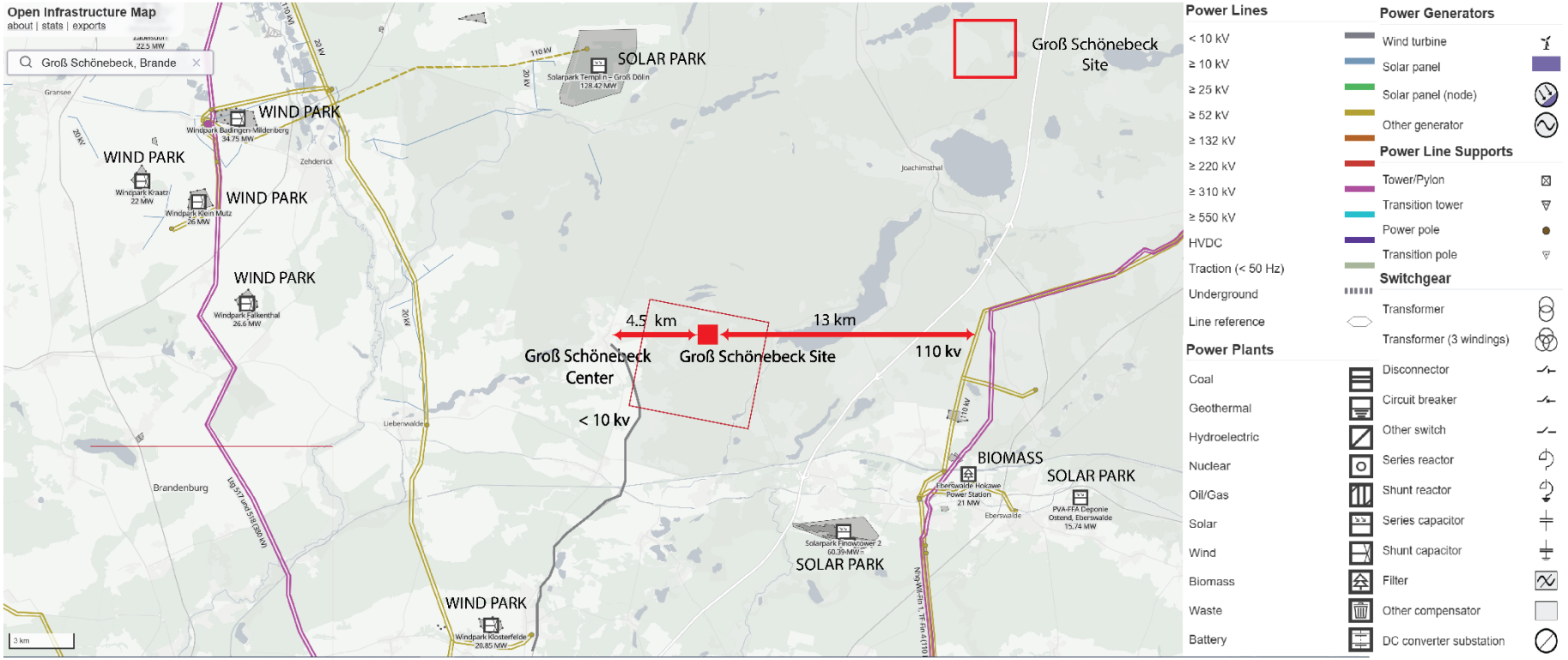

Figure 2.4: Nearby power grids, power plants and the research area of the Groß Schönebeck. Source: https://openinfrastructuremap.org/. (Accessed November 2024).

2.5 Compliance of interventions with current spatial planning documentation

The research platform of the Groß Schönebeck site is registered under the mining license of Groß Schönebeck/Eichhorst with the details listed in **Table 2.2**.

Type of mining authorization	Permit for exploration for commercial purposes
Authorization area	Groß Schönebeck/Eichhorst
Field number	1498
Mineral Resource	Brine and geothermal heat
Permit holder	Helmholtz-Zentrum Potsdam Deutsches Geoforschungs-Zentrum - GFZ
Application date	03.07.2000
Origin date	26.10.2000
Expiry date	26.10.2027

Table 2.2: Detail of mining license of Groß Schönebeck/Eichhorst.

2.5.1 Land use

The study area, depicted in **Figure 2.5**, covers an area of approximately 238.223 square kilometres. According to the CORINE Land Cover (CLC) classification in **Table 2.3** (CORINE, 2018), the main land uses are nature park conservation areas (class 3), accounting for 68.3%, followed by agricultural areas (class 2) with 22.5%, industrial areas (class 1) at 6.8%, and water bodies and wetlands (classes 4 and 5) with around 2%.

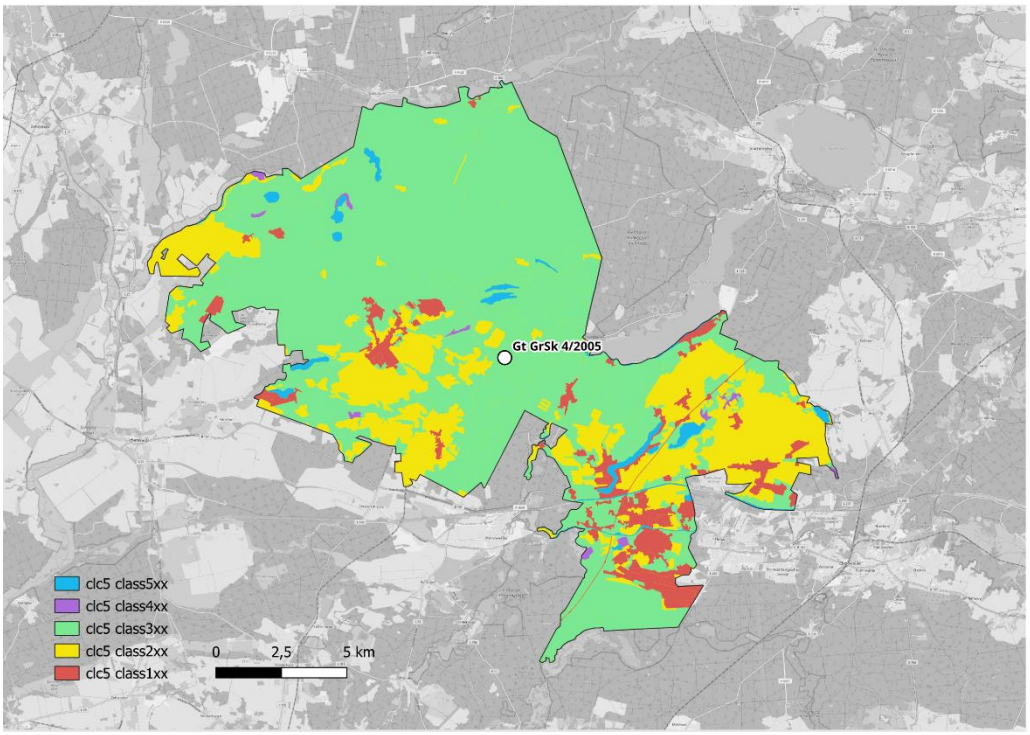

Figure 2.5: Overview of land use in Schorheide - Chorin (CORINE, 2018).

Class	Description of the class category
1	Continuous/discontinuous urban fabric, industrial or commercial units and public facilities, road and rail networks and associated land, port areas, airports, mineral extraction sites, dump sites, construction sites, green urban areas, sport and leisure facilities.
2	Non-irrigated arable land, vineyards, pastures/meadows/ permanent grasslands under agricultural use, complex cultivation patterns, land principally occupied by agriculture with significant areas of natural vegetation.
3	Broad-leaved forest, coniferous forest, mixed forest, natural grassland, moors and heathland, transitional woodland/shrub, beaches, dunes and sand plains, bare rock, sparsely vegetated areas, burnt areas, glaciers and perpetual snow.
4	Inland marshes, peatbogs, coastal salts marshes, intertidal flats.
5	Water courses, water bodies, coastal lagoons, estuaries, sea and ocean.

Table 2.3: Description of class category (CORINE, 2018).

2.5.2 Spatial development plan of the municipality of the pilot site

The municipality of Schorfheide is characterised by its inclusion within the Schorfheide-Chorin Biosphere Reserve, which was established in 1991 and recognised by UNESCO. Around 75% of the municipality's territory is within the reserve's boundaries, making a significant contribution to regional and national biodiversity conservation efforts. The landscape is defined by a unique interplay of glacial features, including morainic hills, numerous lakes such as Großsee, Werbllinsee, Üdersee, Großer Bukowsee, Schleusenteich, Grimnitysee and expansive forested areas such as the Schorfheide Forest. The reserve's diverse habitats support rich flora and fauna, including protected species such as the white-tailed eagle and the European bison, which has been successfully reintroduced, as well as various rare plant communities. Tourism plays a significant economic role in the municipality, largely driven by the unique natural and cultural assets of the Schorfheide-Chorin Biosphere Reserve. The plan recognizes the potential for sustainable tourism development, emphasizing ecotourism and nature-based experiences. Key tourism attractions include the extensive network of hiking and cycling trails, opportunities for water sports on the lakes, and the historic Chorin Monastery. The plan promotes the development of high-quality, environmentally friendly accommodation and visitor facilities within the transition zones, while safeguarding the integrity of the core and buffer zones. The Schorfheide-Chorin Biosphere Reserve represents a fundamental cornerstone of the municipality’s environmental policy. The spatial development plan is committed to the long-term conservation of biodiversity, the preservation of natural resources, and the promotion of sustainable development.

3. Research area

3.1 Description of research area

As described by Norden (2023), located within the North German Basin (NGB), a component of the Central European Basin System extending from Middle England to North Germany, Poland, and the Baltic States (**Figure 3.1**), the Groß Schönebeck deep geothermal research platform resides in a low-enthalpy geothermal setting. The NGB's development occurred during the late Carboniferous and early Permian periods, driven by thermal relaxation, crustal extension, and tectonic subsidence (van Wees et al., 2000). This resulted in the deposition of sedimentary rocks, reaching up to 6,500 m in thickness in the eastern NGB (Hoth et al., 1993; DEKORP-BASIN Research Group, 1999). Similar to other sub-basins within the Permian Basin System, the NGB was historically targeted by the hydrocarbon industry, with significant seismic campaigns and deep drillings, including investigations of Permian Rotliegend sediments in northeast Brandenburg (**Figure 3.1**).

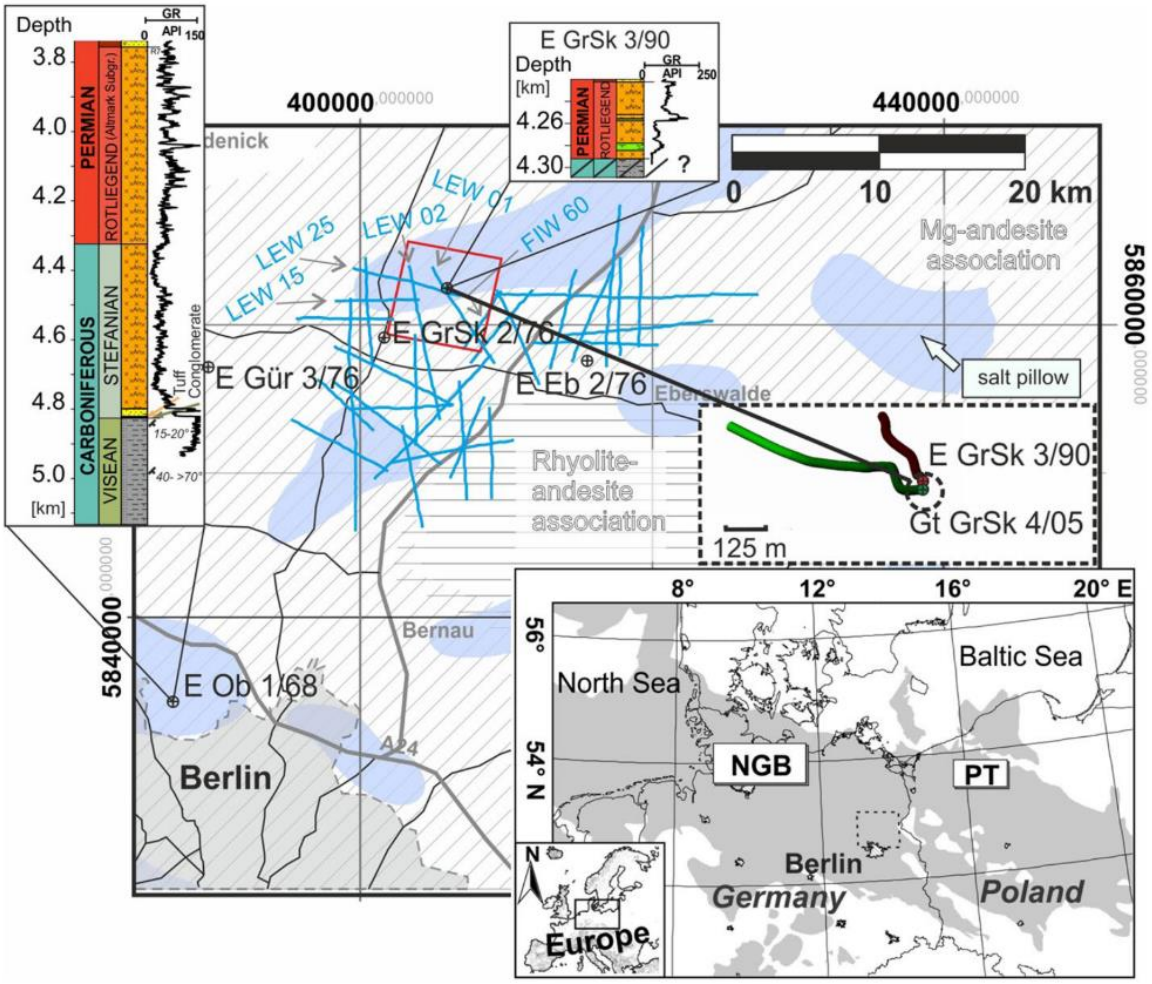

Figure 3.1: Site map of Northeast Brandenburg showing the Groß Schönebeck research area (Norden et al., 2023).

3.2 Available infrastructure at the pilot site

The Groß Schönebeck research site, depicted in **Figure 3.2**, features a former gas exploration well (E-GrSk 3/90) and a geothermal well (GtGrSk 4/05 (A2)), with coordinates listed in Table 2.1. The facility, located at Eichosterch Chaussee 99, includes a fenced drill site, office space, an ORC power plant with cooling systems, water supply wells, electrical grid access, and emergency power.

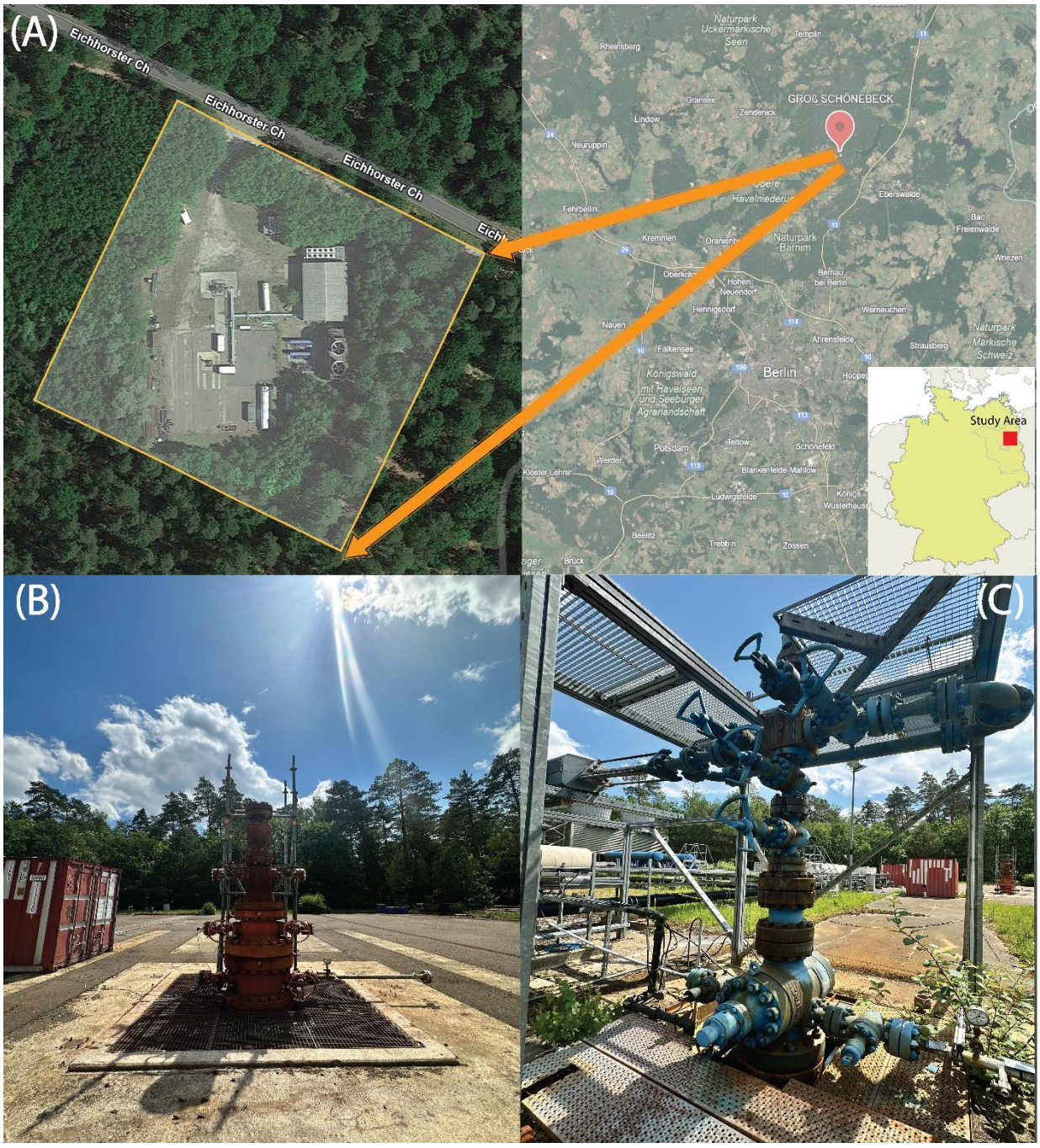

Figure 3.2: The Groß Schönebeck research site. (A) Location of the well site; (B) well Gt GrSk 4/05 (A2); (C) well E GrSk 3/09 (Christi et al., 2025). Source: https://www.google.com/maps/place/16244+SchorfheideGro%C3%9F+Sch%C3%B6nebeck/@52.9326553,13.4190752,25634m/. (Accessed August 29, 2025).

3.2.1 Geothermal research at Groß Schönebeck

As reported by Huenges et al. (2007), the first well (E GrSk 3/90), which was originally completed in 1990 as a gas exploration well but abandoned due to non-productivity, was reopened in 2000 and hydraulically stimulated on several occasions between 2002 and 2005. In 2006, the second well (Gt GrSk 4/05) was drilled for the extraction of thermal waters, forming a doublet system of hydraulically connected boreholes. In this second well, the Lower Permian sandstones and the underlying volcanic rock are the target formations for stimulation by hydrofracturing. The resulting reservoir should demonstrate increased productivity, with a minimal requirement for auxiliary energy to drive the thermal water loop (reservoir-surface-reservoir), and with minimal risk of a temperature short circuit of the system during the planned 30-year utilization period. Thermo-hydraulic modelling based on data from the first well, along with regional structural analyses, identified the optimum well path geometry for the second well (Zimmermann et al., 2007). The borehole was designed with a parallel orientation to the minimum horizontal stress direction and perpendicular to the hydraulic fractures. The new well (Gt GrSk 4/05) was located at the same drill site as E GrSk 3/90 (27 m distance), but with a bottom hole some 472 m apart as shown in **Figure 3.3**.

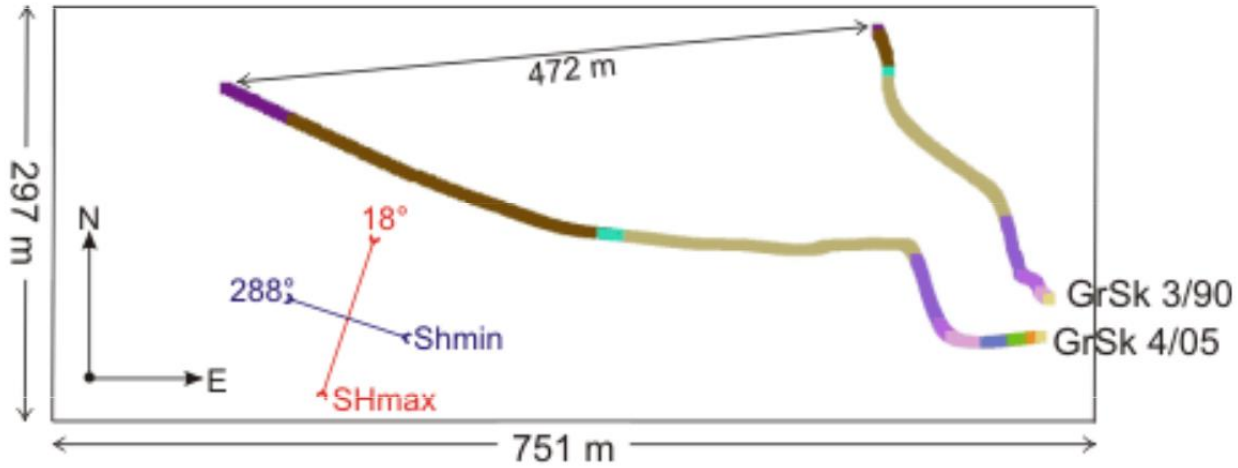

Figure 3.3: Top view projection of the doublet wells at Groß Schönebeck. The deviation of GrSk 4/05 is parallel to the minimum horizontal stress direction to facilitate a set of parallel hydraulic fractures (Huenges et al., 2007).

The geothermal exploitation concept has thus far relied on a matrix-dominated approach, with sparsely distributed 2D seismic profiles acquired in 1987being used to establish a preliminary 3D geological model of the Groß Schönebeck area. This model forms the foundation for the initial exploitation concept and the well design of the Gt GrSk 4/05 borehole (Moeck et al. 2009). In conclusion, the experiences made with this concept did not prove successful. Following the productivity decline observed during the 2012 tests, further investigation by Blöcher et al. (2016) revealed that early EGS development at this site had stalled. The analysis identified five potential causes for this decline: 1) electro-chemical reactions between reservoir fluid and casing, 2) scale accumulation in the well, 3) unsustainable hydraulically induced fractures, 4) reduced reservoir permeability due to scaling or two-phase flow with free gas, and 5) reservoir compartmentalization. In relation to the productivity of the well, from 2011 to 2013, hydraulic tests on the E GrSk 3/90 and Gt GrSk 4/05 (A2) were carried out. It was found that the productivity was lower during this time. The reasons for the drop in productivity during these tests have been explained by Blöcher et al. (2016) and looked into by Regenspurg et al. (2015, 2016). These studies looked closely at problems like clogging and corrosion in the production liner of Gt GrSk 4/05 (A2). This issue is making it hard to move forward with the EGS development concept at Groß Schönebeck, which is mostly focused on the matrix. A test in 2021 (Regenspurg et al., 2024) showed that the productivity index (PI) of 0.6 $m^3h^{-1}MPa^{-1}$ has not

changed in the last ten years. It should be noted that during this period, the well has not been pumped, except for small amounts used for testing and sampling.

Consequently, an engineered fracture-dominated exploitation approach – designed to establish a continuous and sustainable geothermal loop – was considered, and is presented in this study. To assess potential structural obstacles, a 3D seismic exploration campaign was conducted. Preliminary processing and interpretation of these data are detailed in Krawczyk et al. (2019), while the complete geological interpretation forms the basis of the recently updated 3D model presented by Norden et al. (2023).

The latest 3D model did not confirm indications of crustal-scale faults, free gas, seismic compartmentalization in the sub-salinar, or a fracture-dominated Rotliegend reservoir (Krawczyk et al., 2019). Instead, a seismic attribute study (Bauer et al., 2020) revealed a diversity of seismic facies in the reservoir target units, suggesting a system of thicker paleo-channels deposited within a subsided landscape and accounting for large-scale thickness variations. These findings led to a revised 3D model that excludes the previously hypothesized compartmentalization and support an advanced geothermal exploitation concept, as outlined in Christi et al. (2025).

3.2.2 Geological-geophysical works and special operations at Groß Schönebeck

The lithology of the Groß Schönebeck site is derived from seismic-well ties with the available logging data and horizon interpretations as shown in **Figure 3.4**. Cores were available for the E GrSk 3/90 borehole only. Most of the data is referring to the borehole that was drilled more or less vertically. The lithological description and the depth correlation of the boreholes were reinterpreted in Norden et al. (2023). The main stratigraphy, lithology, and the master gamma ray logging data for each well is provided in Norden et al. (2022). Details on the seismic data can be found in Krawczyk et al. (2019) and for the picking and geological modeling in Norden et al. (2023).

The well-logging data comprises data covering the total length of the boreholes and data covering only the geothermal reservoir targets of the Permo-Carboniferous. Legacy data (obtained in 1990/1991) was scanned and digitized. From logging campaigns after 2000/2001, logging data is available in digital form. A list of early logging operations performed in Groß Schönebeck can be found in Huenges & Winter (2004). The petrophysical interpretation of the reservoir zone provides measured bulk density, sonic travel time, neutron porosity, pulsed neutron log permeability, and derived properties like total and effective porosity, fractional volume of clay, permeability based on the Coates equation (Coates et al., 1991), thermal conductivity, thermal diffusivity, and specific heat capacity.

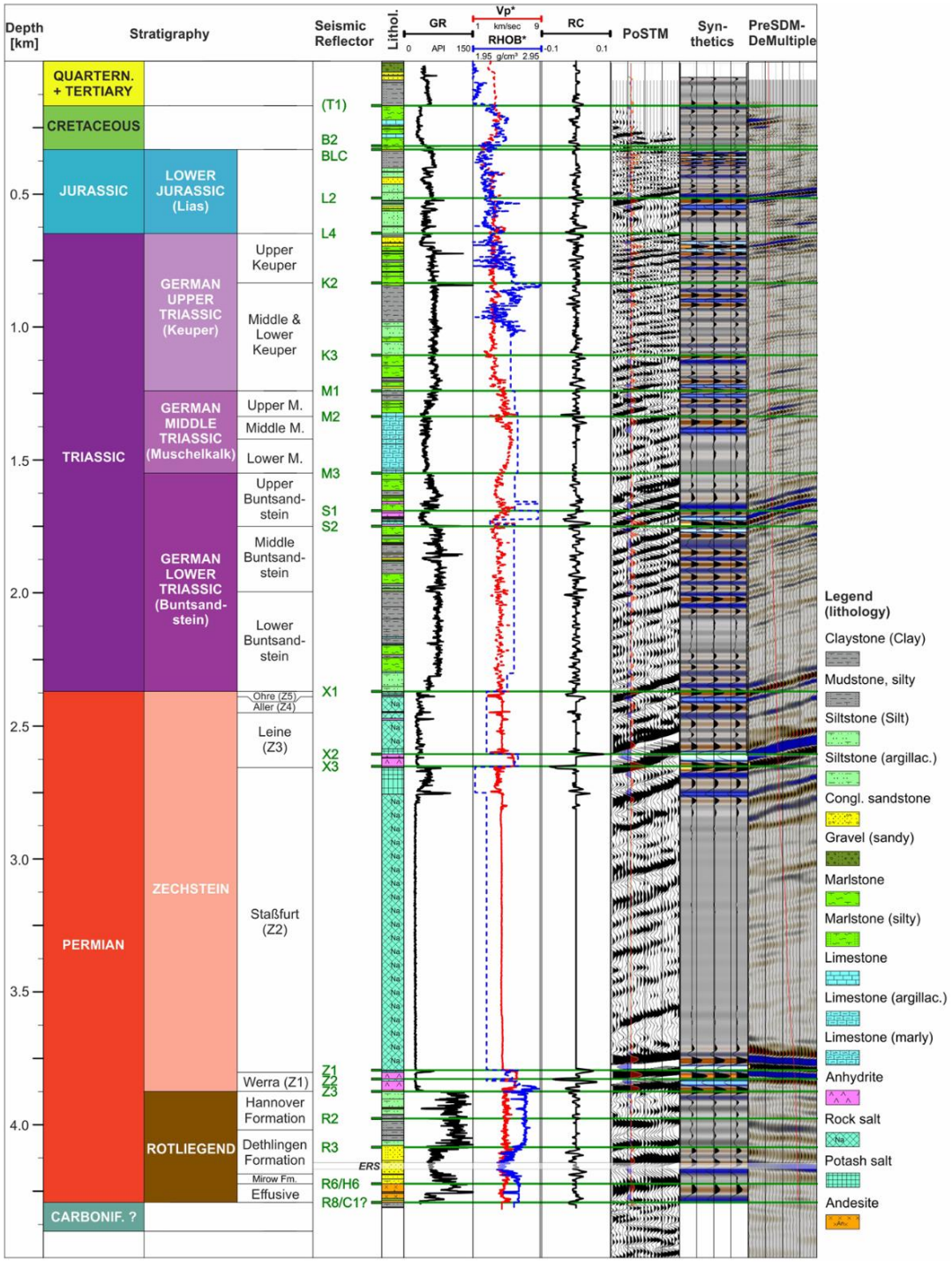

Figure 3.4: Seismic-well tie of borehole data (E GrSk 3/90 borehole) and seismic volumes (Norden et al., 2023). Vp* refers to p-wave velocity (in km/s), RHOB to bulk density logging (in 10^3kg/m or gcm^{-3}), and RC represents the reflector coefficient, ERS: Elbe reservoir sandstone. The synthetic seismic response based on the applied wavelet is shown together with two processed seismic volumes: PoSTM (post-stack time migration) and PreSDM (pre-stack depth migration with suppression of seismic multiples). Stippled lines of the sonic-density composite plot (Vp*, RHOB*) indicate interpolated log responses.

3.2.3 Well configuration at Groß Schönebeck site

The well configuration at the Groß Schönebeck site is described in **Table 3.1**.

Casing Type	Size - Outer Diameter (inch)		Depth/Top (m. MD)		Depth /Bottom (m. MD)		Grade	
Well	P	I	P	I	P	I	P	I
Conductor casing	25 63/64	13 3/8	0	0	41.6	18		
Surface casing	18 5/8	13 3/8	0	0	741.2	205	L80/X56	J55
Production casing	16	9 5/8	0	0	723	2375	N80/HCN 80	P110/DE/E
	13 3/8		723		1680		P110	
	13 5/8		1680		1803		Q125	
	13 3/8		1803		2381.5		P110	
Liner	7	7	2333	2309	3878	3874	L80	N80
Open hole section		5 7/8		3820		4305	L80	
Liner	5		3761		4355		HCl 10	L80
Perforated liner	5	5	4355	3820	4389		C95	
Production tubing with ESP pump installation	4 1/2		0		1163.3		13Cr/J55 (Isol. Joint)	
Injection tubing		4 1/2		0		305		J55

Table 3.1: (P) Well Gt GrSk 4/05 (A2) and (I) Well E GrSk 3/90 configurations.

3.2.3.1 Well E GrSk 3/90

The most recent evaluation of E GrSk 3/90 was conducted between 2000 and 2002. As summarized by Legarth et al. (2002) and Christi et al. (2025), casing inspection caliper (CIC) for casing inspection and a sonic log to assess cement bond condition were carried out after the reopening of the well. However, the majority of these tests were focused on depths between 3853–4294 m MD or below the casing shoe of the 7" liner. As reported by Huenges et al. (2002), a 40% reduction in wall thickness was observed at several points in the 7" liner section below the 9.625" casing. While this reduction does not compromise the overall integrity of the casing configuration and no leaks were found, it is strongly recommended to perform new CIC and integrity tests.

3.2.3.2 Well Gt GrSk 4/05 (A2)

The most recent well assessment was conducted in 2018. The series of logging activities conducted by Schlumberger is shown in **Table 3.2**. The evaluation of casing integrity from PMIT runs revealed that the 7" x 7.625 " casings were in satisfactory condition. An anomaly was encountered at depths ranging from 3360.7 to 3361.5 m MD. Consequently, it was recommended to verify the completion component at that depth. For the 13.375" and 13.625" casing configurations, the PowerFlex results were evaluated. The overall casing for this section was found to be in good condition, except several points showed varying degrees of ovalization (at 1710 m, 1725 m, 1745 m, and at the interval depth of 2170-2200 m MD) and high variance in the thickness at the levels of 777.5 m to 789 m MD. The evaluation of cement bond quality was carried out for the completion section of 7", 7.625", 13.375", and 13.625". The intervals exhibiting low cement bond quality were identified below the 18.625" casing shoe, between 925 m and 1310 m MD, 1668 m and 1820 m MD, 2505 m and 2705 m MD. These intervals primarily consist of liquid, suggesting that they are unlikely to provide annular isolation. In the case of the 16" casing, it was found that PowerFlex and ASLT tools

underwent swelling after being retrieved back from the borehole. This led to a deterioration in signal quality within the 16" section. It was attributed to the presence of water and gas in the well up to 200 meters below the wellhead. To address this issue, it was recommended to fill the well with water and to conduct measurements using a tool string with PowerFlex and PMIT with 120 fingers for this casing size.

Run No	Casing/Liner	Tool
1	Full wellbore/drift	Casing collar locator (CCL), Slickline Jar, Slickline Gauge cutter 76 mm. This run was successfully tagged the final depth of 4235.2 m MD
2	5” liner	Platform Multifinger Imaging Tool (PMIT), 40 finger caliper tool.
3	5” liner	Slim cement mapping tool (SCMT)
4	5” liner	Ultrasonic cement and casing imager (USIT)
5	7”, 7.625”, 5” liner	Platform Multifinger Imaging Tool (PMIT), 40 finger caliper tool.
6	16”, 13.375’, 13.625” casing	Casing& PowerFlex ultrasonic for cement and casing imager; Array sonic logging tol (ASLT) for Cement bond log (CBL) and Variable density log (VDL)
7	7”, 7.625” liner	Array sonic logging tol (ASLT) for Cement bond log (CBL) and Variable density log (VDL)

Table 3.2: Series of logging runs for integrity test conducted in GrSk 4/05 (A2).

3.3 Planning of new wells in Groß Schönebeck site

A research proposal was prepared to drill two new wells at the Groß Schönebeck site. The first well would be drilled as an exploration well to investigate the suitability for hydrothermal heat production from the target horizons Muschelkalk and Buntsandstein. If funded, both target horizons would be fully cored and an extensive logging program would be carried out to develop a reference data set of these horizons for further geothermal development opportunities in nearby districts of the municipality of Schorfheide.

Option A - Drilling up to the red sandstone (1250 m core from the top of the Muschelkalk to the base of the red sandstone), positive production test in the red sandstone.

At the start of drilling, the drilling site would need to be expanded to include a new drill pad and a new standpipe. A 26-inch section would then be drilled, an 18 5/8-inch casing installed and cemented to a depth of approx. 200 m. This would be followed by the $17^1/_2$-inch section with a $13^3/_8$-inch casing to a depth of 1,150 m. The third section will be drilled with $12^1/_4$ inches and completed with a $9^5/_8$-inch liner to a depth of approx. 2,300 m. The final depth is planned at 2,375 m and should be at the top of the Zechstein. The completion is accompanied by a fiber optic cable that would be installed to the final depth of the well to monitor operational parameters in real time. The lower section will be used as an open borehole with a diameter of $8^1/_2$ inches for a hydraulic production test. If this test is deemed successful in terms of productivity and hydrochemical properties, the Buntsandstein horizon would be developed using well construction techniques, including filters and, if possible, gravel packing or, alternatively, a pre-packed liner of a suitable diameter and material.

Option B - Drilling including 1,250 m core to the Buntsandstein, production test Buntsandstein negative, re-cementation to the 13-3/8” casing, side-track to the Muschelkalk, production test Muschelkalk.

Option B would be used if Option A is not successful, specifically, if the Buntsandstein horizon does not have sufficient productivity or the hydrochemical conditions are uncontrollable. In this case, recementation would be carried out to approx. 1,000 m and a side-track would be drilled into the Muschelkalk horizon. This is cased with a 9-5/8-inch liner and cemented to the top of the Muschelkalk. The lower section, down

to the final depth, is drilled with 8-½ inches and is to be used as an open borehole for a hydraulic production test. The well is then developed using the same methods as in Option A.

3.4 Fracture-dominated multi-stage stimulation of horizontal wells as an alternative EGS development concept for Groß Schönebeck

An alternative or additional development approach implements the latest concept of multi-stage fracturing on parallel horizontal doublet wells as described by Christi et al. (2025). This concept followed the blueprint of the state-of-the-art commercial EGS successfully demonstrated in the Blue Mountain project (Dadi et al., 2023 and Norbeck et al., 2023). In the design of the well configuration, the reuse of the existing wells with the possibility of well modification was considered to avoid the potential causes of productivity decline that was observed in the past. A new fracture-dominated EGS concept with a parallel horizontal well doublet with a side-track from a pre-existing well was proposed for Groß Schönebeck. This concept will optimize the existing infrastructure by repurposing Gt GrSk 4/05 (A2) as an injection well, drilling a new production well, and repurposing E GrSk 3/90 as a monitoring well. The possibility of well layout configuration, simplified side-track well projection, and design are shown in **Figure 3.5** and **Figure 3.6.**

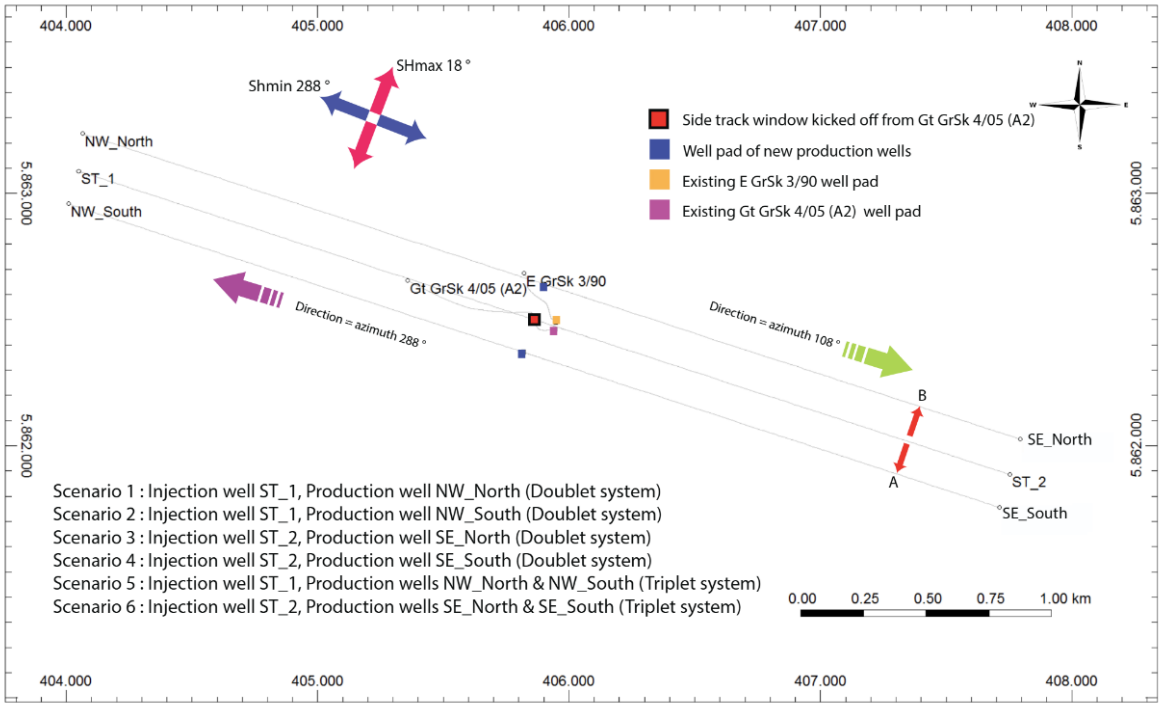

Figure 3.5: Multiple potential well layouts for fracture-dominated EGS concept (Christi et al., 2025).

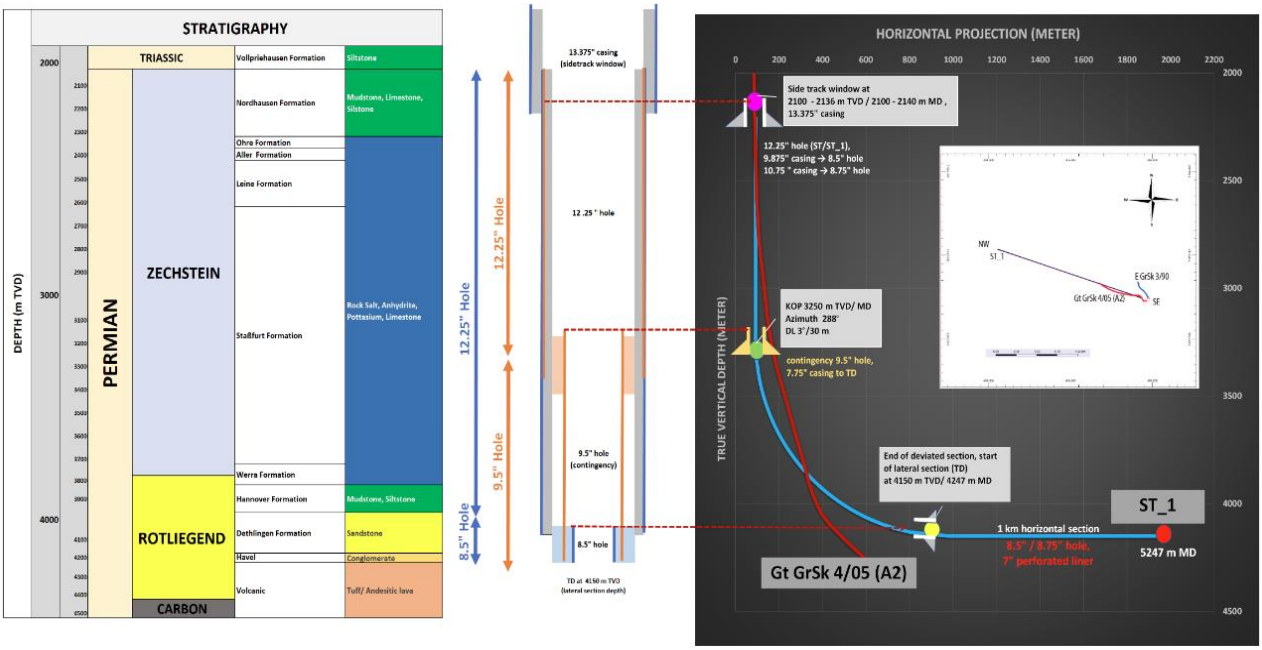

Figure 3.6: Expected casing design (left) and planar view of side-track trajectory of new injection for new fracture-dominated EGS concept (right) (Christi et al., 2025).

3.5 Reuse of a single well as Deep Borehole Heat Exchanger (DBHE)

Groß Schönebeck's geothermal energy can be harnessed cost-effectively and with a low risk by repurposing the existing wells as Deep Borehole Heat Exchangers (DBHE). The proposed system involves installing vacuum-insulated tubing to a measured depth of 3,800 metres, targeting the highly conductive salt layer within the 1.5-kilometre-thick Zechstein Formation. The DBHE can access temperatures of up to 138 °C within the Straßfurt Formation of the Permian Zechstein, utilising existing wells with a maximum casing diameter of 7 inches. This approach is considered both technically feasible and economically viable for well reuse, offering a sustainable energy solution for the region.

4. Geology structure of the geothermal reservoir at the potential location and available data for broader locations

The geology of Groß Schönebeck comprises Cenozoic, Upper Cretaceous, Cretaceous – Jurassic (Lias), Upper Triassic (Keuper), Middle Triassic (Muschelkalk), Lower Triassic (Buntsandstein), Upper Permian (Ohne, Ahler, Leine), Lower Permian (Zechstein), Upper Rotliegend (Hannover Formation and Dethlingen), Lower Rotliegend (Havel group, and effusive volcanic) and Carboniferous. Recent interpretation of the 3D seismic data by Norden et al. (2023) shows that large offset faults in the Rotliegend sediments do not appear to be present in the study area. The putative faults interpreted on reprocessed 2D seismic lines using attribute analysis (Moeck et al., 2009) were not confirmed by the 3D seismic.

4.1 Lithology description for each well at Groß Schönebeck

A full description of the lithology is given in Norden et al. (2023) and provided generally in **Figure 3.4**. The interpretation of the geological structure in the Groß Schönebeck area is mainly based on the drilling reports of Gt GrSk 3/90, geophysical logging data, interpretation of seismic and DAS-VSP data and regional correlation based on the Brandenburg Geological Atlas. For Gt GrSk 4/05, the interpretation is based on the correlation and interpretation of seismic data associated with well E GrSk 3/90. A recent interpretation by Norden et al. (2023) incorporated 3D geological data (**Figure 4.1**) and used data from the nearby boreholes E-Gür-3/76, E-GrSk-2/76 and E-Gwd-1/75, as shown in **Figure 3.1**.

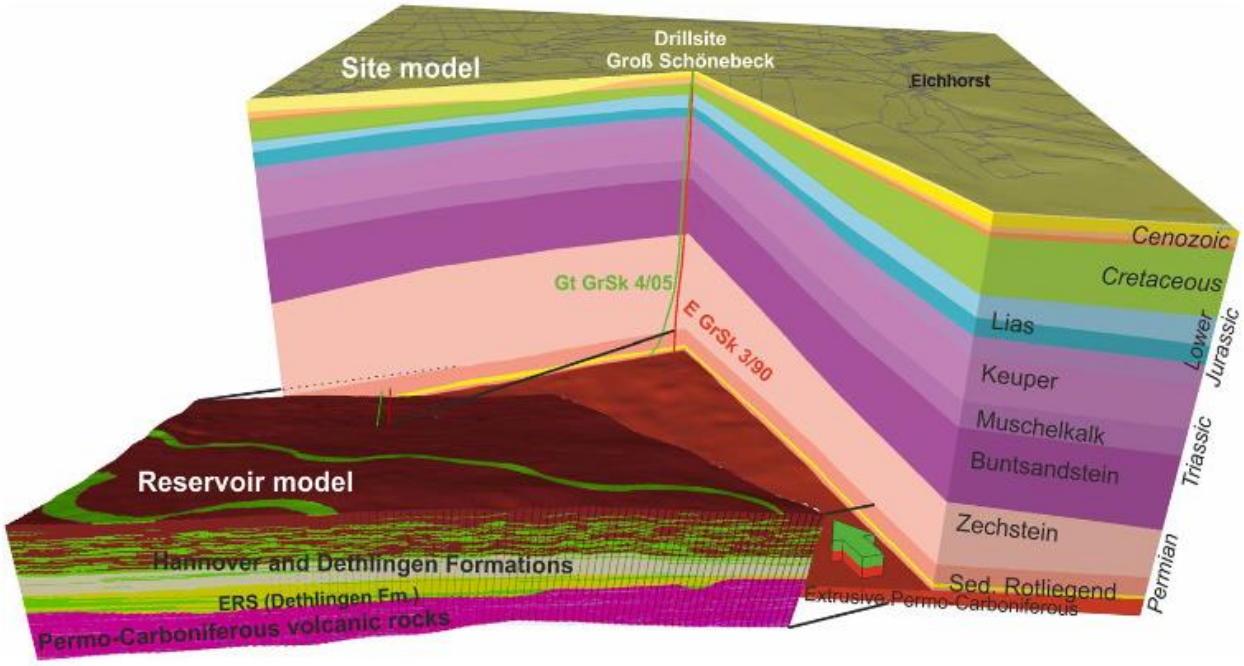

Figure 4.1: 3D view geology model of Groß Schönebeck and targeted reservoir model for geothermal exploration and exploitation in this area (Norden et al., 2023). The size of the site model is 10 km × 10 km, the size of the reservoir model 6.5 km × 6.5 km.

4.2 Series of testing carried out for the development of the Groß Schönebeck site

The series of wells drilled early in the field development were deliberately designed to target the Rotliegend as the main geothermal reservoir interest in the study area. The chronology and details of the Groß Schönebeck site development are presented by Christi et al. (2025). In parallel with the site development, the chronology of hydraulic stimulation and well testing is summarized by Blöcher et al. (2016). **Table 4.1(a)** describes the early development of well E GrSk 3/90 and **Table 4.1(b)** describes the development of the site into a doublet well EGS research and demonstration research platform.

The locations of the hydraulic stimulations carried out in the field are described in **Figure 4.2.** The stimulations targeted the Rotliegend formation, which consists of the Hannover Formation, Elbe Alternate Sequence, Elbe Base Sandstone I and II, Havel Formation and volcanic rocks. The objective of the hydraulic stimulation is to improve the permeability of the Rotliegend formation and the well productivity/injectivity. The parameters are summarized by Blöcher et al. (2016) and provided in **Table 4.2 (a)** and **Table 4.2 (b)**.

Year	Activity	Details (methodology/technology/achievement)
2000	A gas exploration well, E GrSk 3/90, was discovered, redrilled and deepened to 4294 m MD into the Permo-Carboniferous volcanic succession (Huenges et al., 2002).	Three layers of cement plugs were drilled at the first phase of reopening the well.
2001 - 2002	(1) Well inspection by performing well integrity related geophysical logging. (2) Reservoir evaluation related logging activities (Pressure, Temperature, Gamma Ray, Integrity test). (3) Initial production test at well E GrSk 3/90.	(A) Well integrity check: Casing Inspection Caliper (CIC) and sonic data (Legarth et al., 2002). (B) Characterization of reservoir: Temperature, Pressure, Mud Resistivity. (C) Fracture identification, geomechanical zoning, and state of stress: caliper, sonic, borehole televiewer (BHTV) and laboratory experiments on cores (Huenges et al., 2002). (D) Downhole inflow test (flow meter log): downhole flowmeter was used to measure the initial flow contribution of the formation (Huenges et al., 2002). (E) Nitrogen lift test showing a productivity index (PI) of 0.97 $m^3h^{-1}MPa^{-1}$ (Huenges et al., 2002).
2002	(1) The first stimulation of well E GrSk 3/90 carried out to propagate and maintain open fractures in the clastic Rotliegend at 4078–4118 m MD and 4130–4190 m MD. (2) The second stimulation in the open hole section from 3883–4294 m MD was carried out targeting the volcanic sequence of the uncased hole. However, during the first attempt of water fracturing, a wellbore instability problem was encountered (Tischner, 2004).	(1) Gel-Proppant and water frac treatments in the open hole section in 2002: the concept involved the application of a retrievable open hole packer system to independently and successively treat the two intervals in the open-hole section of the well (Legarth et al., 2003). The annulus between frac string and casing was filled with saline water – NaCl (1120 kg/m^3) during stimulation (Wolfgramm et al., 2003). (2) Water frac treatment in the open-hole section.
2003	1) E GrSk 3/90 was deepened to 4305 m MD and a 5" perforated liner was installed from 4134 m to 4395 m MD (Tischner, 2004). (2) The third stimulation in the perforated liner section was performed at the interval depth of 4134 to 4305 m MD	Water frac treatment in the perforated section. The PI of well E GrSk 3/90 increased to 4.0 m^3/ h/ MPa

Table 4.1 (a): The chronology of E GrSk 3/90 development, an example of how the well was transformed from a gas exploration well into an injection well for EGS development (Christi et al., 2025).

Year	Activity	Details (methodology/technology/achievement)
2006	Drilling a new geothermal production well Gt GrSk 4/05 (A2).	Directional drilling of deviated well.
2007	Three consecutive stimulations. The details of the hydraulic stimulations, including treatment parameters and fracture dimensions have been presented by Zimmermann et al. (2009, 2010), Zimmermann and Reinicke (2010), Blöcher et al. (2010), Zimmermann et al. (2011) and Blöcher et al. (2016).	(1) Water frac at 4350-4404 m MD in the open-hole section. (2) 1st gel-proppant frac at 4204-4208 m MD in the perforated liner. (3) 2nd gel-proppant frac at 4118-4122 m MD in the perforated liner. (3) 2 nd gel-proppant frac at 4118-4122 m MD in the perforated liner.
2009	Acid treatment was performed in Gt GrSk 4/05 (A2) to remove the residual drilling fluid (Reinsch et al., 2015b).	Acid treatment was performed in the perforated section.
2010	Final completion of the production well Gt GrSk 4/05 (A2).	The installation of a 4.5" production liner as well as the Electrical Submersible Pump (ESP) installed at 1293 m MD.
2011	Preparation of the communication test between E GrSk 3/90 and Gt GrSk 4/05 (A2).	PI of 8.9 $m^3h^{-1}MPa^{-1}$ measured in June 2011 (Reinsch et al., 2015a; Blöcher et al., 2016).
2011 - 2013	139 hydraulic tests were conducted to understand hydrothermal processes during simultaneous production and injection, as well as to investigate reservoir performance in relation to surface facility integration.	PI of 1 -2 $m^3h^{-1}MPa^{-1}$

Table 4.1 (b): The chronology of E GrSk 3/90 development, an example of how the well was transformed from a gas exploration well into an injection well for EGS development (Christi et al., 2025).

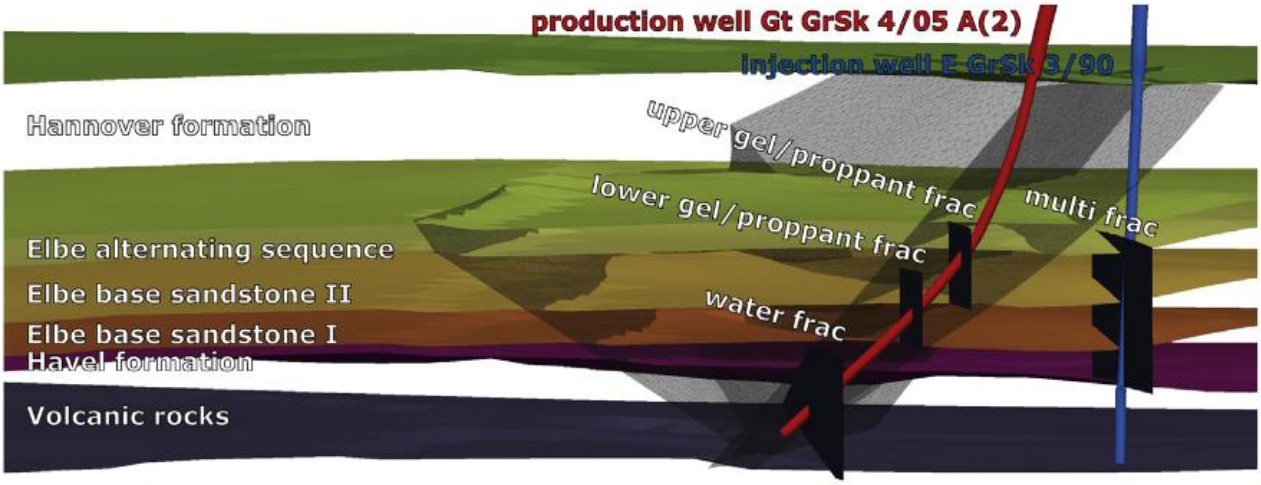

Figure 4.2: Targeted formations for hydraulic stimulations, the Rotliegend formation as a deep geothermal reservoir (Blöcher et al., 2016).

Well	E GrSk 3/90							Gt GrSk 4/05 (A2)		
Treatment	Unit	Initial Frac	1st gel/ Proppant	2nd Frac	2nd gel/ Proppant Frac	1st Water Frac	2nd Water Frac	Water Frac	1st gel/ Proppant	2nd gel/ Proppant
Date and time										
Year		2002	2002	2002	2002	2003	2003	2007	2007	2007
Duration	[h]	1.9	9.3	1.7	9.5	96	67	106.5	1.5	2
Treatment parameter										
Frac interval	[MD]	4140 - 4200	4140 -4200	4088 - 4128	4088 - 4128	3882 - 4294	4135 - 4305	4350 - 4404	4204 - 4208	4118 - 4122
Completion		Open hole	Open hole	Open hole	Open hole	Open hole	Slotted liner	Slotted liner	Perforated liner	Perforated liner
Maximum flow rate	[m^3/h]	153 (stepwise)	138	121 (stepwise)	120	86.4	144	540	240	210
Cummulative volume	[m^3]	129	107	103	120	4284	7291	13170	280	310
Maximum well head pressure	[MPa]	54.6	45.2	50.2	44.9	22	25	58.6	35	40
Gel type		HTU[a]/brine	HTU[a]/brine	HTU[a]/brine	HTU[a]/brine	-	-	-	Cross-linked	Cross-linked
Proppant type		-	Carbo-Lt	-	Carbo-Lt	-	-	Quartz sand	High strength	High strength
Proppant mesh size		-	2040	-	2040	-	-	-	2040	2040
Proppant mass	[kg]	-	8796	-	8580	-	-	24400	95000	113000
Fracture dimension										
Half length	[m]	-	32	-	-	-	160	190	57	60
Height	[m]	-	72	-	-	-	96	135	115	95
Aperture	[cm]	-	0.16	-	-	-	0.5	0.8	0.53	0.53

Table 4.2 (a): Chronological sequence of all induced hydraulic fractures including treatment parameters and fracture dimensions (Blöcher et al., 2016). [a] cationic, hydrophilic, and polymer base gel.

Well	E GrSk 3/90						Gt GrSk 4/05 (A2)		
Well test		Casing lift	Casing lift	Casing lift	Flow back	Flow back	Injection	Casing lift	Caisng lift
Date and time									
Year		2001	2002	2002	2003	2003	2007	2007	2009
Relative time		Before Initial Frac	After First Gel/proppant frac	After First Gel/proppant frac	After First Water Frac	After Second Water Frac	Before Water frac	After Hydraulic Tretaments	After Acidizing
Duration	[h]	12.24	8	13.92	5.76	24	13.4	11.8	4
Well test parameter									
Flow rate	[m^3/h]	13.5	14.8	22.4	59	35.8	31.6[a]	30.2	35
Cummulative volume	[m^3]	167	100	307	338	859	424[b]	356	140
Pressure difference	[MPa]	14	7.5	10.5	14.7	6.7	13.3	3.5	2.8
Reservoir performance									
PI/II	[m^3/(hMPa)]	0.97	2	2.1	4	7.5	2.4	10.1	14.7
PER		Initial	2.1	2.2	4.1	7.7	Initial	4.3	6.2

Table 4.2 (b): Chronological sequence of well tests including hydraulic parameters, reservoir performance, productivity enhancement ratio (PER) (Blöcher et al., 2016). [a]Average of three single tests in different depths; [b]Sum of three single tests in different depths.

4.3 Characteristics of the aquifers in the research area

As described by Feldrappe et al. (2007), the following criteria were used for classification as a geothermal aquifer (cf. Wormbs et al., 1992). The temperature should be between 40°C and 100°C or higher, which can be expected at a depth interval of about 1000-3000m. An assumed minimum production rate of 50 m^3/h requires an aquifer thickness of at least 10 – 15 m and an effective porosity of more than 20%, preferably 25%. The permeability of the rock should exceed the minimum value of 0.25-05 Darcy. The most important aquifers for geothermal applications in the wider area of North German Basin (NGB) are the sandstones of the Middle Bunter, the Schilfsandstein (Middle Keuper), the sandstone complex of the Rhaetian and Liassic, the Dogger-ß sandstone (Aalenian) and the Lower Cretaceous sandstones (Feldrappe et al., 2007). These horizons are distributed basin-wide and often reach the required thicknesses. Later, Frick (2023) investigated the geothermal resources and ATES potential of Mesozoic reservoirs in the North German Basin. Five of the most promising and widespread Mesozoic reservoirs in northern Germany were identified. An analysis of the heat storage potential, which describes the geothermal reservoirs and associated depths that are most promising for technical use, points to 5 promising reservoirs in the NGB for heat production: Lower Cretaceous, Middle Jurassic, Lower Jurassic and Middle Triassic. The relevant aquifers suitable for geothermal energy production identified in Groß Schönebeck (E GrSk 3/09) are listed below, following the preceding interpretation and description carried out by Feldrappe et al. (2007) for the regional geothermal potential aquifers and by Norden et al. (2023) for local Groß Schönebeck area.

4.3.1 Upper Triassic – Lower Jurassic sandstones (Rhaetian-Liassic aquifer complex)

According to Feldrappe et al. (2007). The Rhaetian is subdivided into three units, which consist of coloured and black mudstones and light to brownish mature sandstones (Beutler, 2005). Sandstones occur in the Lower Rhaetian (Postera beds), in the Middle Rhaetian (Contorta beds) and locally in the Upper Rhaetian (Triletes beds). The sandstones of the Rhaetian and Triassic are mostly very good aquifers, because of their high porosity, and low content of matrix and cement. The high quality especially of the Rhaetian aquifers is proven by geothermal installations in Waren, Neustadt Glewe and Neubrandenburg. Numerous laboratory measurements and the interpretation of the well logs imply porosities of 20-35% as well as good and rarely moderate to good permeabilities (500 - 1000 mD), respectively. The production rate is estimated of about 50 – 250 $m^3h^{-1}MPa^{-1}$.

At Groß Schönebeck, only Lower Jurassic (Northern Lias Group) sediments are present in the drillings on the salt pillow (Norden et al., 2023) and it was identified at the depth of 600 – 700 m at well E GrSk 3/90 with the temperature range of 30℃ - 40 ℃. The deposits represent marine shale facies and are partly interfingering with shallow-marine sands and limnic and terrestrial sediments.

4.3.2 Middle Keuper - Upper Triassic

The Schilfsandstein beds (Stuttgart Formation) are a sandy to muddy sequence of the Middle Keuper. They are distributed throughout the basin, with the exception of the areas of the island of Rügen and the Altmark, which are typical swells regions during the Middle Keuper. The storage properties of these sandstones are very good in the north-eastern and eastern parts of the basin, with effective porosities varying between 20 and 35%. These sandstones in the north-eastern and eastern parts of the basin have very good reservoir properties, with effective porosities varying between 20 and 35%. The sandstones in the western part have slightly lower porosities (15-25%). Good permeability (>1D) is also expected in the eastern part, while moderate (to good) permeability is expected in the western part. The productivity of the aquifers reaches up to 100 $m^3h^{-1}MPa^{-1}$. The Keuper sediments are mainly characterized by fine-grained sediments of perennial and fluvial facies, with subordinate marine facies. The Groß Schönebeck salt structure formed during the

Keuper and represents a salt pillow with only minor hiatuses of less than 30 m (Beutler and Franz 2015; Norden et al., 2023).

At Groß Schönebeck, Middle and Lower Keuper up to the Upper Keuper are present in the drillings at well E GrSk 3/90 and Gt GrSk 4/05 (A2) at depths of approximately 600 – 1200 m TVD with a temperature range of 30°C - 65 °C. The deposits represent marine shale facies and are partly interfingering with shallow-marine sands and limnic and terrestrial sediments.

4.3.3 Lower Triassic (Middle Buntsandstein)

The Middle Bunter Formation is subdivided into the Volpriehausen, Detfurth, Hardegsen and Solling Formations. The porosity of the sandstones was determined using core samples and borehole measurements. These values range between 10 and 30%, with the higher values occurring in the north-eastern part of the NGB. In this area, permeabilities are estimated to be moderate to good. The productivity of the Solling sandstone in Vorpommern is estimated at around 100 $m^3h^{-1}MPa^{-1}$ on the basis of porosity measurements and the productivity of geothermal wells. At Groß Schönebeck, the thickest sandstone interval occurs in the Dethfurt Formation with a thickness of 10 m, showing a cleaner sand interval of about 6 m and temperatures of 85 °C at a depth of 1870 m.

4.3.4 Permian Rotliegend

Rotliegend is one of the most targeted reservoirs for hydrocarbon exploration in the North German Basin. The Rotliegend formation itself consists of quartz-dominated sandy deposits that represent one of the geothermal reservoir targets (Norden et al., 2023), the Elbe Reservoir Sandstone (ERS) (Bauer et al. 2020). The ERS consists of the Dethlingen Formation, the Hannover Formation, and possible parts of the Mirow Formation. In well E GrSk 3/90, the ERS shows a thickness of about 40 m within the Dethlingen Formation (Bauer et al. 2020). In open hole logs, the ERS is characterized by low gamma ray values and shows a high quartz content. In addition, reduced P-wave velocities observed by sonic logging indicate an increase in porosity (Trautwein and Huenges 2005). These two observations explain the general interest in the ERS as a geothermal target. It hosts water at a temperature of around 150 °C in Groß Schönebeck, with an initial productivity and injectivity index of 0.97 $m^3h^{-1}MPa^{-1}$, and a permeability of no higher than 5 mD (Huenges, 2002).

5. Geothermal features of the potential location

5.1 Geothermal reservoir at the area

As detailed in Chapter 3, the geothermal resources in Groß Schönebeck present three potential development approaches: (1) Enhanced Geothermal System (EGS) targeting the Rotliegend Formation (maximum temperature of 150°C), (2) Hydrothermal System (HE) targeting the Muschelkalk and Buntsandstein (maximum temperature of 85°C), and (3) Deep Borehole Heat Exchanger (DBHE) targeting the Zechstein Formation (maximum temperature of 138°C). The stratigraphic profile in **Figure 5.1** delineates the horizons and corresponding upper and lower boundaries of the targeted geothermal reservoirs for each technology.

5.1.1 New drilling plan

- **HE development** will depend on the success of initial drilling and connectivity between the first and second wells. A minimum 500 m distance between doublet wells should be achieved within the planning of the second well drilling as the practical industrial standard.

5.1.2 Repurposing concepts for the existing infrastructure concepts

- **EGS development**, the reservoir size is defined by the area surrounding the stimulated fractures between well doublets, based on the fracture length (**Table 5.1** and **Figure 5.2**) and the cross-sectional area of the fractures within the well doublet.

- **DBHE development,** effective DBHE development hinges on near-wellbore reservoir characteristics, as the coaxial system relies on conductive heat transfer from the reservoir to a closed-loop working fluid. At the Groß Schönebeck site, geothermal resources within the Zechstein formation can be accessed at depths up to 3800 m TVD with a minimum 7” liner.

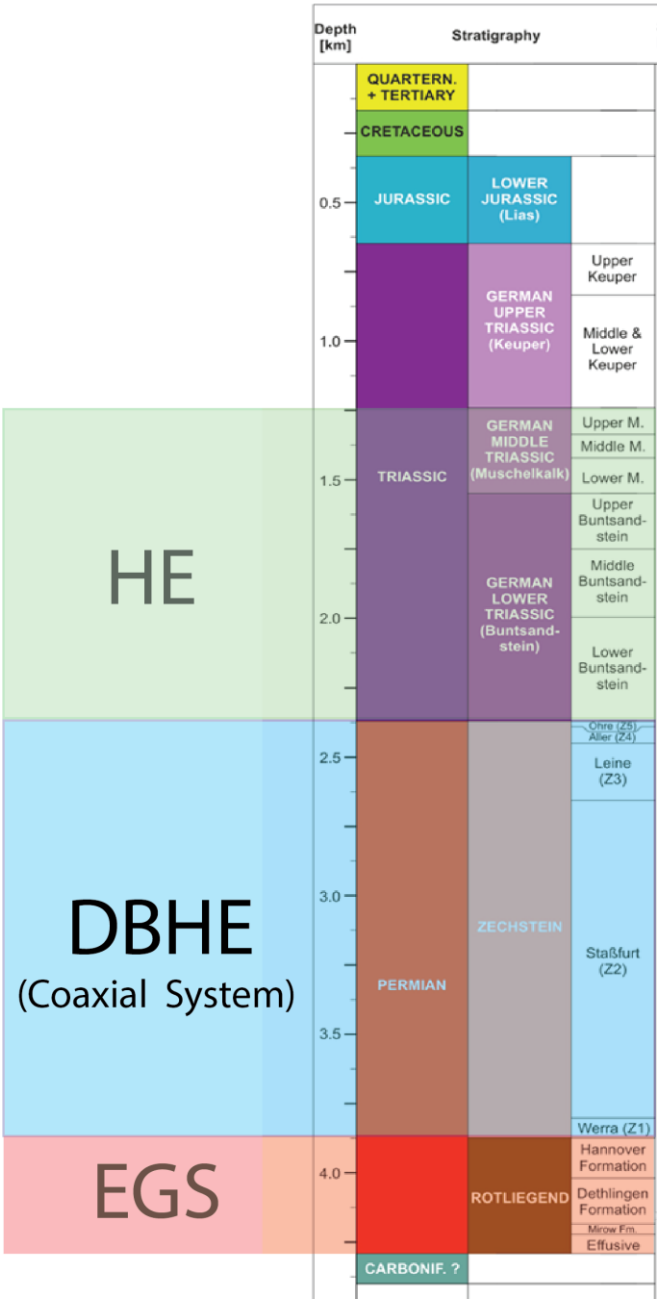

Figure 5.1: Potential multi-layered geothermal resources and their respective technological development approaches (modified from Norden et al. (2023).

Well	Type of fracturing	Depth (m)	Height (m)	Half length (m)	Fracture aperture (a) in (mm)
E GrSk 3/90	Multifrac	-4004 to -4147	143	160	0.228
Gt GrSk 4/05 (A2)	Water frac	-4098 to -4243	145	190	0.228
Gt GrSk 4/05 (A2)	Gel-proppant	-3996 to -4099	103	60	0.228
Gt GrSk 4/05 (A2)	Gel-porppant	-3968 to -4063	95	60	0.228

Table 5.1: Dimensions and hydraulic properties of the induced fractures under in-situ conditions (Zimmermann et al., 2010).

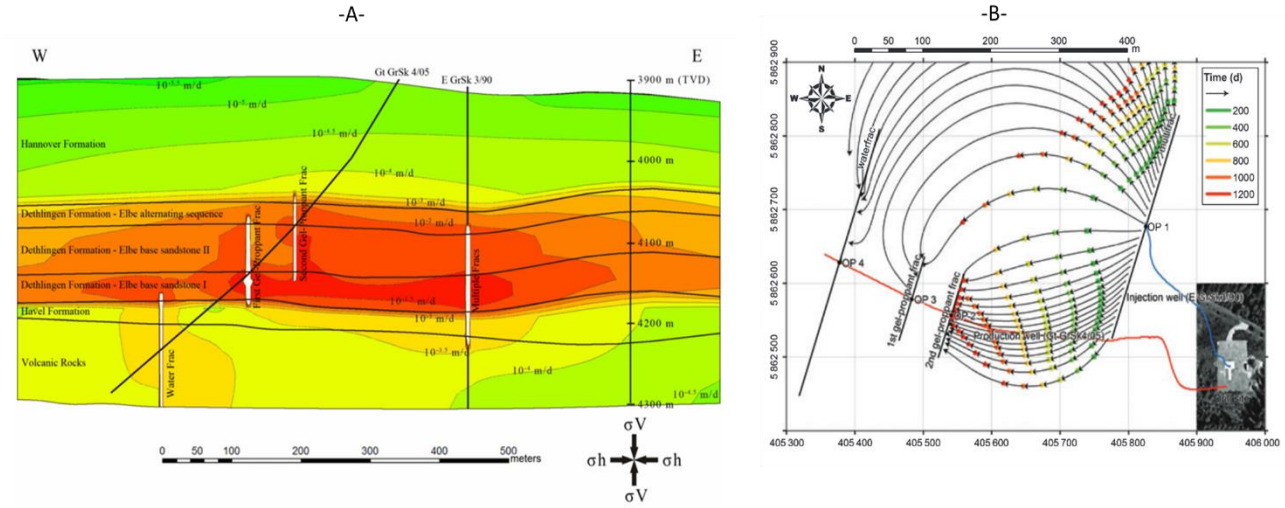

Figure 5.2: Fractures dimensions relatively to the doublet well location at the Groß Schönebeck. (-A-) taken Zimmermann et al., (2009), (-B-) from Blöcher et al., (2010).

5.2 Initial pressure and temperature conditions of the reservoir

As reported in the TRANSGEO engineering workflow document (Hofmann et al., 2025), **Figure 5.3** shows the initial conditions of the geothermal reservoir. These initial conditions are based on a series of T-P-MRES-GR (temperature, pressure, mud resistivity and gamma ray) measurements performed at well E GrSk 3/90 in 2001, immediately after the borehole was opened (Huenges et al., 2002). The initial temperature of the reservoir is 149 °C at a depth of 4,230 m TVD. The average water level is 255 m below the bottom of the well at a TVD of 4290 m. The initial pressure is 45.5 MPa at a depth of 4290 m TVD. This was measured during the first 100-hour flow test, prior to the hydraulic stimulation series.

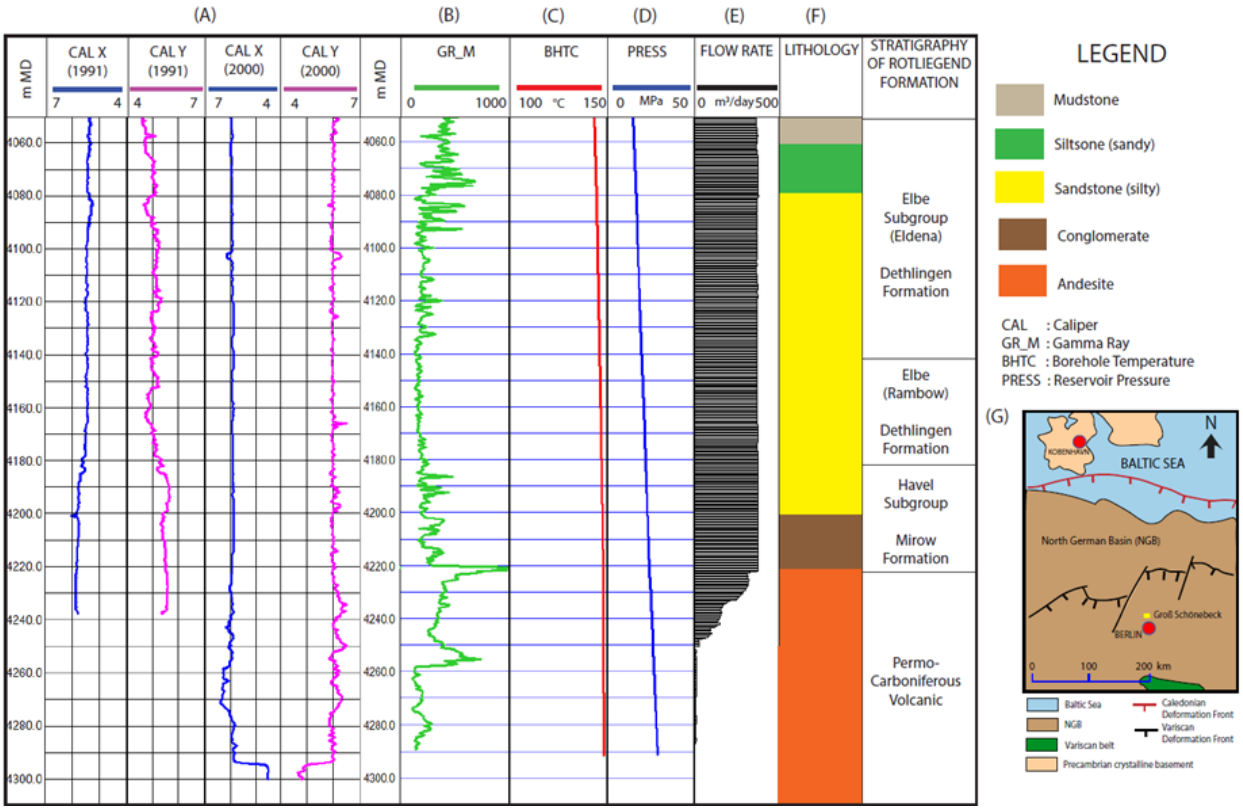

Figure 5.3: (A) Caliper measurement results in 1991 and 2000. (B) Gamma Ray (GR_M), (C) Temperature (BHTC), (D) Pressure (PRESS) measured in 2001. (E) Inflow measurement with down-hole flow meter after the re-opening of E GrSk 3/90 in January 2001. (F) Lithology and stratigraphy of well E GrSk 3/90 (modified from Huenges et al. (2002) and Norden et al. (2023). (G) Tectonic setting of the surrounding Groß Schönebeck site (modified from DEKORP, 1999). The Rotliegend formation covers the area described in Figure (G). The graphic is taken from (Christi et al., 2025).

5.3 Characteristics of the reservoir fluid

As reported by Wolfgramm et al. (2023), the fluids of the Rotliegend formation are generally characterised by temperatures and salinities of 150 °C and 280 g/l, respectively (Lehmann, 1974 a,b; Naumann, 2000). The chemical composition of the deep Rotliegend fluids from the GrSk 3/90 well was determined by several analyses of deep samples (4231-4247 m). The formation fluids of the GrSbk 3/90 show a total dissolved solids (TDS) content of 260-265 g/l. A pH value of 6.2 and an Eh value related to the standard hydrogen electrode of 50 mV were measured prior to the stimulation tests. Chemical analysis showed predominance of calcium (54,000 mg/l) and sodium (38,000 mg/1) with minor amounts of magnesium and potassium. Chloride (167,000 mg/l) is the major anion. The deep fluid can be assigned to a Ca-Na-Cl type and classified as a Rotliegend fluid (**Figure 5.4**). The Rotliegend fluids of the E GrSk 3/90 well contain ammonium and sulphate with up to 130 and 150 mg/l respectively. HS^- and S^{2-} were not detected. Relatively high values of copper (9 mg/l), zinc (65 mg/l), iron (200 mg/l), lead (100-225 mg/l) and manganese (230 rag/l) indicate a metal-rich source rock. The composition of gases from deep samples was determined in the laboratory using a quadrupole mass spectrometer (Bakers Omnistar, Balzers QMG 421) and the ratios of noble gases were measured using a sector field mass spectrometer (VG 5400) (Giese et al., 2002). A summary of geothermal composition is provided in **Figure 5.4**. The average density of reservoir fluid is 1115 kgm^{-3}, however, depending on the pressure and temperature, the density of the reservoir fluid under injection and production conditions differs, as indicated in **Figure 5.5**.

Cations	mg l^{-1}	mEq l^{-1}	Anions	mg l^{-1}	mEq l^{-1}
Ca^{2+}	54 000	2694.61	Cl^-	167 300	47 18.92
Na^+	38 400	1670.29	Br^-	300	3.75
K^+	2900	74.17	SO_4^{2-}	140	2.91
Sr^{2+}	1900	43.37	HCO_3^-	18.9	0.31
Mg^{2+}	430	35.38			
Mn^{2+}	270	9.83			
Fe^{2+}	200	7.16			
Li^+	204	29.39			
Pb^{4+}	180	3.48			
NH_4^+	75	4.16			
Zn^{2+}	74	2.26			
Ba^{2+}	34	0.50			
Cu^{2+}	7	0.22			
Cd^{2+}	1.8	0.03			
As^{3+}	1.4	0.06			
Total	98 677.2	4574.91		167 758.9	4725.90

Error of ion balance $= \frac{\sum \text{cations}(mEq\,l^{-1}) - \sum \text{anions}(mEq\,l^{-1})}{\sum \text{cations}(mEq\,l^{-1}) + \sum \text{anions}(mEq\,l^{-1})}$ = −0.016

Dissolved SiO_2 = 80 mg l^{-1}

Total dissolved solids (TDS) = 266.5 g l^{-1}

pH = 5.7

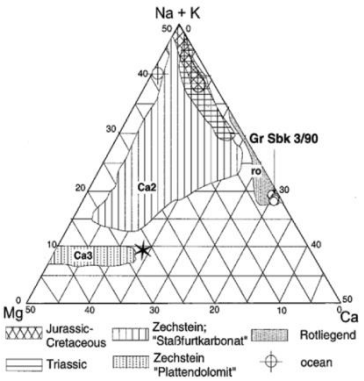

Fig. 2. Fluid composition of basinal waters of NE German basin according to Müller (1969); circles show water composition of well Gr Sbk 3/90, values in mval%, sum of all cations is 50 mval%.

Figure 5.4: Composition of the Groß Schönebeck Rotliegend reservoir fluid. Reservoir composition table is taken from Blöcher et al., (2010), the trilinear diagram is taken from Wolfgramm et al. (2003).

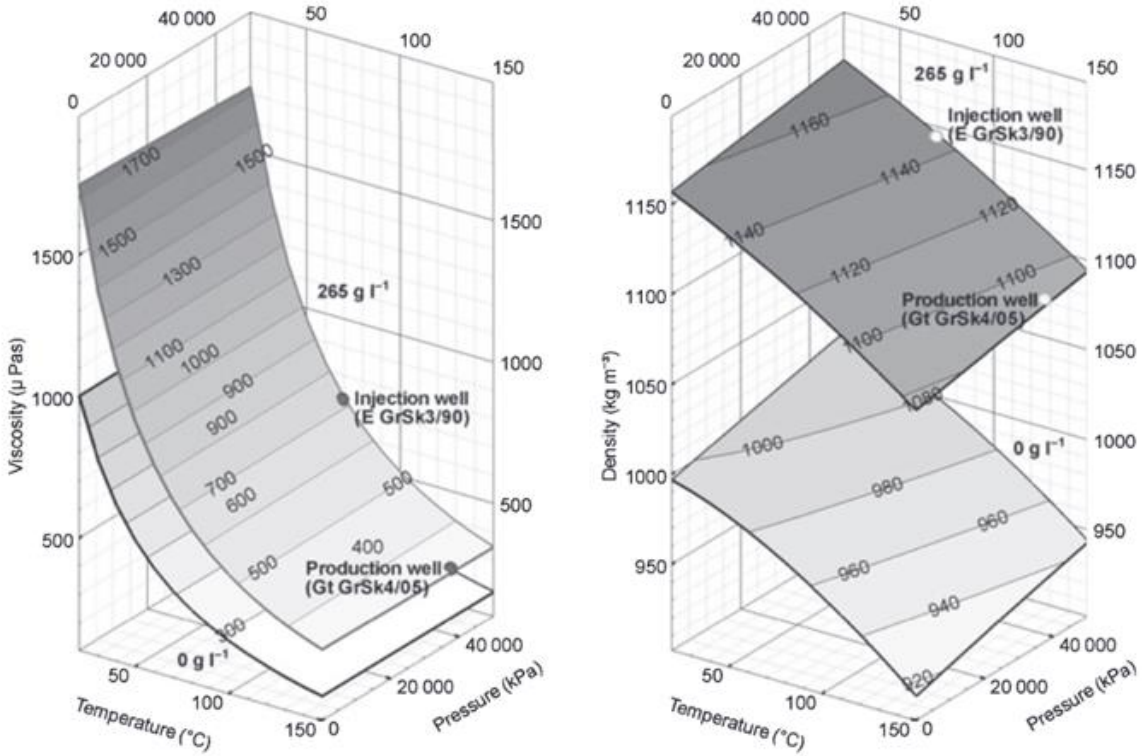

Figure 5.5: Pressure and temperature dependent density and viscosity of the Groß Schönebeck reservoir fluid (Blöcher et al., 2010).

5.4 Physical properties of rocks

The physical properties of the reservoirs are based on the report for model validation of EGS technology in the TRANSGEO Engineering Workflow document (Hofmann et al., 2025). The rock thermal conductivity and volumetric heat capacity were obtained from Blöcher et al. (2010). Due to the low porosity of the reservoir rock, it is assumed that the properties of the solid fraction are similar to the bulk properties used by Blöcher et al. (2010). The porosity and permeability parameter values were obtained from the facies simulation parameterisation provided by Norden et al. (2023). The top-to-bottom layer properties required for the DBHE, which focus on the variation in thermal conductivity of each formation, are based on Norden et al. (2008; 2012; 2023). These properties are summarised in **Tables 5.2** and **Table 5.3** for EGS and DBHE technology approaches respectively.

Geological unit	Φ (%)	k (m^2)	λ ($Wm^{-1}K^{-1)}$	VHC ($MJ\ m^{-3}K^{-1}$)
I. Hannover (Mellin Peckensen)	0.05	3.57×10^{-23}	1.90	2.40
II. Dethlingen (Eldena)	0.10	3.57×10^{-23}	1.90	2.40
III. Dethlingen (Rambow)	0.10	4.44×10^{-15}	2.80	2.40
IV. Havel subgroup	0.11	4.44×10^{-15}	3.00	2.60
V. Volcanic rock sequence (Permo - Carboniferous Volcanic)	0.11 – 0.13	1.77×10^{-21}	2.30	3.60

Table 5.2: Thermal and hydraulic properties applied in the reservoir model of EGS system. φ is porosity, λ is thermal conductivity, and VHC is volumetric heat capacity (Christi et al., 2025).

Parameter	Symbol	Unit		
Porosity of Zechstein Formation	ϕ	-	0.05	
Permeability of Zechstein Formation	k	m^2	9.87×10^{-20}	
Formation Compressibility	CP_{rock}	kPa^{-1}	4.50×10^{-7}	
Formation	Rock Thermal Conductivity (λ_r), ($Wm^{-1}K^{-1}$)		Rock Heat Capacity (C_{pr}), ($MJm^{-3}K^{-1}$)	Thickness (m)
Surface - Tertiary	2.38		1.65	168
Cretaceous	2.82		2.29	165
Lias	2.53		2.53	315
Keuper	2.71		2.32	593
Muschelkalk	2.30		2.25	309
Bundsandstein	2.27		2.32	819
Zechstein (Staßfurt - Werra Fm.)	4.50		2.32	1498
Rotliegend (Hannover Fm.)	1.90		2.40	208
Rotliegend (Dethlingen Fm.)	2.80		2.40	100
Rotliegend (Havel Fm.)	3.00		2.60	38
Rotliegend (Effusive Rotliegend)	2.30		3.60	70
Permo-Carboniferous Volcanic	2.30		3.60	217

Table 5.3: Thermal and hydraulic properties applied in the reservoir model of DBHE system (Christi et al., 2025).

6. Technological aspects of geothermal energy technology application at Groß Schönebeck

6.1 Determination of working conditions

During the test phase, well E GrSk 3/90 was operated as an injection well and well Gt GrSk 4/05 as a production well. The wells were connected to a small-scale binary facility for testing purposes. The aim was to produce electricity from the produced brine. Both wells, E GrSk 3/90 and Gt GrSk 4/05 (A2), have a negative wellhead pressure of ~2.5 MPa in the shut-in condition, with the water level at approximately 230 m below the ground surface. The operating condition measurements (wellhead pressure, bottomhole flow pressure, ESP flow quantification, surface temperature, Productivity Index (PI) and Injectivity Index (II) were obtained during the 139 production tests between the two wells from 2011 to the end of 2013, as shown in **Figure 6.1** and **Figure 6.2**. The complete datasets of the 139 production tests are presented in Blocher et al. (2016) and Reinsch et al. (2015). The complete well completion configuration during the production test period can be found in Figure 2 and Figure 3 of (Christi et al., 2025).

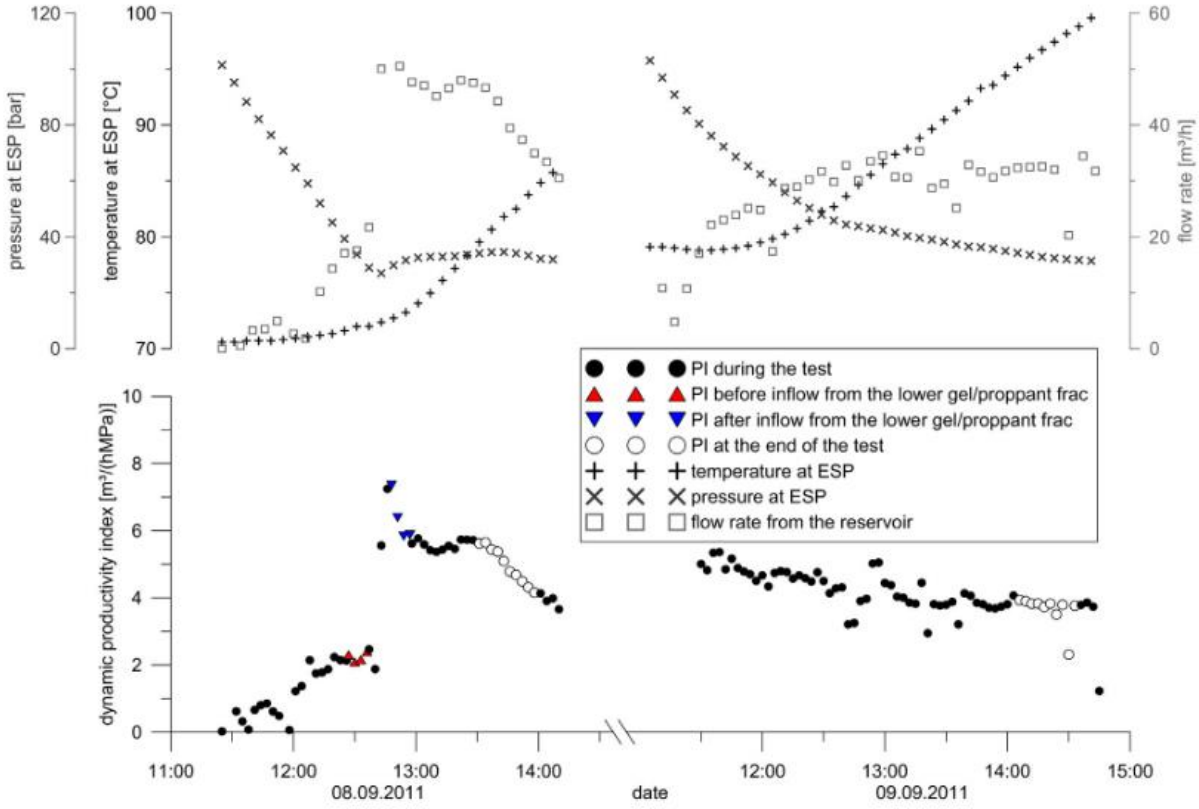

Figure 6.1: Measured temperature and pressure at the ESP and calculated flow rate from the reservoir with corresponding dynamic productivity index (PI dynamic) of the production test on September 8, 2011 (Blöcher et al., 2016).

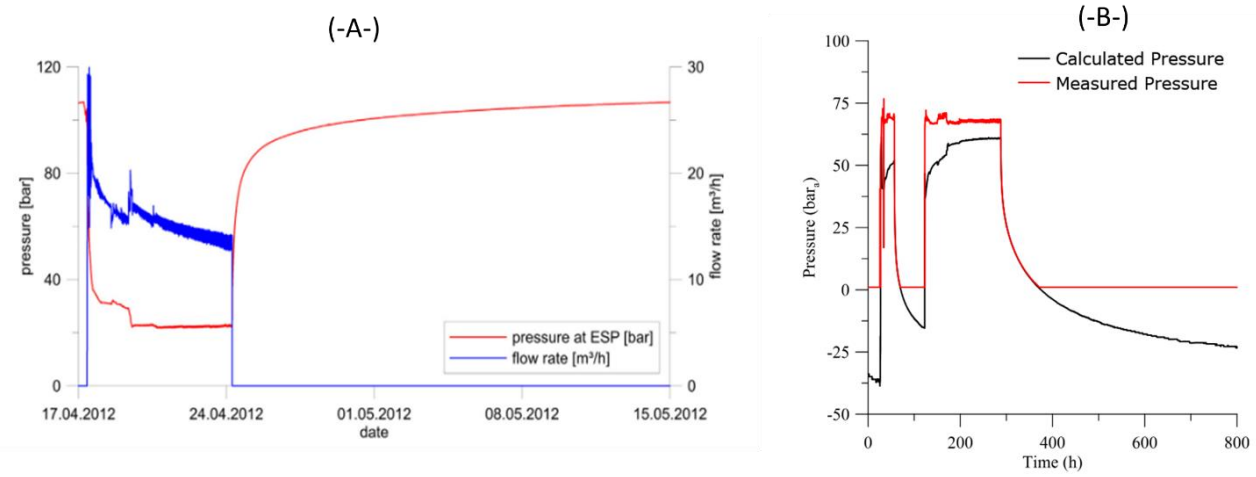

Figure 6.2: (-A-) Progression of the hydraulic tests from April 2012. The graphic shows the flow rate and the pressure at the ESP installed a depth of 1200 m MD. (-B-) Measured and corrected well head pressure during the communication test in April 2014 (Reinsch et al., 2015 and Blocher et al., 2016).

6.2 Reservoir simulation

6.2.1 Reservoir model for EGS system

The reservoir model was validated, with the results presented in the Engineering Workflow document (Hofmann et al., 2025) and in the work of Christi et al. (2025). For the purpose of the feasibility study, the predictive model was derived from the calibrated model in order to forecast the thermal power output over a 30-year lifespan. In the predictive model, the reservoir simulation adopted the new fracture-dominated development concept as shown in **Figure 6.3.** The details of the modelling method and parameterization are described in Christi et al. (2025). The scenarios modelled in this feasibility study following the design of well layout configuration presented in **Figure 3.5**.

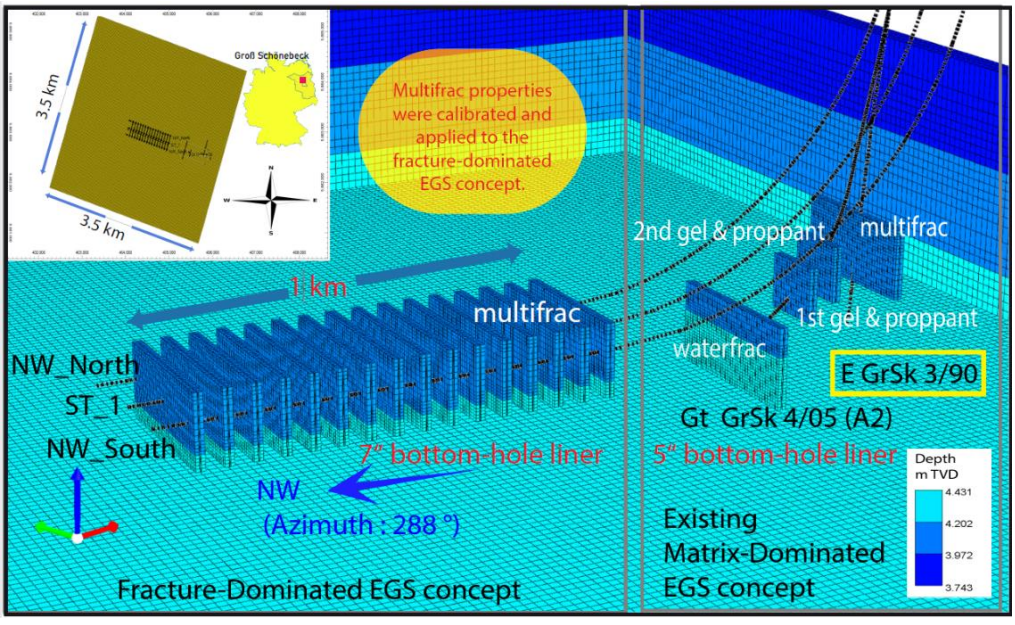

Figure 6.3: The 3D conceptual model of new fracture-dominated EGS development concept (Christi et al., 2024).

- **Scenario 1 (1 injection well: Side track ST_1 and 1 production well: NW_North)**

Scenario 1 represents the location of the new injection well in the same direction as the Gt GrSk 4/05 (A2) to the northwest and the new production well pad which is 150 m away, from the existing production well pad to the northeast. The risk of this configuration, based on the 3D geological model, is that the new production well will have the closest distance of 15 m to the former injection well E GrSk 3/90 at a depth between 3993 and 4055 m TVD. The new fractures are located approximately 800 m away from of the existing 1st induced fracture to the northeast.

- **Scenario 2 (1 injection well: Side track ST_1 and 1 production well: NW_South)**

Scenario 2 is designed in the same direction as the existing wells, with the new production well pad located 150 m to the southwest of the current well pad. In this configuration, the location of the multi-stage fracture does not interfere with the existing wells and fractures. It also means that the new well will be located approximately 600 meters from E GrSk 3/90.

- **Scenario 3 (1 injection well: Side track ST_2 and 1 production well: SE_North)**

The objective of Scenario 3 is to target an area in a direction that is opposite to that of the existing well configuration. In order to achieve the optimum trajectory, the drilling target is oriented to the southwest with an azimuth of 108° for the side-track section of the injection well. The new production well is located in the northwest region of the existing well pad of Gt GrSk 4/05 (A2). The rationale for this option was to explore a previously unexplored area that would be accessible by reusing Gt GrSk 4/05 (A2) in a new configuration.

- **Scenario 4 (1 injection well: Side track ST_2 and 1 production well: SE_South)**

In Scenario 4, the well configuration has been set in the same direction as in Scenario 3 and the location of the production well pad is to the southeast of the current well pad of Gt GrSk 4/05 (A2). The production well in this scenario is in the opposite direction to the production well configuration in Scenario 2.

- **Scenario 5 (1 injection well: Side track ST_1 and 2 production wells: NW_South & NW_North)**

In Scenario 5, the configuration consists of two production wells and one injection well. The location of the production well, designated NW_North, is identical to the production well used in Scenario 1. Similarly, the production well, designated NW_South, is identical to the one used in Scenario 2.

- **Scenario 6 (1 injection well: Side track ST_2 and 2 production wells: SE_South & SE_North)**

In Scenario 6, two production wells and one injection well are positioned in a southeast direction, the opposite to the orientation of well configuration in Scenario 5. The location of the production well, designated SE_North, is identical to that of the production well utilized in Scenario 3. Similarly, the production well, designated SE_South, is identical to that used in Scenario 4. The advantage of this well configuration is that it allows for the creation of a new reservoir system without disturbing the existing matrix-dominated system.

The result of simulation quantified the performance of the reservoir in terms of Productivity/Injectivity index (PI/II) and thermal breakthrough time as shown in **Figure 6.4**. The best performance was evaluated in terms of maximum achievable flow rate, thermal breakthrough time, productivity and injectivity indices. The wellbore flow was a single-phase fluid flow. The flow regime was laminar with flow rates of 60 m^3h^{-1}, 180 m^3h^{-1} and 360 m^3h^{-1}. The thermal breakthrough time in this study was set at the point where the reservoir temperature drops below 100°C. This concept, comprising 16 fractures with a parallel horizontal well configuration, demonstrates a 16-fold increase in the Productivity Index (PI) and Injectivity Index (II) at a production rate of 60 m^3h^{-1} compared to the previous matrix-dominated EGS development concept.

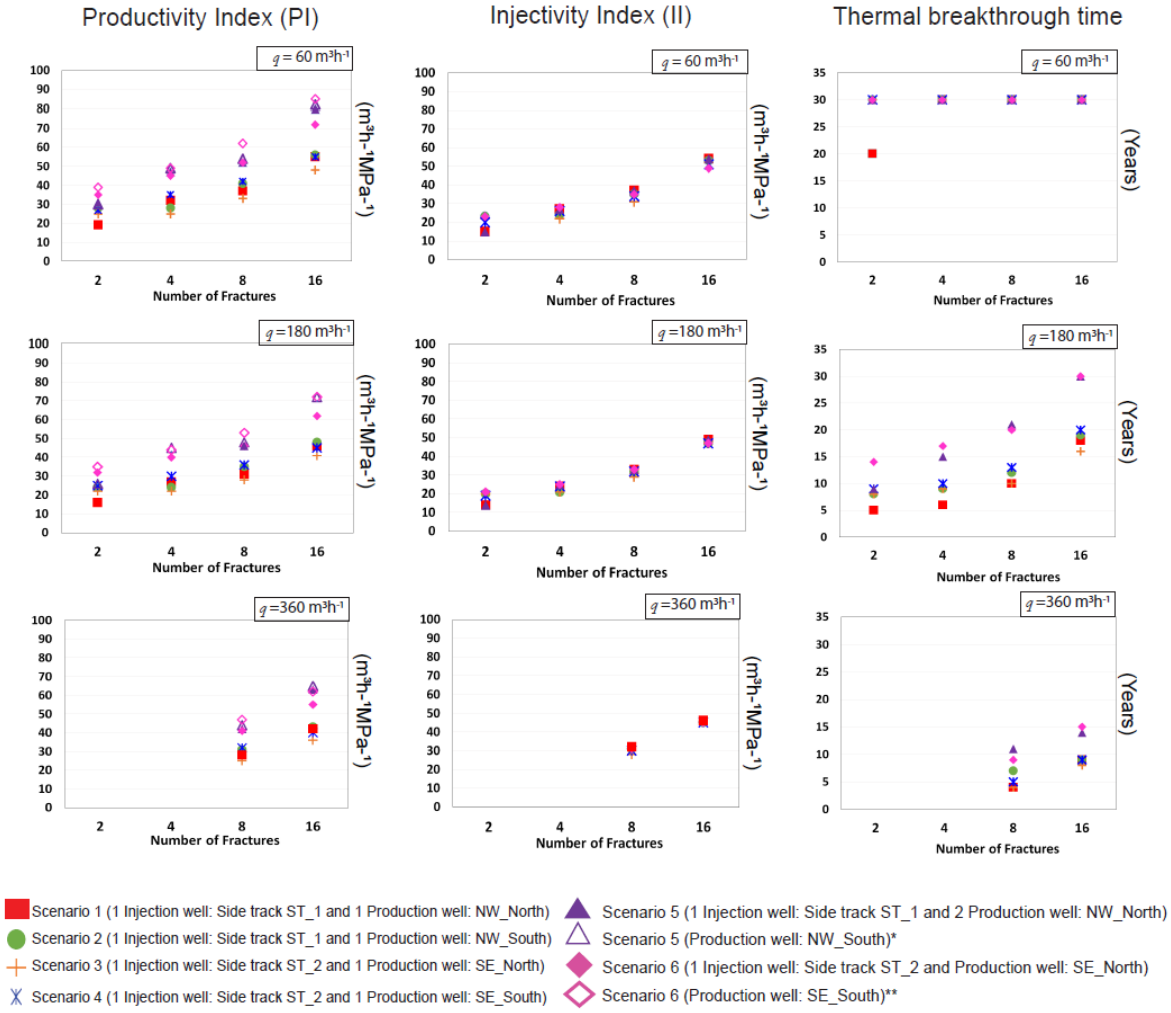

Figure 6.4: Simulation results of the fracture-dominated EGS concept. The results represent PI, II, and thermal breakthrough time at constant production rates (*60 m^3h^{-1}, 180 m^3h^{-1}, 360 m^3h^{-1}*). In the case of double production wells, PI of each well was calculated separately: *PI of production well NW_South (scenario 5); **PI of production well SE_South (Scenario 6) (Christi et al., 2025).

The predicted thermal power capacity produced by the fracture dominated EGS is shown in **Figure 6.5**, The results demonstrate that with 4 to 16 fractures at a minimum production rate of 60 m^3h^{-1}, the thermal power capacity produced from geothermal wells could reach as much as 5 MW_{th} and achieves the latest thermal breakthrough of all simulated scenarios. If the higher flow rate of 180 m^3h^{-1} and 360 m^3h^{-1} are used, the maximum calculated thermal power capacity reaches 15 MW_{th} and 30 MW_{th} respectively, with shorter time to thermal breakthrough. In the 2 and 4 fractures configuration, the reservoir could not achieve the maximum flow rate of 360 m^3h^{-1}. This flow rate could only be achieved with 8 and 16 fractures configuration for all the six scenarios. The results of the various scenarios above indicate that a 16-fracture design, combined with an optimum flow rate of 180 m^3h^{-1}, represents the most optimum case among the simulated scenarios. With two production wells, a 30-year production life can be achieved without thermal breakthrough. However, it is noteworthy that at a higher production rate of 360 m3h-1, the viability of double thermal power capacity is enhanced in the beginning, but severe temperature and pressure drop as indicated by lower PI and II could lead to the reduced heat production.

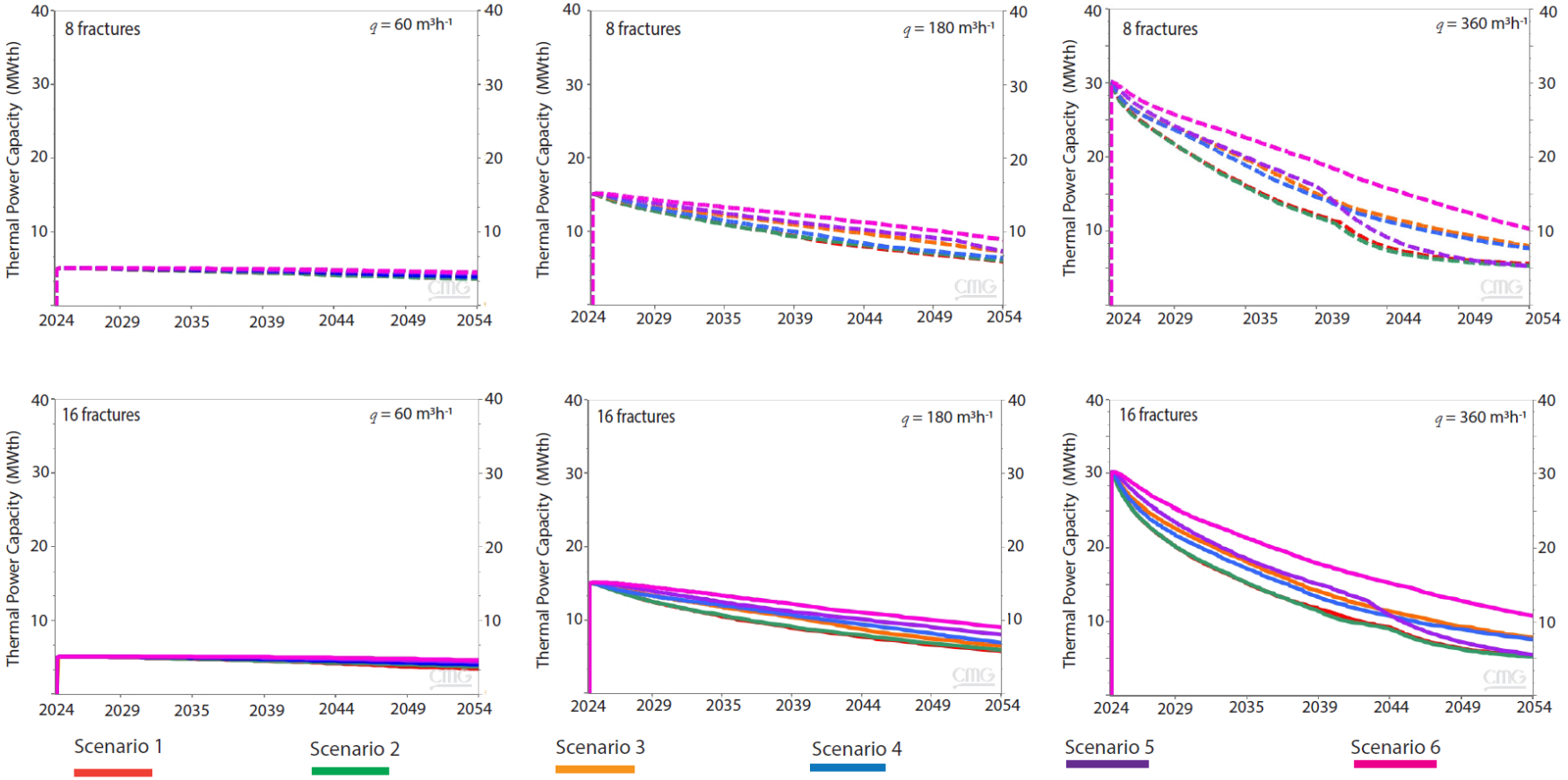

Figure 6.5: Thermal power capacity of production wells. The graph shows the power generated by varying 8 and 16 fractures, well layout setups, and at production-injection flow rates of 60 m^3h^{-1}, 180 m^3h^{-1}, 360 m^3h^{-1} (Christi et al., 2025).

Nonetheless, from an economic standpoint of drilling less production well, the scenario involving the 16-fracture design and the flow rate of 180 m3h-1 emerges as the optimal choice. In terms of the sustainability of the thermal harvest, the production scheme with a constant flow rate of 60 m3h-1 shows a 30% decline in the estimated thermal power capacity of the geothermal wells over the projected 30-year reservoir lifetime, which is the lowest of the other higher flow rate scenarios. An analysis of the well configuration and target location for the new production wells indicates that the results of scenarios 2 and 4, which include a single production well, are the best option.

It is therefore reasonable to assume that the newly developed reservoir system, located opposite the existing system and to the south-east and south-west, is the most viable option for further exploration. As shown in Figure 6, the calculated thermal power capacity produced by geothermal wells from the six scenarios with 8 and 16 fractures is presented in a ranking from highest to lowest: (1) Scenario 6; (2) Scenario 5; (3) Scenario 4; (4) Scenario 3; (5) Scenario 2; and (6) Scenario 1.

6.2.1 Reservoir model for DBHE system

The stratigraphic profile (**Figure 5.1**) illustrates that wells E GrSk 3/90 and Gt GrSk 4/05 penetrated the Zechstein Formation to a depth of 3.8 km TVD. This thermally conductive and impermeable formation, approximately 1.5 km of which consists of salt, is well-suited for DBHE applications, offering a maximum temperature of 138°C accessible with a 7” liner diameter (**Table 3.1**).

Salt structures strongly influence the subsurface temperature field at Groß Schönebeck (Huenges et al., 2002; Norden et al., 2023), inducing significant small-scale thermal anomalies – often referred to as the chimney effect (Jensen, 1983; Fromme et al., 2010; Noack et al., 2010; Kaiser et al., 2011; Balling et al., 2013; Sippel et al., 2013; Koltzer et al., 2024). This increased temperature potential within and above these structures can be effectively tapped using closed-loop systems – near-surface, intermediate-depth, or deep borehole heat exchangers (Fromme et al., 2010). In petroleum systems, salt formations act as tight, sealing caprocks for hydrocarbon reservoirs (Grunau, 1981; Jin et al., 2006; Liu et al., 2017), contributing to their extremely low permeability. The subsurface of the entire North East German Basin (NEGB) is characterized by salt structures – including rounded diapirs, elongated salt stacks, and salt walls (Fromme et al., 2010) – features common to many Permian sedimentary basins. Consequently, hydrocarbon wells targeting these sediments, particularly idle wells, are promising candidates for geothermal conversion (Koltzer et al., 2024).

To model a coaxial borehole heat exchanger at maximum depth of 3800 m MD, achieving this maximum temperature with a minimum 7” liner diameter, a numerical simulation was conducted using CMG STARS. The existing well configuration significantly influences the completion depth for DBHE installation, coaxial tubing dimensions, and accessible borehole temperature.

The reservoir model geometry was defined based on a 3D geological model derived from the latest 3D seismic interpretation of the Groß Schönebeck site (Norden et al., 2023). Fifteen geological units intersected by the well doublet are represented in the 3D model with dimensions of 0.45 km (x) x 0.32 km (y) x 4.50 km (z). Each grid cell has dimensions of 10 m (Δx) x 10 m (Δy), with the vertical length (Δz) varying according to the thickness of each geological unit (**Table 6.1**). For coaxial DBHE modelling, the grid was designed to cover the reservoir area with a 50 m margin. Local refinement, with a factor of 5 in all directions (x, y, z), was applied within the area intersected by both wells (**Figure 6.6**). Model parameters are summarized in **Table 6.2**. The model incorporates different tubing materials and sizes to evaluate the optimal design of coaxial Deep Borehole Heat Exchanger systems at Groß Schönebeck. The wellbore properties are described in **Table 6.3**.

Formation	Thickness (m)	Spatial model layers
Surface - Tertiary	168	3
Cretaceous	165	2
Lias	315	6
Keuper	593	11
Muschelkalk	309	6
Bundsandstein	819	16
Zechstein (Staßfurt - Werra Fm.)	1498	29
Rotliegend (Hannover Fm.)	208	3
Rotliegend (Dethlingen Fm.)	100	2
Rotliegend (Havel Fm.)	38	1
Rotliegend (Effusive Rotliegend)	70	2
Permo-Carboniferous Volcanic	217	4

Table 6.1: Geological units defined for DBHE systems in Groß Schönebeck (*Christi et al., under review*).

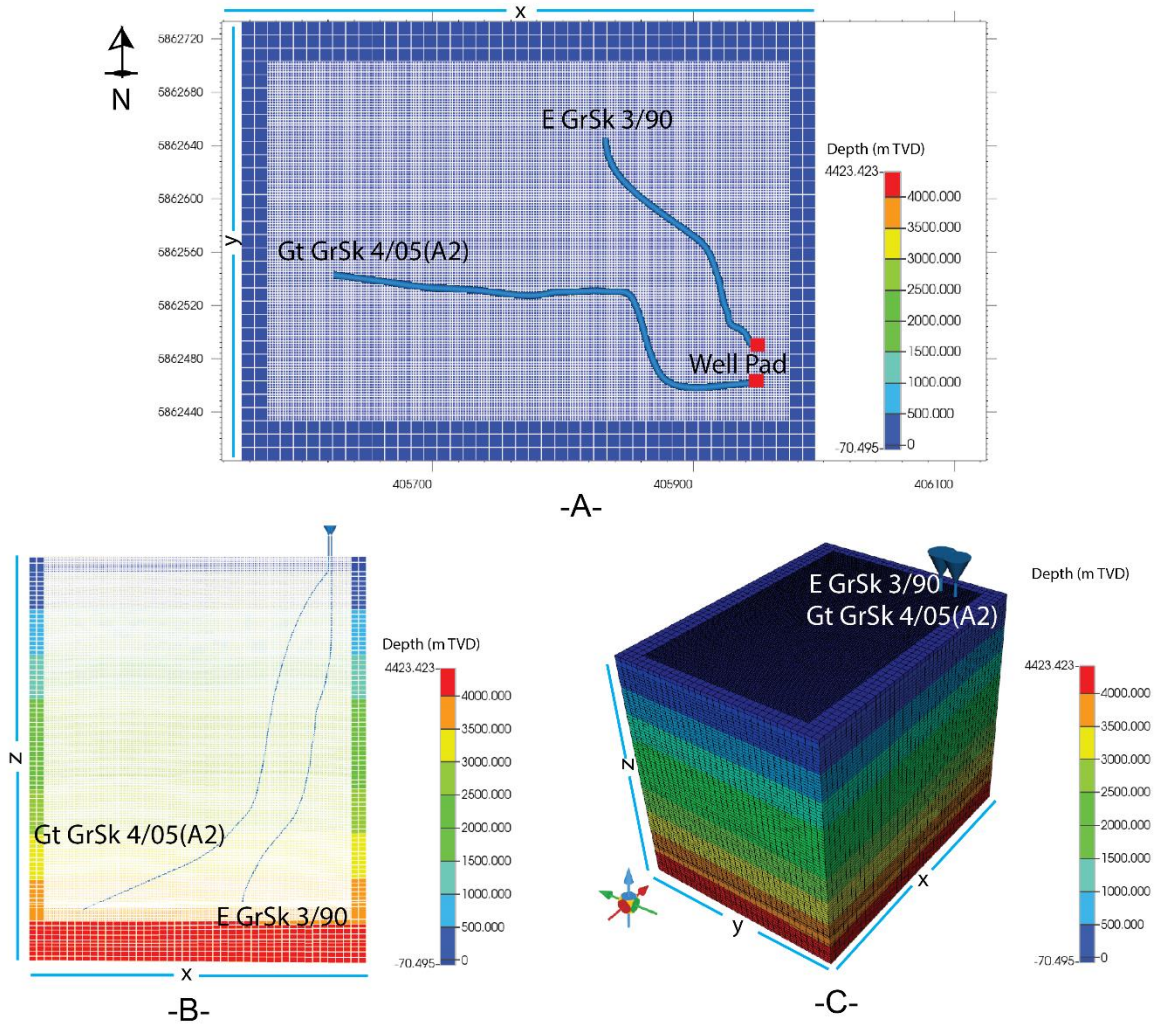

Figure 6.6: Coaxial DBHE model setup in CMG STARS. [-A-] 2D aerial view; [-B-] Vertical cross-section; [-C-] 3D view (*Christi et al., under review*).

Parameter	Unit	
Initial conditions		
Surface temperature	°C	10.00 (IEA,2022)
Surface pressure	MPa	0.1
Temperature gradient	°C m^{-1}	0.032
Pressure at 4290 m TVD	MPa	45.5
Reservoir and Working Fluid: Water		
Thermal conductivity	$Wm^{-1}K^{-1}$	0.6065 (Ramires et al., 1995)
Density	kg m^{-3}	temperature and pressure dependent (Younglove and Ely, 1987)
Viscosity	mPa s	temperature and pressure dependent (Schmelzer et al., 2005)
Compressibility	kPa^{-1}	4.7×10^{-7}
Specific heat capacity	MJ $m^{-3}K$	4.19

Table 6.2: Reservoir and working fluid parameters (*Christi et al., under review*).

Component	Thermal Conductivity ($Wm^{-1}K^{-1}$)	Heat Capacity (MJ $m^{-3}K^{-1}$)	Outer Diameter (inch)	Inner Diameter (inch)
Cement	1.37	1.85	8.75-17.75	9.63 - 18.63
Casing - Carbon Steel	45.00	3.82	7.00 - 16.00	6.00 - 14.85
Tubing - Carbon Steel	45.00	3.82	2.88	2.44
Tubing- VIT 13 Cr	0.06	3.54	2.88	2.44
Tubung- Fiberglass	0.20	1.65	2.88	
Insulator	0.19	0.003	Thickness: 1.215	

Table 6.3: Wellbore properties (*Christi et al., under review*).

The simulation scenario was designed to assess the feasibility of retrofitting existing wells with coaxial Deep Borehole Heat Exchangers (DBHEs). Key parameters were selected to optimize performance and ensure practical implementation. Well depth was fixed, reflecting a constraint inherent in retrofit applications. Tubing dimensions were then varied to evaluate commercially available options and identify designs that maximize heat extraction for a given well configuration. Operating parameters – specifically flow rate and inlet temperature – were systematically assessed to determine the optimal combination for achieving maximum surface temperature and thermal energy output, while remaining within allowable bottom hole and total pressure limits. This approach leveraged existing literature (Alimonti et al., 2018; Brown et al., 2023; Kolo et al., 2024) and production test data from the Groß Schönebeck site (Blöcher et al., 2016). To further refine the analysis, three different tubing materials were considered. This comprehensive approach facilitates the assessment of heat extraction efficiency, considering the relationship between annulus and tubing surface areas, and heat transfer characteristics of each material. These parameters are summarized in **Table 6.4**. The primary objective of these simulations was to identify an optimal well design for coaxial DBHEs, based on numerical modeling, and to provide a sound basis of energy yield and economic evaluation for future implementation considering the energy yield and economic evaluation.

Parameter	Unit	Range of Value	Literature Review	
Depth (b.s.l)	m	3600 and 3800	Min: 305 (Feng et al., 2015)	Max: 6000 (Alimonti and Soldo, 2016)
Tubing size (OD/ID)	inch	4.50/3.96, 4.50/4.05, 3.50/2.99, 2.88/2.44, 2.38/1.99	Min: 1.57/0.78 (Templeton et al., 2015)	Max: 9.25/8.81 (le Lous et al., 2015)
Vacuum space	inch	0.45 - 1.56	Min: 0.4 (Noorollahi et al., 2015)	Max: 4 (Nalla et al., 2005)
Tubing material	-	Carbon Steel, Fiberglass, VIT 13Cr	Silwa et al. 2015	
Flow rate	m^3h^{-1}	3.60, 18.00, 36.00, 54.00	Min: 3.6 (Kohl et al., 2002)	Max: 42.84 (Noorollahi et al., 2015)
Inlet temperature	°C	10, 25, 30, 40, 50, 60, 70, 80, 90, 100	Min: 3.8 (Silwa et al., 2015)	Max: 95 (Brown et al., 2023)

Table 6.4: Wellbore design and operation condition parameters for simulation scenarios (*Christi et al., under review*).

The simulation results were used to optimize the DBHE design at the Groß Schönebeck site, considering: (1) maximum flow rate based on bottom-hole and tubing pressure; (2) bottom-hole and outlet temperature variations by tubing material; (3) 30-year bottom-hole temperature decline; and (4) thermal power output for varying operating parameters. The detail results and explanation are as follows:

(1) Maximum flow rate based on bottom-hole and tubing pressure

At a base case inlet temperature of 10°C, bottom-hole pressures at constant flow rates of 3.60, 18.00, 36.00, and 54.00 m^3h^{-1} are shown in **Figure 6.7(A)**. These pressures were calculated assuming full exposure of the 3800 m TVD perforation to the impermeable Zechstein formation, providing a constraint on the maximum allowable flow rate for the closed-loop system. **Figure 6.7(B)** illustrates the wellbore pressure in the annulus at the initial time-step for wells E GrSk 3/90 and Gt GrSk 4/05 (A2), demonstrating a constant pressure profile at all flow rates. This indicates that annulus pressure does not increase with flow rate and is an important factor in determining the optimal coaxial tubing installation depth for a given maximum tubing pressure, which is constrained by the properties of commercially available Vacuum Insulated Tubing (VIT).

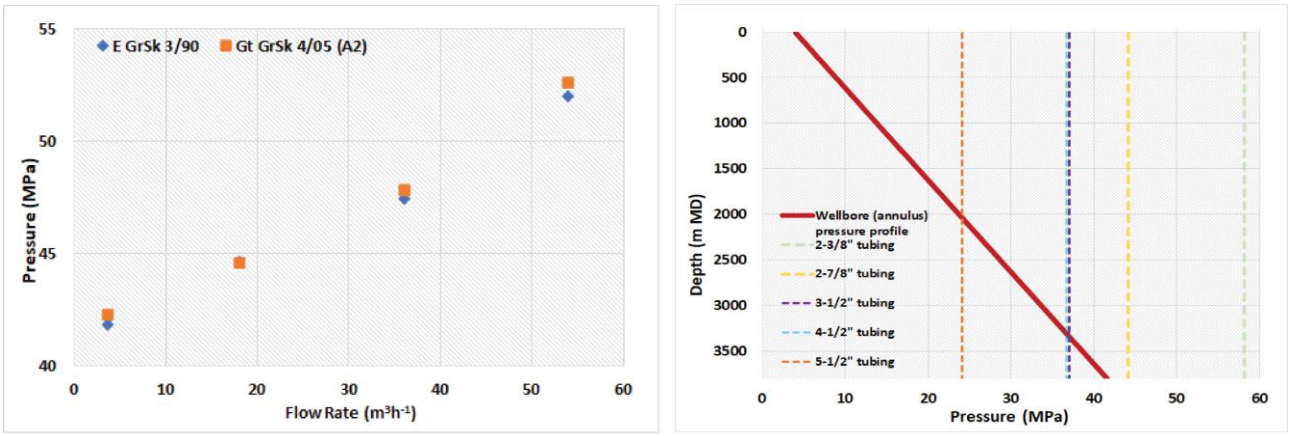

Figure 6.7: (A) Well pressure at 3800 m TVD for different flow rates. (B) Wellbore pressure profiles of wells E GrSk 3/90 and Gt GrSk 4/05; dashed lines indicate the maximum allowable tubing pressure specified by the manufacturer *(Christi et al., 2025)*.

Figure 6.8 shows the result of flow rate versus tubing pressure for different coaxial tubing sizes. The 2.88-inch/2.44-inch (OD/ID) tubing best accommodates the range of flow rates tested, though a pressure test is recommended to verify well configuration integrity as this size exceeds the 44.2 MPa pressure limit at 54.0 m^3h^{-1}. Smaller 2.38-inch/1.99-inch (OD/ID) tubing exhibits a maximum pressure of 72 MPa. Larger 3.5-inch and 4.5-inch tubing sizes are limited by their maximum pressure ratings. The 4.5-inch tubing is recommended for shallower wells, with a maximum installation depth of 2000 m MD at 36.7 MPa. The 3.5-inch tubing, offering higher pressure rating, is suitable for installation up to 3300 m MD. In practice, installation depth and tubing size selection can be efficiently determined through pressure gradient calculations.

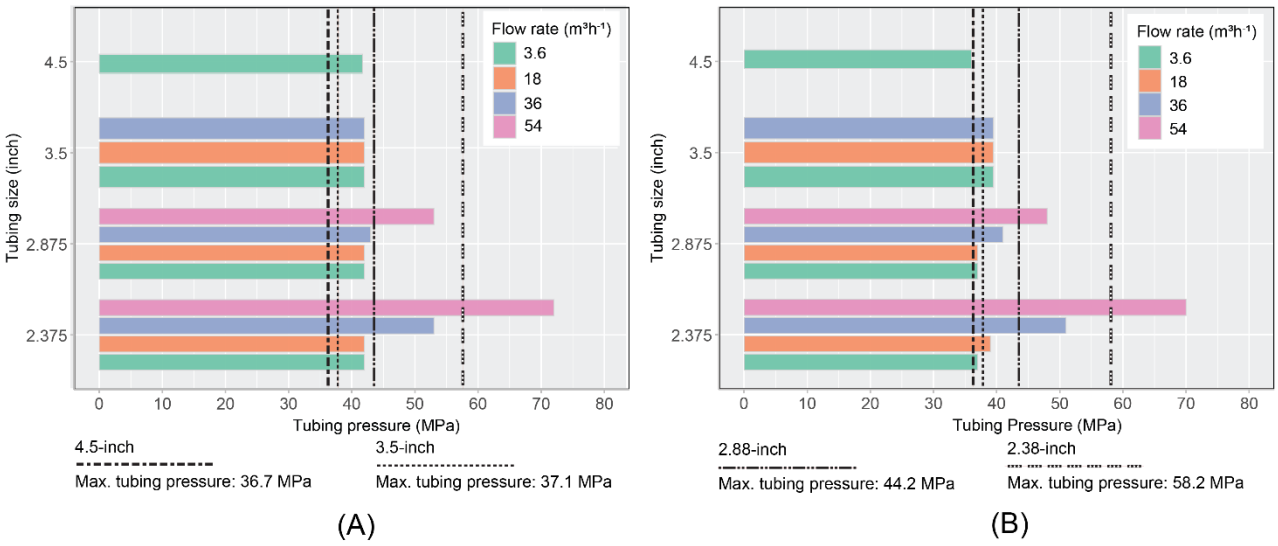

Figure 6.8: Flow rate vs. Tubing pressure for different sizes of coaxial tubing. (A) Tubing pressure at 3800 m MD; (B) Tubing pressure at 3600 m MD *(Christi et al., under review)*.

(2) Inlet and outlet temperature variations by tubing material

In accordance with the maximum allowable pressure as explained in **Figure 6.7 and Figure 6.8**, the baseline configuration of the coaxial tubing arrangement utilized tubing with a diameter of 2.88-inch for all the scenarios. Each scenario was run for a 30-year simulation period.

- ***Carbon Steel – temperature profiles***

Figure 6.9 illustrates the effect of carbon steel with the highest thermal conductivity. A flow rate of 18 m^3h^{-1} indicates significant heat extraction, achieving the maximum possible degree for this carbon steel material.

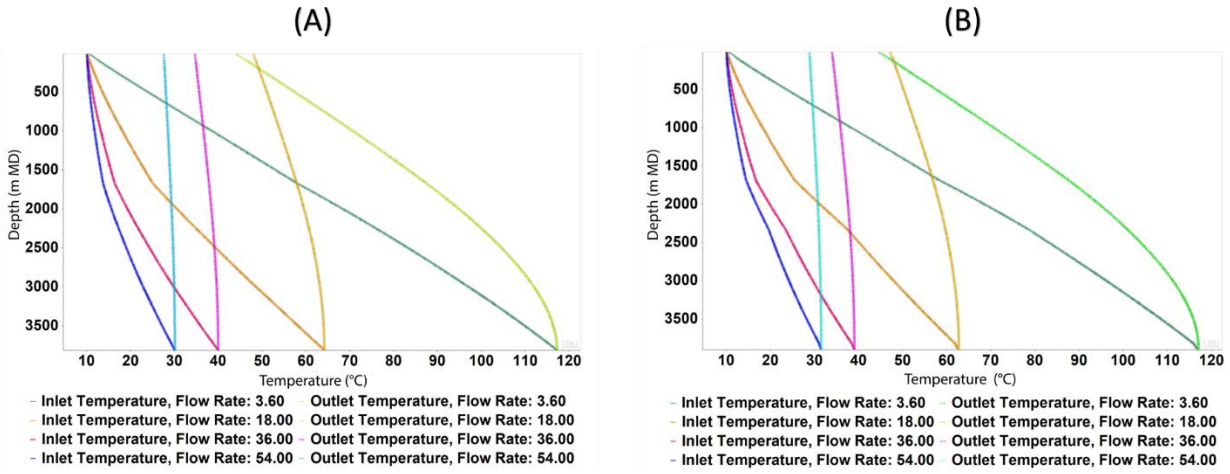

Figure 6.9: Temperature profiles using carbon steel tubing with a constant injection temperature of 10°C at different flow rates for (A) E GrSk 3/90 and (B) Gt GrSk 4/05.

- ***Fiberglass – temperature profiles***

Figure 6.10 illustrates the effect of fiberglass material, which has medium thermal conductivity falling between that of carbon steel and VIT. Fiberglass performs best at flow rates less than 18.00 m^3/h, with optimal temperature gain achieved at the low flow rate of 3.60 m^3h^{-1}.

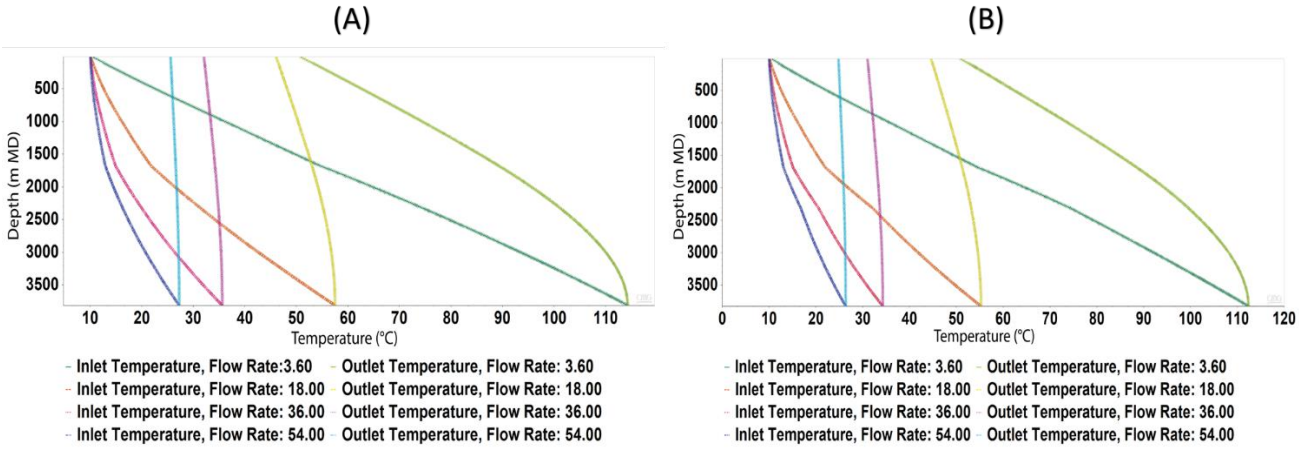

Figure 6.10: Temperature profiles using fiberglass with a constant injection temperature of 10 °C at different flow rates. (A) E GrSk 3/90; (B) Gt GrSk 4/05.

- *VIT – temperature profiles*

Figure 6.11 illustrates the effect of VIT material, which has the lowest thermal conductivity. VIT outperforms the other materials at a low flow rate of 3.60 m^3h-1. The outlet temperature can reach 79.4°C using VIT for both well E GrSk 3/90 and Gt GrSk 4/05 (A2).

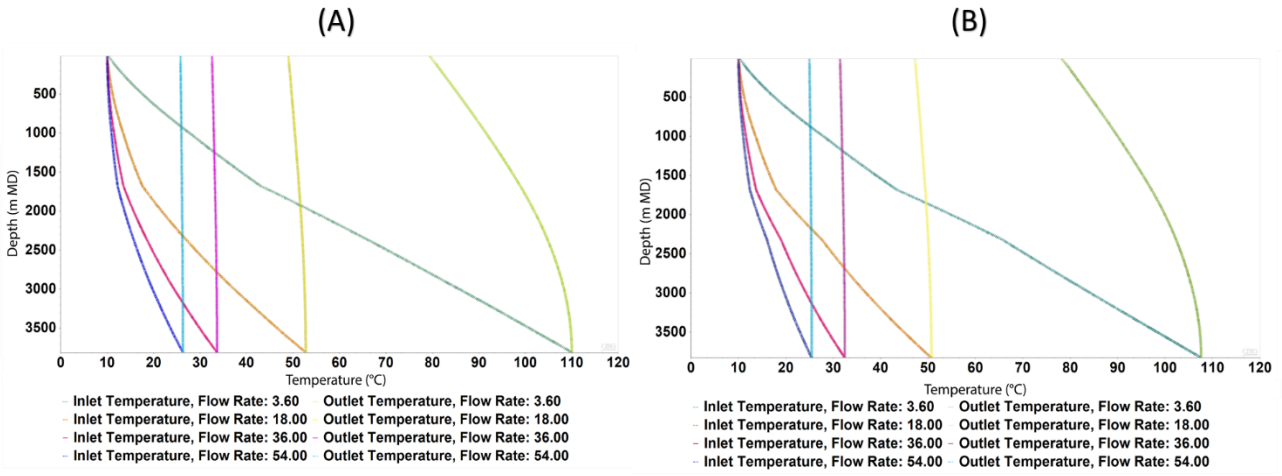

Figure 6.11: Temperature profiles with a constant injection temperature of 10 °C at different flow rates. (A) E GrSk 3/90; (B) Gt GrSk 4/05 (A2).

The impact of varying tubing material is substantial at flow rates less than 20 m^3h^{-1}. VIT demonstrates superior efficiency in maintaining elevated temperatures at low flow rates, although the temperature gain at the bottom-hole is marginally lower than that observed with carbon steel and fiberglass.

(3) 30-year bottom-hole temperature decline

As shown in **Figure 6.12**, at the end of the 30-year simulation period, bottom-hole temperature, outlet temperature, and thermal power generation are nearly equivalent at the maximum flow rate of 54.0 m^3h^{-1}. This indicates that increasing the flow rate minimizes the influence of tubing material on system performance.

The primary observed variation over the 30-year exploitation period is a reduction in bottom-hole reservoir temperature (**Figure 6.12 (-C-)**). This reduction was 36% for well E GrSk 3/90 and 35% for well Gt GrSk 4/05 (A2), with lower flow rates resulting in less pronounced temperature decline. VIT consistently exhibited the lowest percentage of thermal decline.

Bottom-hole reservoir temperature reduction is significantly influenced by completion depth and flow rate. In the context of well retrofits, the depth of the exploited reservoir is determined by well length and trajectory deviation. Notably, the initial bottom-hole temperature of Gt GrSk 4/05 (A2) was 4 °C lower than that of E GrSk 3/90. While well lengths are equivalent, Gt GrSk 4/05 (A2) exhibits greater trajectory deviation (Figure 6.14), resulting in a higher reservoir temperature at the bottom-hole for E GrSk 3/90.

(4) Thermal power output for varying operating parameters

Thermal power output was evaluated for tubing lengths of 3600 m MD (**Figure 6.13**) and 3800 m MD (**Figure 6.14**), using both carbon steel and VIT. Results indicate that both wells can generate approximately 1000 kW of thermal power at these depths, with the 3800 m MD installation yielding a slightly higher output (a 100 kW difference at maximum flow rate),

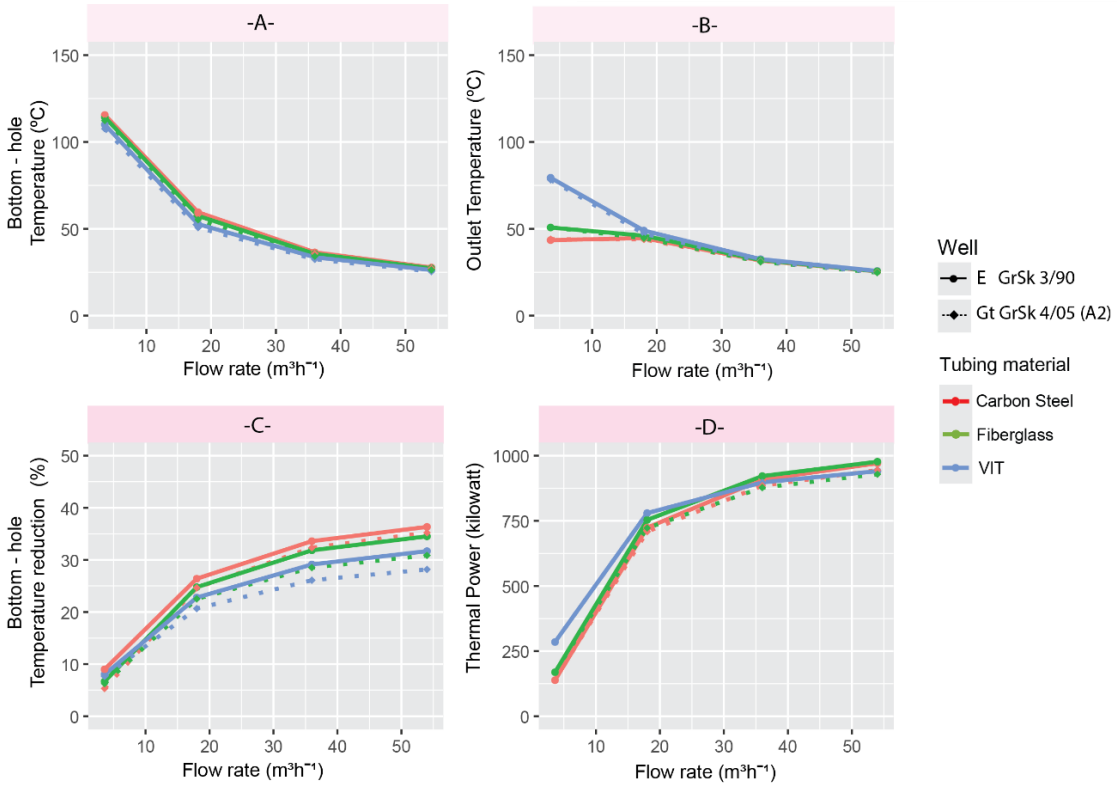

Figure 6.12: Result of base case scenario simulation after 30 years continuous production with 2.88-inch coaxial tubing size at 3800 m MD using different tubing materials. Correlation of given flow rates vs (-A-) Bottom-hole temperature; (-B-) Outlet Temperature; (-C-) Rate of temperature reduction; (-D-) Thermal Power at injection temperature of 10 °C *(Christi et al., under review)*.

Consistently high thermal power was achieved with flow rates of at least 36 m^3h^{-1} and inlet temperatures of 20 °C or less. While well E GrSk 3/90 consistently exhibits higher thermal power, it also demonstrates a greater rate of thermal decline under these conditions. Simulations conducted up to an injection temperature of 100 °C revealed that temperatures exceeding 80 °C resulted in decreased thermal power, establishing an upper operational limit of 80 °C.

This study considered two potential applications of DBHE technology: electricity generation and direct heating. Optimizing several factors – including maximum accessible depth for bottom-hole temperature gain, tubing material selection, and operating parameters, is crucial. For thermal power generation, a high flow rate (≥ 36 m^3h^{-1}) is generally recommended to maximize thermal power output. Analysis indicates that tubing material efficiency remains consistent at higher flow rates, minimizing the importance of material selection. However, achieving outlet temperatures of 60 – 70 °C is crucial for maximizing the efficiency of an Organic Rankine Cycle (ORC) system. While VIT, with a minimum injection temperature of 10 °C, is a viable option, this approach may result in a lower flow rate and reduced thermal power generation, rendering it economically unattractive. For direct heating applications, as previously studied by Koltzser et al. (2024), maintaining a minimum outlet temperature of 60 °C is essential. The optimal outlet temperature gain can be achieved by VIT with inlet temperature ranging from 10 °C - 25 °C and a low flow rate of < 12 m^3h^{-1}.

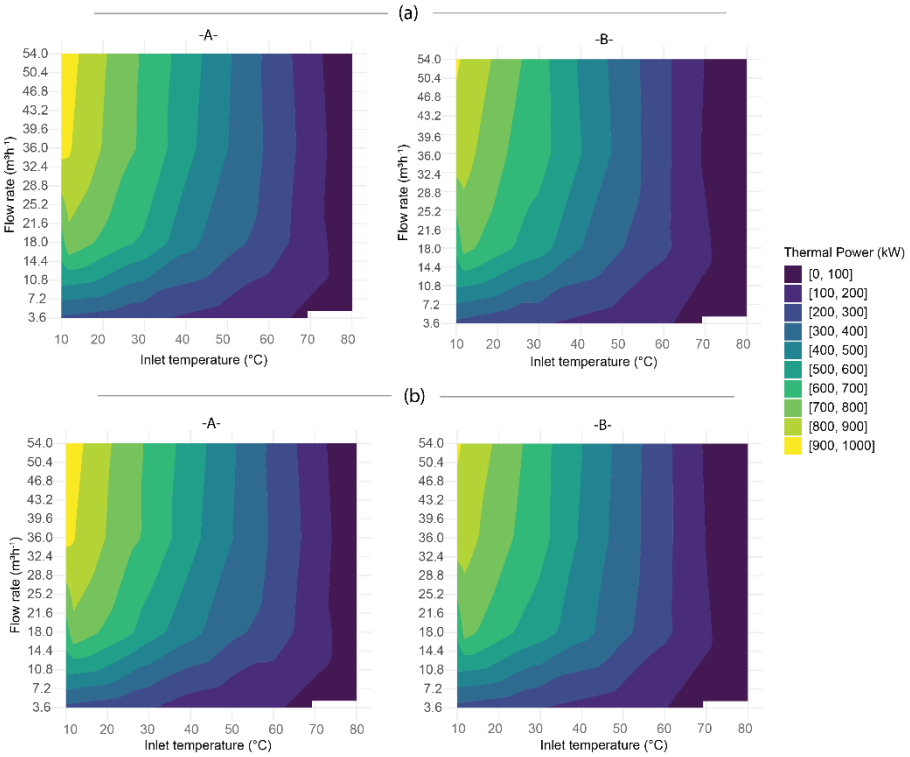

Figure 6.13: Thermal power generated at 3600 m MD for a 2.88-inch tubing size, comparing carbon steel (a) and VIT (b) materials. Wells are indicated as [-A-] E GrSk 3/90 and [-B-] Gt GrSk 4/05 (A2) *(Christi et al., under review)*.

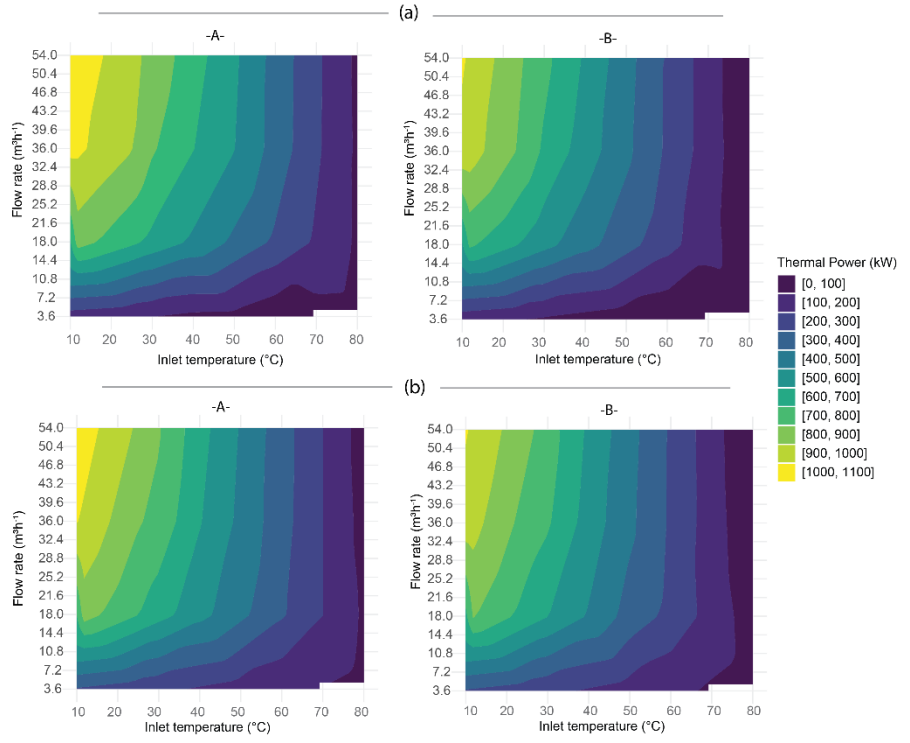

Figure 6.14: Thermal power generated at 3600 m MD for a 2.88-inch tubing size, comparing carbon steel (a) and VIT (b) materials. Wells are indicated as [-A-] E GrSk 3/90 and [-B-] Gt GrSk 4/05 (A2) *(Christi et al., under review)*.

6.3 Feasibility of reusing infrastructure in Groß Schönebeck and technical challenges for further development of the site

6.3.1 EGS technology approach

To support the reuse of the existing well configuration, this study proposes converting the production well Gt GrSk 4/05 (A2) into an injection well. This can be achieved by creating a side-track from the 13.375″ casing at 2116–2200 m MD. Tests and fluid sampling in 2021 (Regenspurg et al., 2024) confirmed accessibility to 2200 m MD, making reuse feasible. Surface space availability further reduces costs and time for land acquisition.

Regenspurg et al. (2024) also highlighted steel corrosion in the casing, underlining the need for an integrity check, particularly above the side-track depth, and the option of plugging and cementing the well from 2300 m MD downward. For completion design, carbon steel should be avoided for liners. Instead, injection tubing extended to side-track depth can isolate casing from reservoir fluids, though it increases frictional pressure losses due to smaller diameter. Compared with E GrSk 3/90, Gt GrSk 4/05 (A2) offers sufficient casing diameter to accommodate an injection string for both fracturing and injection. The planned trajectory includes ~3000 m drilling (1000 m vertical, 1000 m deviated, 1000 m horizontal) with two completions at most, requiring an 8.50″ hole and 7″ casing in the horizontal section. E GrSk 3/90 could additionally be reused as a monitoring well with geophone chains and fiber optics.

Experience from Gt GrSk 4/05 (A2) drilling highlights uncertainties: no core data were obtained, and stratigraphic interpretation relied on logs correlated to E GrSk 3/90. The interval 2381–3000 m MD proved complex, complicated by rock salt (2300–3800 m TVD), which poses risks of salt movement, column trapping, washouts, and cementation failures (Amer et al., 2016; Folsta et al., 2011). Future drilling should integrate salt imaging to anticipate and mitigate these challenges.

The EGS concept remains in the research and development stage, and its practicality requires further validation across several key elements before it can become economically feasible and commercially viable. To enhance the viability of fracture-dominated EGS, further investigation is recommended in the following areas:

- Sustainability of hydraulically induced fractures
- Stimulation methods to increase fracture half-length and delay thermal breakthrough
- Longer lateral sections to enable the creation of more fractures
- Multi-fracture development in low-permeability reservoirs
- Wellbore chemistry modeling to address scaling and clogging issues observed in matrix-dominated EGS concepts
- Well completion designs that can withstand electro-chemical reactions between reservoir fluids and casing materials, enabling access to higher temperatures in the deeper Rotliegend formation

Due to the low technology readiness level, economic assessment of an EGS project at Groß Schönebeck remains highly uncertain. The high drilling costs and the difficulty of predicting long-term performance make any reliable economic evaluation challenging. For this reason, no economic assessment has been performed in this study, to avoid drawing misleading conclusions about the feasibility of commercial EGS development at Groß Schönebeck. Nevertheless, continued technological advances, improved stimulation methods, and supportive policy frameworks may enhance the economic viability of EGS in the future, making further EGS research in this field both necessary and promising. Groß Schönebeck has the potential to continue being a key EGS research and development site.

6.3.2 DBHE technology approach

The technical feasibility of applying DBHE technology at Groß Schönebeck is being assessed, considering the following two key factors:

- **Well-specific condition**

The Groß Schönebeck site offers a significant advantage for well reuse due to its uniquely deep well and high bottom-hole temperature – exceeding those of comparable projects in Weggis, Landau, Prenzlau, and Kikunhalas. This minimizes modification costs and risk. While salt structures present challenges for open-loop geothermal, they are well-suited for closed-loop applications like DBHE.

This study analyzed two application approaches for DBHE installation and concluded that the technology is best suited for heating purposes, utilizing vacuum-insulated tubing or equivalent systems and materials with a thermal conductivity of 0.06 $Wm^{-1}K^{-1}$ or less. Low thermal conductivity is essential to minimize heat loss from bottom-hole to the well-head, requiring further laboratory and field testing to validate tubing material,effective insulation technique and formation heat transfer parameters. The established DBHE system operates optimally with inlet temperatures between 10 – 25 °C and flow rates below 26 m^3h^{-1}, consistently delivering outlet temperatures of 49 – 67 °C after 30 years of simulation. This performance yields a thermal power output of 500–750 kW.

Successful DBHE implementation requires confirming and maintaining well integrity, optimizing well design, utilizing effective insulation, and employing a high-performing working fluid like water. While earlier systems were limited by low temperatures and material lifespan, advancements in insulated tubing enable long-term, reliable operation. However, DBHE systems require a consistent heating demand to maintain productivity and cost-effectiveness; fluctuating needs may reduce their viability.

- **Subsurface uncertainty**

While DBHE systems offer greater control and reduce reliance on reservoir fluids, accurately quantifying conductive heat transfer between the formation, casing, tubing, and working fluid remains a critical challenge. Establishing optimal control parameters – specifically inlet temperature and flow rate – to maximize thermal power output and minimize pumping costs requires comprehensive field measurements and long-term testing. Validating thermal conductivity, specific heat capacity, and optimal insulation materials is essential for accurate forecasting and successful project implementation.

Resource characteristics at Groß Schönebeck – a bottom-hole temperature of 138°C – is accessible with a 7” liner, supported by data from comparable operating projects such as Weissbad (Kohl at al. (2000); Alimonti et al. (2018) and Landau (LBEG, 2021), which similarly utilizes deep borehole heat extraction. Data from these projects demonstrate bottom-hole temperatures between 45 °C -112 °C and flow rates of 9.6-22.6 m^3h^{-1}. Consequently, higher outlet temperatures and thermal power outputs are anticipated, supporting a high probability of success for DBHE demonstration.

For further evaluation of the feasibility of using the existing deep wells as DBHEs, we conducted an economic analysis. This preliminary assessment considered capital costs for system installation, ongoing operating costs, and projected revenue from thermal power for heating solution. As the soon-ready-to-implement technology is within reach, further detailed economic modeling and field testing are planned to refine these projections.

6.3.3 Hydrothermal technology approach

6.3.3.1 Overall project summary

This research project proposal intends to the economic viability of medium-depth geothermal energy extraction from salt structures in the North German Basin. The project employs a hydrothermal concept and deep drilling at Groß Schönebeck to characterize reservoir potential, develop innovative completion techniques, and address the challenges of hypersaline water intrusion. **Figure 6.15** illustrates the concept.

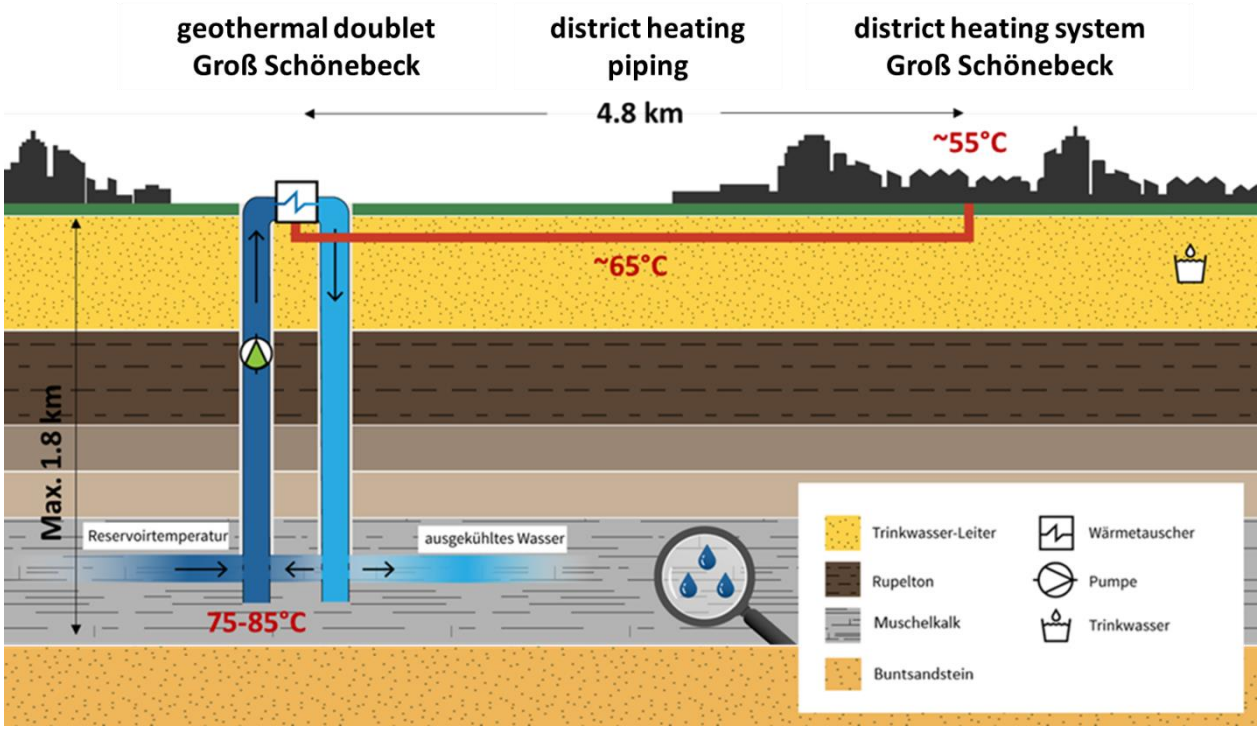

Figure 6.15: Concept of hydrothermal technology research and development at Groß Schönebeck (Picture credit: GFZ).

6.3.3.2 Specific research objectives

- **Reservoir characterization & thermal water extraction:** To explore and characterize the shell limestone and red sandstone formations adjacent to the salt dome at Groß Schönebeck, assessing their potential for sustained thermal water extraction.
- **Innovative hydrothermal doublet development:** To develop and demonstrate an innovative hydrothermal doublet system tailored for medium-depth geothermal energy utilization in salt structure environments, addressing permeability variations and potential hypersaline water contact.
- **Process design optimization for hypersaline conditions:** To determine and implement optimized process design parameters – including material selection, pressure maintenance, and heat transfer systems – to mitigate risks associated with hydraulic contact with hypersaline formation waters and ensure long-term operational stability.
- **Knowledge transfer and industry engagement:** To actively engage and coordinate with the district heating industry throughout the project lifecycle, facilitating knowledge transfer and accelerating the adoption of medium-deep geothermal energy solutions within the North German Basin.

6.3.3.3 Justification & site selection

This research leverages the advantageous location at Groß Schönebeck, capitalizing on existing infrastructure, high-quality geological subsurface data (including 3D seismic and wells GrSk3 and GrSk4), and favorable regulatory conditions. This site presents a critical opportunity to pioneer deep geothermal development in the central North German Basin, a region currently limited by data and operational experience. The unique geological complexities associated with salt structures necessitate tailored solutions, and the results of this project will contribute to the broader deployment of sustainable geothermal energy resources across the region.

6.3.3.4 Planned technical surveys to enhance project feasibility

The following technical surveys will be conducted to reduce exploration risk and improve the feasibility of the project:

- **Reprocessing of 3D Seismic Data & 2D Seismic Profiles:** The existing 3D seismic data (acquired February 20 – March 10, 2017, RissDom-A funding reference number: 0324065) will be reprocessed with a focus on the Buntsandstein and Muschelkalk formations for geothermal and hydrogeological evaluation. This will be supplemented by new 2D seismic profiles targeting these formations.
- **Vertical Seismic Profiling (VSP):** ***VSP will be conducted in the existing wells (EGrSk 3/90 and GtGrSk4/05) for seismic monitoring to further refine subsurface imaging and reduce exploration risk.***
- **Vertical Exploration Well with Core Drilling:** A vertical exploration well will be drilled to a depth of 1250m, obtaining a continuous core from the top of the Muschelkalk to the base of the Buntsandstein.
- **Geoscientific Support (Cores, Logging):** Core samples will be obtained from the overburden (Quaternary to Keuper) to characterize hydraulic and geomechanical properties, assess drilling-related issues, and examine hydraulic integrity and geochemical properties.
- **Fluid Monitoring:** Formation fluids obtained from production tests will be analyzed on-site and in the laboratory. Horizontal selective depth samples will be collected to characterize in-situ formation fluids, including dissolved and entrained gases.
- **Production Test:** A production test will be conducted in either the Buntsandstein or Muschelkalk formations, utilizing either a casing lift test with liquid nitrogen or a pump installation. The test will aim to achieve stable flow rates comparable to those expected during operational use and will generate valuable data on the geo-hydraulics of Mesozoic target horizons in salt rim areas.

7. Economic aspects of geothermal energy application at Groß Schönebeck

7.1 Cost estimation for implementing the hydrothermal concept at Groß Schönebeck

This section assesses the economic feasibility of extracting geothermal heat from the Muschelkalk and Buntsandstein formations. Due to the lack of prior exploration in these formations, the cost estimation includes all exploratory activities and associated testing required to establish technical feasibility. A detailed breakdown of these costs can be found in **Table 7.1.**

Details	Cost
Reprocessing of 3D seismic data + Quaternary/Tertiary hydrogeological assessment Interpretation of Muschelkalk/Buntsandstein	72.5 k€
2D-Seismic and VSP surveys	545 k€
Planning and approval	600 k€
Environmental aspect opinion	50 k€
Drilling: **A. Option A**: Drilling up to the red sandstone (1250 m core from the top of the Muschelkalk to the base of the red sandstone), positive production test in the red sandstone. **B. Option B**: Drilling including 1,250 m core march to the Buntsandstein, production test Buntsandstein negative, re-cementation to the 13-3/8" casing, side-track to the Muschelkalk, production test Muschelkalk.	**7231.5 k€** **9438.5 k€**
Borehole monitoring	290 k€
Geoscientific support (cores, logging)	517.5 k€
Fluid-Monitoring	145 k€
Reservoir characterization including well testing	435 k€
Feasibility study	100 k€
Production test including pumps	450 k€
Total cost **Option A** **Option B**	 **10436.5 k€** **12543.5 k€**

Table 7.1: Cost estimation for hydrothermal implementation at Groß Schönebeck. **) Personnel cost is included in each listed operation activity.

7.2 Economic assessment of DBHE application at Groß Schönebeck

Due to the unavailability of field data, a sensitivity analysis was conducted to estimate DBHE performance under a range of operational scenarios and to identify key areas for future investigation. This analysis is a critical step in translating the technical assessment of DBHE into a comprehensive economic evaluation, providing essential insights into project feasibility and informing decisions regarding implementation pathways. The findings from the Effect estimate, Sobol, and Morris analyses have consistently demonstrated that inlet temperature and flow rate are the primary drivers of thermal power. The subsequent Monte Carlo analysis refined the identification of promising parameter combinations based on their probability distributions on the percentiles basis (P10, P50, P90). The sensitivity analysis was conducted subsequently with techno-econmic analysis based on operational and economic parameters given in **Table 7.2**.

Probability	P10		P50		P90	
Well	E GrSk 3/90	Gt GrSk 4/05 (A2)	E GrSk 3/90	Gt GrSk 4/05 (A2)	E GrSk 3/90	Gt GrSk 4/05 (A2)
Inlet Temperature (℃)	21.58	21.61	17.51	17.49	13.40	13.41
Flow Rate (m^3/hour)	20.60	25.70	16.80	21.00	10.80	12.20
Outlet Temperature (℃)	65.88	68.24	52.32	58.00	45.63	52.49
Annual total Thermal Power Production (MWh_{th})	6892	6564	6327	5960	4750	4631
Surface pump power (kW)	40 kW					
Radiation effect (kW)	18 kW					
CAPEX (€)	1,200,000					
OPEX (€)/year	250,000 – 350,000					

Table 7.2: Operational and techno-economic analysis parameters (*Christi et al., 2025, under review*).

The techno economic analyses were conducted using the formula of Levelized Cost for Heating (LCOH) and Levelized Cost for Electricity developed by Beckers et al. (2022) as shown below:

$$LCOH = \frac{sum\ of\ cost\ over\ lifetime}{sum\ of\ heat\ produced} = \frac{\sum_{t=1}^{n}\frac{C_t+O_t}{(1+r)^t}}{\sum_{t=1}^{n}\frac{E_{h,t}}{(1+r)^t}} \qquad LCOE = \frac{sum\ of\ cost\ over\ lifetime}{sum\ of\ electricity\ generated} = \frac{\sum_{t=1}^{n}\frac{C_t+O_t}{(1+r)^t}}{\sum_{t=1}^{n}\frac{E_{e,t}}{(1+r)^t}}$$

In this analysis, C_t denotes the CAPEX in year t, O_t represents the operating and maintenance expenditure in year t, and n is the expected production lifetime (30 years) of the DBHE system. The discount rate is denoted by r and the heat produced in year t is indicated by E_h. The electricity generated in year t is denoted by E_e. The techno-economic analysis considers the use of a surface pump, an Organic-Rankine-

Cycle (ORC) system efficiency for electricity generation, and the expected radiation effect of insulated tubing.

The projected lifespan of the production system is a key factor in evaluating the economic potential of a geothermal project. This analysis assumes a 30-year operational period—a typical benchmark—to determine total costs and assess economic feasibility. Securing long-term power purchase agreements and attracting investment relies on a stable production estimate, which in turn provides confidence in future revenue streams. The economic evaluation utilised the probability distribution of annual average heat generation from the sensitivity analysis. The capital expenditure (CAPEX) budget covered the costs of subsurface-to-wellhead and surface pipeline facilities. It did not include customer connection costs.

Under optimistic conditions (10% Organic Rankine Cycle efficiency and outlet temperatures between 65.88 and 68.24 ℃), the Levelized Cost of Electricity (LCOE) ranges from 0.68 to 0.99 €/kWh for Well E GrSk 3/90 and from 0.71 to 1.01 €/kWh for Well Gt GrSk 4/05 (A2). Consequently, electricity production using Deep Borehole Heat Exchanger (DBHE) technology is currently uneconomical, as these costs significantly exceed typical offtake prices of 0.25–0.40 €/kWh. While theoretical efficiencies of 10% are possible with selective fluids (Ottaviano, 2021), this assessment demonstrates that DBHE-driven electricity generation remains technically feasible but economically unsustainable given the observed low temperatures and flow rates. As a for heating application, characterized by 99% heat production efficiency **Figure 7.1** presents a detailed LCOH calculation result for DBHE systems, recognizing that both production cost and revenue are directly dependent on total heat generation over time.

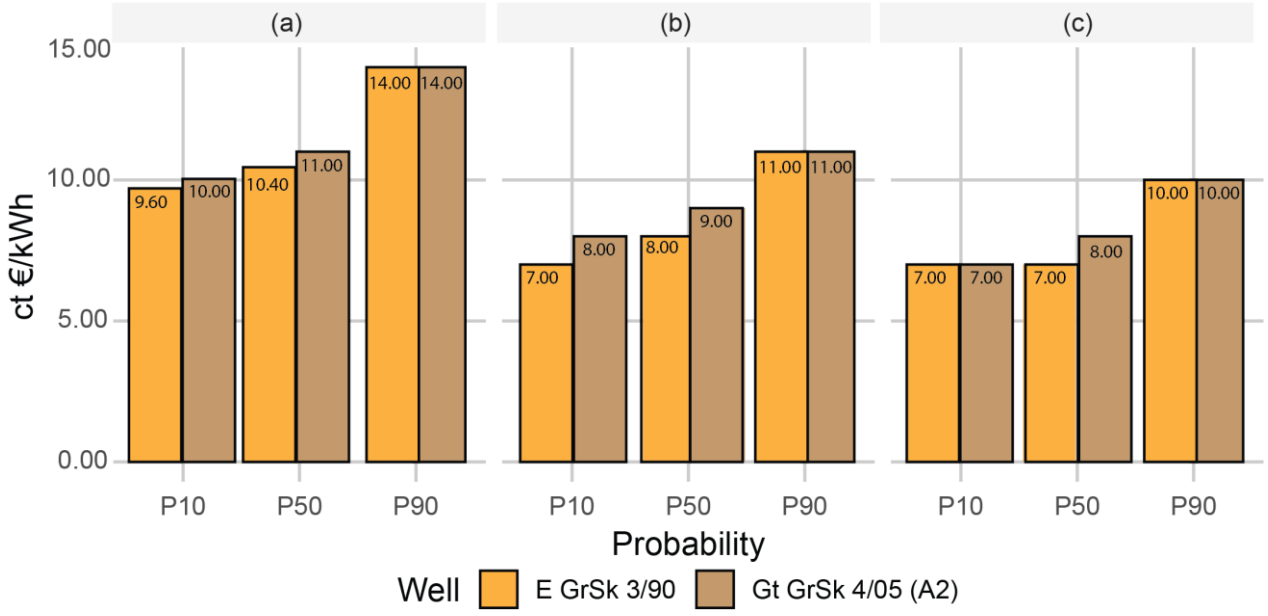

Figure 7.1: Comparison of LCOH values at probability levels of P(10), P(50), and P(90) for annual operating hour scenarios of (a) 4380 h; (b) 6570 h; (c) 8060 h (*Christi et al., under review*).

The Interest Returned Rate (IRR) is calculated by taking into account general financial modelling parameters such as the debt-equity ratio, depreciation period, loan term, loan interest and income tax, and incorporating them into a 30-year cash flow model which are described in **Table 7.3**. **Figure 7.2** presents a financial evaluation of revenue streams, expressed as the Internal Rate of Return (IRR), based on varying annual heat generation and operational hours. As shown in Table 7.3, which presents the simplified financial parameters, a positive IRR can be achieved with both the P(10) and P(50) development schemes, requiring tariffs between 15 and 20 ct €/kWh. To achieve a competitive tariff of 10 ct €/kWh, it is necessary to use

the P(10) and P(50) heat generation schemes alongside sustained, near-full-capacity operation (8060 hours). These results demonstrate the critical interplay between operational efficiency, resource utilisation and economic viability for this DBHE technology.

Parameters	
Heating Cost	12 – 25 ct €/kWh
Debt share investment	80%
Discount rate	6%
Tax (Income)	25 %
Interest (Loan)	20 %
Term (Loan)	15 years
Deprecation period	15 years

Table 7.3: Operational and techno-economic analysis parameters (*Christi et al., under review*).

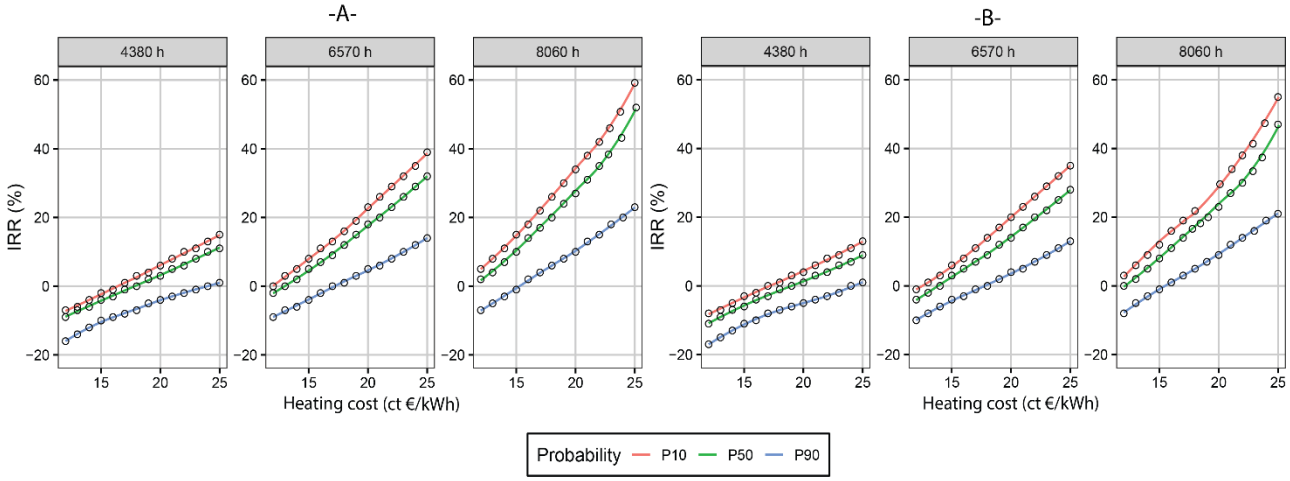

Figure 7.2: IRR versus heating cost (tariff) based on the operating hours scenario (a) 4380 h; (b) 6570 h; (c) 8060 h. [-A-] E GrSk 3/90 and [-B-] Gt GrSk 4/05 (A2) (*Christi et al., under review*).

Under optimal operating parameters and the economic assumptions of this study, the Levelized Cost of Heat (LCOH) is estimated to be between 10 and 14 ct €/kWh. This metric represents the average cost per kilowatt-hour of heat delivered over the project's lifetime, encompassing all associated costs – capital investment, operation, maintenance, and resource extraction. Importantly, this LCOH calculation considers investment costs up to the well-head only, and excludes the expenses related to heat distribution networks. While the geothermal resource possesses potential for energy production, electricity generation is not currently

economically feasible due to the combination of low fluid temperatures and limited flow rates. These factors preclude efficient power generation via conventional turbine technologies. Therefore, this analysis indicates that the geothermal resource is best suited for direct heating applications – such as district heating systems, agricultural uses like greenhouses, or industrial process heat – where the thermal energy can be utilized directly without conversion to electricity.

7.3 Geothermal energy in Groß Schönebeck: economic viability and next steps

This assessment demonstrates the significant potential of diverse geothermal resources at Groß Schönebeck, though economic viability varies by technology. While Enhanced Geothermal Systems (EGS) require further technological advancements and supportive policy frameworks to overcome high initial costs, Deep Borehole Heat Exchangers (DBHE) offer a more immediately feasible pathway for repurposing existing wells and providing cost-competitive heat if the consumer is nearby or existing heat transfer infrastructure can be used. Medium-depth hydrothermal resources present a promising avenue for expanding geothermal contributions to the regional energy mix. The successful realisation of these opportunities depends on leveraging the region's existing strengths, which include a high penetration of renewable energy, established grid infrastructure (including 10kV and 100kV lines) and a strong demand for heat, supported by existing district heating networks. Integrating geothermal resources with other renewables, such as solar, wind and biomass, in combination with energy storage solutions, will create a resilient and cost-effective energy system, providing a reliable baseload supply and reducing reliance on fossil fuels. The continued research and demonstration projects and innovative business models being undertaken in this favourable environment will facilitate a transition towards a fully sustainable and resilient energy system at Groß Schönebeck.

8. Compliance to the local Brandenburg mining regulation

The Groß Schönebeck boreholes have been used for research purposes so far. The original gas well E GrSk 3/90 (4240 m) was deepened to 4309 m and converted into a geothermal well (injection well) (2001). A second well was drilled (Production well Gt GrSk 4/05). The doublet reaches the Rotliegend formation. After a considerable drop in production, the doublet has been abandoned.

8.1 Reusing the Groß Schönebeck wells

The E GrSk 3/90 and Gt GrSk 4/05 wells are located within the exploration field Groß Schönebeck/Eichhorst (Permit for exploration for commercial purposes) (**Table 2.2**). In **Figure 8.1** the steps of creating a new geothermal project is depicted in a simplified manner – the current status of the Groß Schönebeck wells is marked with a green circle.

8.2 Scenarios for reuse of existing infrastructure at the Groß Schönebeck geothermal research site

8.2.1 Scenario 1: EGS

- The injection well E GrSk 3/90 would be used as a monitoring well;
- The production well Gt GrSk 4/05 (A2) would be used as an injection well (cementing, deviation drilling into the Rotliegend formation and then horizontal)

- Drilling a new production well (into the Rotliegend formation)

To realize the project, an application for a mining license at the mining authority has to be undertaken, also the operational plans have to be approved by the mining authority.

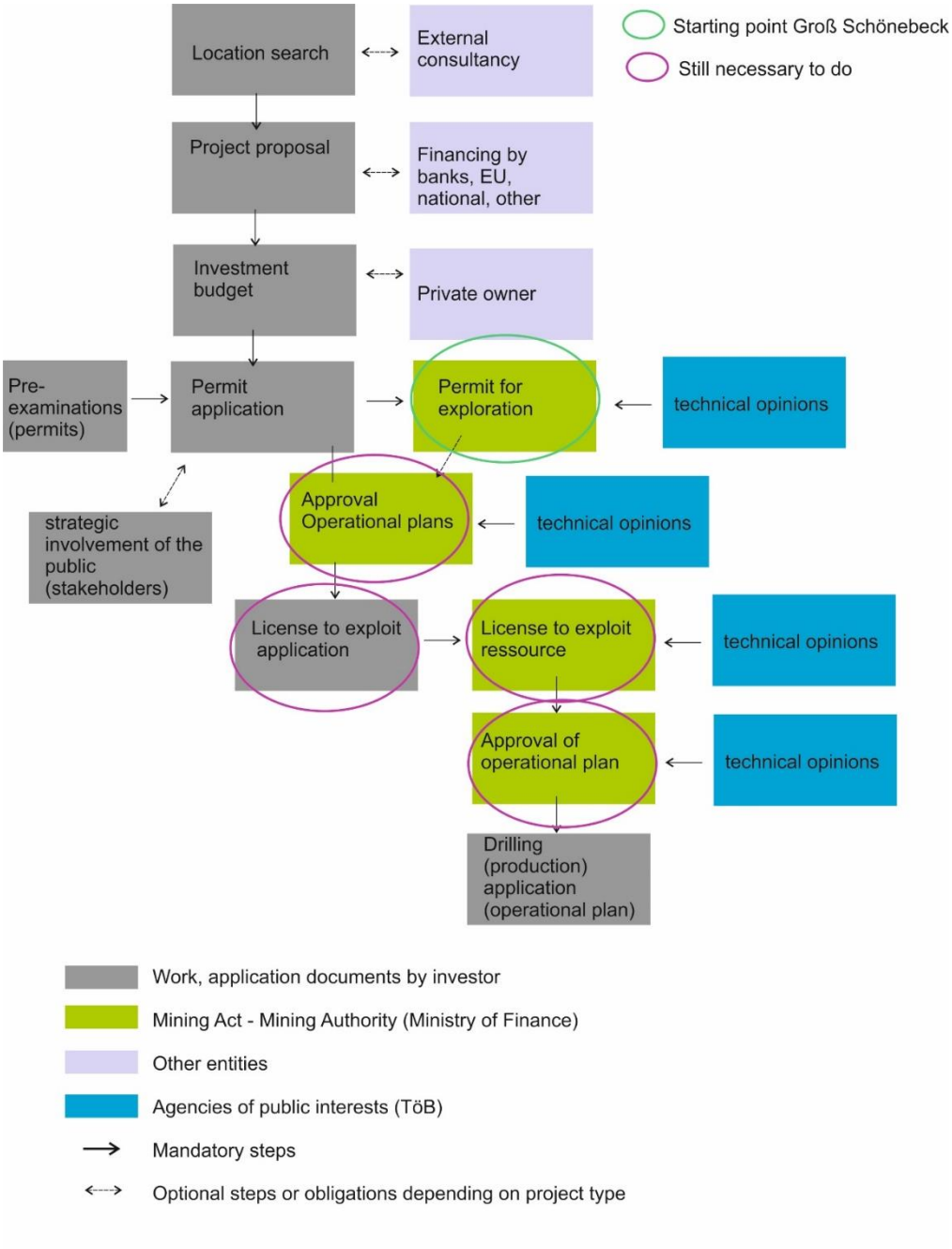

Figure 8.1: Workflow of permitting application modified for the Groß Schönebeck site.

8.2.2 Scenario 2: DBHE

- Injection well E GrSk 3/90 would be cemented until 3900 or 3800 and then tubing would be installed
- Production well Gt GrSk 4/05 (A2)) would be cemented until 3900 or 3800 and then tubing would be installed

8.2.3 Scenario 3: Hydrothermal Concept

- The injection well E GrSk 3/90 and Gt GrSk 4/05 (A2) would be used as monitoring wells
- Drilling new well following the Option A and Option B as explained previously above

8.2.4 Common procedures for the three scenarios

(1) The licensed area has so far been used for research purposes; it could be considered to apply for a new license area or to continue with the existing one (since a permit for the exploration of mineral resources for commercial purposes already exists)

(2) In any case a new working plan has to be created and presented to the mining authority

(3) If it can be proven that the resource (in this case "geothermal energy and brine") can be technically extracted, an application for a production license can be undertaken

(4) Operational plans must also be submitted that cover all work on the existing wells.

(5) Operational plans for the well to be drilled (new)

The application of the issuance of the permit is provided as an appendix file to this feasibility report.

9. Appendix

LAND BRANDENBURG

Brandenburg State Office for Mining, Geology and Raw Materials

LBGR Landesamt für Bergbau, Geologie und Rohstoffe Brandenburg

Information sheet**

on the application for a permit to explore for mineral resources for commercial purposes pursuant to § 7 BBergG (section 7 of the Federal Mining Act)

The cited sections/subsections refer to the relevant provisions of the Federal Mining Act (BBergG) of August 13, 1980 (BGBl. I S. 1310), as amended.
The Brandenburg State Office for Mining, Geology and Raw Materials (LBGR) requires the following information and documents to process a permit application:

1. Application

❑ A written application must be submitted in compliance with the present structure. The application must be personally signed by the applicant or, in the case of legal entities, by the authorized representative(s). Official documents attached to the application must generally be submitted as originals or as certified copies.

The LBGR will decide on the number of additional application copies to be submitted depending on the extent of the public interest participation process. The number must be agreed upon with the LBGR.

2. Personal information of the applicant

Legal entities or commercial partnerships respectively

- ❑ Company name and registered office
- ❑ Representation of the company
- ❑ Current trade register excerpt
  (not older than three months; only for the first copy of the application)
- ❑ Shareholder agreement *(for companies in the process of being founded)*
- ❑ Presentation of the management
  (persons authorized to represent)

Natural entities

- ❑ Last name, first name; permanent residence
- ❑ Date of birth
- ❑ Profession
- ❑ Business registration *(only for the first copy of the application)*

3. Designation of the mineral resources

❑ Detailed designation of the mineral resources to be explored (§ 11 Nr. 1 i.V.m. § 3 Abs. 3 BBergG; section 11 in conjunction with section 3, subsection 3 of the Federal Mining Act).

4. Map

❑ The representation and design of the map must be in accordance with the Mining Ordinance on Surveying and Safety Documents (UnterlagenBergV) of November 11, 1982 (Federal Law Gazette I, p. 1553). Depending on the size of the field, the map should be prepared on the basis of a current official topographic map of the state of Brandenburg at a scale of 1: 25,000, 1: 50,000, or 1: 100,000; if legibility and clarity require it, a scale of 1: 10,000 may also be used. The field must be delimited by straight-line connected corner points in accordance with

Information sheet on an application for a permit to explore mineral resources

Section 4, subsection 7. The field corner points must be specified in the Gauss-Krüger-Bessel coordinate system (RD 83 position system). Elevations must be specified in the DHHN2016 height reference system.

Map content

Titel

- ❑ Type and name of the authorization
- ❑ Designation of the mineral resources to which the application relates
- ❑ Location of the field (*district, municipality)*
- ❑ The field corner points are to be listed in a table
- ❑ Indication of the area of the field *(the area should be calculated based on the coordinates of the corner points, taking into account the projection distortion, and rounded down to the nearest hundred square meters).*
- ❑ Scale
- ❑ Elaboration note (place, date, and original signature of the person who created the map; name of the creator in block letters, possibly with the addition "Mine Surveyor" or "Publicly Appointed Surveying Engineer").

Representation of the field

- ❑ Entry of the field corner points on the map with continuous numbering in a clockwise direction; straight-line connection of the corner points.
- ❑ Within the field boundary, the designation of the field corner points of the authorization (field name) and the mineral resources to which the application relates, must be entered.
- ❑ All entries should be made in black. The field boundaries are to be marked in red (carmine) on the inside.
- ❑ The numbers of the field corner points, the designation of the mining permit, and the mineral resources are to be underlined in red (carmine).

The attached annex is part of this information sheet and shows a sample map for the graphical representation of the field.

5. Obligations of the applicant

- ❑ The applicant must commit to the LBGR to promptly disclose the results of the exploration upon its completion, no later than when the permit expires, upon request (see § 11 No. 4).
- ❑ If a permit for scientific purposes or a permit for large-scale exploration is applied for, the applicant must commit to the competent authority to participate in the exploration within the requested field, upon request, as a holder of mining rights in accordance with § 11 No. 5.

6. Work program

The submitted work program constitutes a significant criterion for the decision on granting the permit, particularly in regard to the priority regulation according to § 14 subsection 2.

- ❑ **Presentation of the exploration activities**

  The principle of reservoir protection must be ensured in order to prevent an excessive field size. Therefore, the work program (§ 11 No. 3) must take the planned field size into account and should include a sensible and systematic exploration across the entire requested field. It must be demonstrated that the planned exploration activities regarding:
  - The type, scope, and purpose of the exploration of the suspected deposit are sufficient and will be carried out within a reasonable period.
  - The necessary work for a proper investigation of the suspected deposit must be sufficiently described in terms of scope and the appropriate exploration methods, including details of the suspected content, depth, and the characteristics/quality of the deposit, as well as the technical feasibility of extracting the suspected mineral resources. If already known, the planned drill hole locations should be shown on an additional overview map, indicating their positions and depths.

  If the applicant has conducted exploration activities in the requested area at an earlier time or if third-party activities are available to them, these activities should be referenced in the application.

- ❑ **Time frame of exploration activities**
  Depending on the expected timeline of the exploration activities, the period for which the permit is requested (duration) must be specified. According to § 16 subsection 5, a period of no more than 5 years may be granted. However, the duration can be extended if necessary for proper exploration.
- ❑ **Technical capability**
  - Declaration indicating which equipment and technical gear the applicant will have for carrying out the project, along with a description of the measures the applicant will take to ensure proper exploration within the permit area.
  - Declaration indicating that a competent company has been commissioned for the exploration or a description of the applicant's mining activities over the past five years.

7. Financial capacity

- ❑ **Information about the expected costs**
  - for proper exploration and evaluation of the survey results,
  - for the rehabilitation of the surface,
  - for operational facilities and equipment that are primarily used for or intended for activities specified in § 2 subsection 1 number 1 or 2, as well as for other financially necessary activities related to these.

- ❑ **Prima facie evidence**
  Considering the estimated costs for the planned project, it must be **credible** that the necessary funds for proper exploration and related activities (according to § 2 subsection 1) can be raised. This can be demonstrated by providing information on the extent to which the expenses are financed through own funds, loans, or grants from public authorities, along with a declaration that the funds are also available for the rehabilitation of the surface.
  In accordance with the estimated exploration costs, **bank statements, credit commitments, balance sheets**, and other documents (§ 11 No. 7) must be submitted in original or as certified copies of the original (only for the first copy of the application)."

The LBGR reserves the right to request additional information and documents regarding the permit application at any time.

For further information about the information sheet, you can contact:
Herr Kaminski *(Tel.: 0355/48640-334, E-Mail: Klaus.Kaminski@lbgr.brandenburg.de)* oder
Herr Fiedler *(Tel.: 0355/48640-359, E-Mail: Peter.Fiedler@lbgr.brandenburg.de)*

Last modified: 24th of June 2025

*** Please note that the legal references mentioned in this document are based on the original German texts and are provided for informational purposes only. The official and binding versions are the original German statutes and regulations."*
The official language of LBGR is German and all applications must be submitted in this language.

REFERENCES

Agemar, T., Alten, J., Ganz, B., Kuder, J., Kühne, K., Schumacher, S., & Schulz, R. (2014). The geothermal information system of Germany. *GeotIS-ZDGG*, *165*, 129-144.

Alimonti, C., & Soldo, E. (2016). Study of geothermal power generation from a very deep oil well with a wellbore heat exchanger. *Renewable energy*, *86*, 292-301.

Alimonti, C., Soldo, E., Bocchetti, D., & Berardi, D. (2018). The wellbore heat exchangers: A technical review. *Renewable Energy*, *123*, 353-381.

Amer, A., Dearing, H., Jones, R., & Sergiacomo, M. (2016, September). Drilling through salt formations: A drilling fluids review. In *SPE Deepwater Drilling and Completions Conference* (p. D021S011R003). SPE.

Balling, P., Maystrenko, Y., & Scheck-Wenderoth, M. (2013). The deep thermal field of the Glueckstadt Graben. *Environmental Earth Sciences*, *70*, 3505-3522.

Beckers, K. F., Rangel-Jurado, N., Chandrasekar, H., Hawkins, A. J., Fulton, P. M., & Tester, J. W. (2022). Techno-economic performance of closed-loop geothermal systems for heat production and electricity generation. *Geothermics*, *100*, 102318.

Beutler G, Franz M. Keuper. In: Stackebrandt W., Franke D., editors. (2015). Geologie von Brandenburg. Stuttgart: Schweitzerbart. p. 194–216.

Beutler, G., Hauschke, N., Nitsch, E., and Vath, U. editors. (2005). Stratigraphie von Deutschland IV - Keuper, in Deutsche Stratigraphische Kommission, Courier Forschungsinstitut Senckenberg, 253: Frankfurt/M, p. 296.

Blöcher, G., Cacace, M., Jacquey, A. B., Zang, A., Heidbach, O., Hofmann, H., Kluge, C., Zimmermann, G. (2018). Evaluating Micro-Seismic Events Triggered by Reservoir Operations at the Geothermal Site of Groß Schönebeck (Germany). *Rock Mechanics and Rock Engineering*.

Blöcher, G., Reinsch, T., Henninges, J., Milsch, H., Regenspurg, S., Kummerow, J., Francke, H., Kranz, S., Saadat, A., Zimmermann, G., Huenges, E. (2016). Hydraulic history and current state of the deep geothermal reservoir Groß Schönebeck. - *Geothermic*s, 63, pp. 27-43.

Blöcher, M. G., Zimmermann, G., Moeck, I., Brandt, W., Hassanzadegan, A., & Magri, F. (2010). 3D numerical modeling of hydrothermal processes during the lifetime of a deep geothermal reservoir. *Geofluids*, *10*(3), 406-421.

Brown, C. S., Kolo, I., Falcone, G., & Banks, D. (2023). Repurposing a deep geothermal exploration well for borehole thermal energy storage: Implications from statistical modelling and sensitivity analysis. *Applied Thermal Engineering*, *220*, 119701.

Christi, L. F., Hofmann, H., Sass, I., Zimmermann, G., Norden, B., Blöcher, G. (2024). Lessons learned from reusing an abandoned hydrocarbon well as Enhanced Geothermal System (EGS): Fracture-dominated EGS development concept for Groß Schönebeck - Tagungsband, *Der Geothermiekongress 2024* (Potsdam, Germany 2024).

Christi, L. F., Sass, I., Norden, B., Blöcher, G., Zimmermann, G., & Hofmann, H. (2025). Repurposing of hydrocarbon wells for Enhanced Geothermal System (EGS) development. *Geothermics*, *128*, 103268.

Christi, L.F., Singh, M., Frick, M., Hofmann, H., Norden, B., Sass, I. (2025). Numerical simulation of a single-well closed-loop deep borehole heat exchanger (DBHX) at the Groß Schönebeck site. In *Proceedings European Geothermal Congress*, 6-10 October 2025, Zurich, Switzerland.

Christi, L.F., Singh, M., Sass, I., Norden, B., Zimmermann, G., Frick, M., Hölzel, M., Hofmann, H. (under review). Design optimization of Deep Borehole Heat Exchangers (DBHE) for well retrofitting. Submitted to *Geothermics*.

Coates, G.R., Peveraro, R.C.A, Hardwick, A., Roberts, D. (1991). The magnetic resonance imaging log characterized by comparison with petrophysical properties and laboratory core data. *SPE Annual Tech Conf Exhib*. https://doi.org/10.2118/ 22723-MS.

Dadi, S., Titov, A., Norbeck, J., Voller, K., Woitt, M., Fercho, S. F., McConville, E., Lang, C., Agrawa, S., Gradl, C., Latimer, T. (2023). Utah FORGE: Reports on Northwestern Nevada Well Doublet Drilling and Testing by Fervo Energy (No. 1530). USDOE Geothermal Data Repository (United States); Fervo Energy.

DEKORP-BASIN Research Group. (1999). The deep crustal structure of the Northeast German basin: new DEKORP-BASIN'96 deep profiling results. Geology.

Europäische ARGE Landentwicklung und Dorferneuerung. (2018). Accessed [December 2024], https://www.landentwicklung.org/aktivitaeten/events/beurteilungen-europaeischer-dorferneuerungspreis-2018/.

European Environment Agency, *CORINE Land Cover*. (2018). Accessed [December 2024], https://land.copernicus.eu/pan-european/corine-land-cover.

Feldrappe, H., Obst, K., & Wolfgramm, M. (2007, May). Evaluation of sandstone aquifers of the North German Basin: a contribution to the „Geothermal Information System of Germany ". In *Proceedings European Geothermal Congress*, Unterhaching, Germany.

Feng, Y., Tyagi, M., & White, C. D. (2015). A downhole heat exchanger for horizontal wells in low-enthalpy geopressured geothermal brine reservoirs. *Geothermics*, *53*, 368-378.

Folsta, M. G., Martins, A. L., Lomba, R. F., Cardoso Jr, W. F., Simão, C. A., Sidi, I. A., & Dannenhauer, C. E. (2011, March). Predicting salt leaching during drilling and cementing operations. In *SPE/IADC Drilling Conference and Exhibition* (pp. SPE-140242).

Frick, M., Kranz, S., Norden, B., Bruhn, D., & Fuchs, S. (2022). Geothermal resources and ATES potential of Mesozoic reservoirs in the North German Basin. *Energies*, *15*(6), 1980.

Fromme, K., Michalzik, D., & Wirth, W. (2010). Das geothermische Potenzial von Salzstrukturen in Norddeutschland. *ZDGG*, *161*(3), 323-333.

Giese, L., Seibt, A., Wiersberg, T., Zimmer, M., Erzinger, J., Niedermann, S., Pekdeger, A. (2002). Zur geochemie der formationsfluide der bohrung E Groß Schönebeck 3/90. Scientific Technical Report STR02/14, 145-170.

Grunau, H. R. (1981). Worldwide review of seals for major accumulations of natural gas. AAPG Bulletin, 65(5), 933-933.

Hofmann, H., Hölzel, M., Hoyer, S., Werkl, P., Brives, J., Christi, L.F., Liu, Y., Blöcher, G., Petrova, E., Kurevija, T., Perković, L., Macenić, M., Sedlar, D.K., Prkič, I.S.M., Sieron, K., Fedor, F., Castro, C.C., Szanyi, J., Kovács, J., Svetina, M. (2025). Engineering workflows for retrofitting abandoned wells. Technical Report. Interreg-Central Europe. URL: https://www.interreg-central.eu/wp-content/uploads/2025/02/TRANSGEO-D1.1.6-Engineering-Workflows-FINAL-December 2024.pdf.

Hoth, K., Ruspült, J., Zagora. K., Beer, H., Hartmann, O. (1993). Die tiefen Bohrungen im Zentralabschnitt der Mitteleuropäischen Senke - Dokumentation für den Zeitabschnitt 1962–1990, vol. 2. Berlin: Schriftenr geol Wiss. p. 145.

Huenges E, Winter H. (2004). Experimente zur Produktivitätssteigerung in der Geothermie-Forschungsbohrung Groß Schönebeck 3/90, Scientific Technical Report, in German.

Huenges et al. (2002): In-situ Geothermielabor Groß Schönebeck 2000/2001. Scientific Technical Report. ISSN 1610-0956.

Huenges, E., Moeck, I., Saadat, A., Brandt, W., Schulz, A., Holl, H., Bruhn, D., Zimmermann, G., Blöcher, G., Wohlgemuth, L. (2007): Directional drilling and stimulation of a deep sedimentary geothermal reservoir. - Scientific drilling: reports on deep earth sampling and monitoring, 5, pp. 47-49.

IEA, 2022. Temperature in Germany, 2000-2020 URL: https://www.iea.org/data-and-statistics/charts/747temperature-in-germany-2000-2020-2. accessed: 2024-08-16.748.

Jensen, P. K. (1983). Calculations on the thermal conditions around a salt diapir. *Geophysical Prospecting*, *31*(3), 481-489.

Jin, Z. J., Long, S. X., Zhou, Y., Wo, Y. J., Xiao, K. H., Yang, Z. Q., & Yin, J. Y. (2006). A study on the distribution of saline-deposit in southern China. *Oil & Gas Geology*, *27*(5), 571-583.

Kaiser, B. O., Cacace, M., Scheck-Wenderoth, M., & Lewerenz, B. (2011). Characterization of main heat transport processes in the Northeast German Basin: Constraints from 3-D numerical models. *Geochemistry, Geophysics, Geosystems*, *12*(7).

Kohl, T., Brenni, R., & Eugster, W. (2002). System performance of a deep borehole heat exchanger. *Geothermics*, *31*(6), 687-708.

Kohl, T., Salton, M., & Rybach, L. (2000, May). Data analysis of the deep borehole heat exchanger plant Weissbad (Switzerland). In *Proceedings World Geothermal Congress* (pp. 3459-3464).

Kolo, I., Brown, C. S., Nibbs, W., Cai, W., Falcone, G., Nagel, T., & Chen, C. (2024). A comprehensive review of deep borehole heat exchangers (DBHEs): subsurface modelling studies and applications. *Geothermal Energy*, *12*(1), 19.

Koltzer, N., Schoenherr, J., Sporleder, M., Niederau, J., & Wellmann, F. (2024). Repurposing idle wells in the North German Basin as deep borehole heat exchangers. *Geothermal Energy*, *12*(1), 35.

Krawczyk CM, Stiller M, Bauer K, Norden B, Henninges J, Ivanova A, Huenges E. 3-D seismic exploration across the deep geothermal research platform Groß Schönebeck north of Berlin/Germany. *Geotherm Energy*. 2019. https://doi.org/10.1186/s40517-019-0131-x.

LBEG. (2021). Geothermische Nachnutzung von Bohrungen Technical Report. Landesamt für Bergbau Energie und Geologie Niedersachsen (LBEG). Hannover, Germany.

LBGR. (2025). Accessed [November, 2024], https://gst.brandenburg.de.

Le Lous, M., Larroque, F., Dupuy, A., & Moignard, A. (2015). Thermal performance of a deep borehole heat exchanger: Insights from a synthetic coupled heat and flow model. *Geothermics*, *57*, 157-172.

Legarth, B. A., Tischner, T., Huenges, E. (2003): Stimulation experiments in sedimentary, low-enthalpy reservoirs for geothermal power generation, Germany. *Geothermics*, 32, 4, pp. 487-495.

Lehmann, H.-W. (1974a). Geochemie der Tiefenwiisser der Nordostdeutschen Senke, Teil 1. Zeitschrift für angewandte Geologic 20, 502-509.

Lehmann, H.-W. (1974b). Geochemie der Tiefenwiisser der Nordostdeutschen Senke, Teil 2. Zeitschrift für angewandte Geologic 20, 551-557.

Liu, W., Zhao, H., Liu, Q., Zhou, B., Zhang, D., Wang, J., Lu, L., Luo, H., Meng, Q., Wu, X. (2017). Significance of gypsum-salt rock series for marine hydrocarbon accumulation. *Petroleum Research*, 2(3), 222-232.

Moeck, I., Schandelmeier, H., Holl, H. (2009). The stress regime in a Rotliegend reservoir of the North-east German Basin. *International Journal of Earth Sciences*, 98, 7, pp. 1643-1654.

Nalla, G., Shook, G. M., Mines, G. L., & Bloomfield, K. K. (2005). Parametric sensitivity study of operating and design variables in wellbore heat exchangers. *Geothermics*, *34*(3), 330-346.

Noack, V., Cherubini, Y., Scheck-Wenderoth, M., Lewerenz, B., Höding, T., Simon, A., & Moeck, I. (2010). Assessment of the present-day thermal field (NE German Basin)—inferences from 3D modelling. *Geochemistry*, *70*, 47-62.

Noorollahi, Y., Pourarshad, M., Jalilinasrabady, S., & Yousefi, H. (2015). Numerical simulation of power production from abandoned oil wells in Ahwaz oil field in southern Iran. *Geothermics*, *55*, 16-23.

Norbeck, J., Latimer, T., Gradl, C., Agarwal, S., Dadi, S., Eddy, E., Fercho, S., Lang, C., McConville, E., Titov, A., Voller, K., Woitt, M. (2023, February). A review of drilling, completion, and stimulation of a horizontal geothermal well system in North-Central Nevada. In *Proceedings of the 48th Workshop on Geothermal Reservoir Engineering* (pp. 6-8). Stanford University California, USA.

Norden, B., Bauer, K., & Krawczyk, C. M. (2022). From pilot site knowledge via integrated reservoir characterization to utilization perspectives of a deep geothermal reservoir: 3D geological model at the research platform Groß Schönebeck in the Northeast German Basin.

Norden, B., Bauer, K., & Krawczyk, C. M. (2022). From pilot site knowledge via integrated reservoir characterization to utilization perspectives of a deep geothermal reservoir: 3D geological model at the research platform Groß Schönebeck in the Northeast German Basin.

Open Infrastructure Map. NLnet Labs, [November 2024]. https://openinfrastructuremap.org/.

Ottaviano, S. (2021). Test bench development, experimental analysis and modelling of micro-organic Rankine cycle for low-grade heat recovery.

Ramires, M. L., Nieto de Castro, C. A., Nagasaka, Y., Nagashima, A., Assael, M. J., & Wakeham, W. A. (1995). Standard reference data for the thermal conductivity of water. *Journal of Physical and Chemical Reference Data*, *24*(3), 1377-1382.

Regenspurg, S., Blöcher, G., Bregnard, D., Hehn, V., Huenges, E., Junier, P., Kieling, K., Kluge, C., Kranz, S., Leins, A., Vieth-Hillebrand, A., Wiersberg, T., Zimmer, M. (2024). Geochemical and microbial processes in a deep geothermal well during seven years of production stop and their potential impact on the well performance. *Geothermics*, *120*, 102979.

Regenspurg, S., Feldbusch, E., Byrne, J., Deon, F., Driba, D. L., Henninges, J., Kappler, A., Naumann, R., Reinsch, T., Schubert, C. (2015). Mineral precipitation during production of geothermal fluid from a Permian Rotliegend reservoir. *Geothermics*, 54, pp. 122-135.

Regenspurg, S., Feldbusch, E., Norden, B., Tichomirowa, M. (2016). Fluid-rock interactions in a geothermal Rotliegend/Permo-Carboniferous reservoir (North German Basin). *Applied Geochemistry*, 69, pp. 12-27.

Reinsch, T., Blöcher, G., Kranz, S. (2015). Data from The Groß Schönebeck Research Platform 2011-06-01 - 2013-12-31 (Datasets)., GFZ Data Services: Potsdam.

Reinsch, T., Blöcher, G., Kranz, S. (2015). Data from the Groß Schönebeck Research Platform 2011-06-01 - 2013-12-31 (Report), (Scientific Technical Report - Data; 15), Deutsches GeoForschungsZentrum GFZ: Potsdam, 71 p.

Schmelzer, J. W., Zanotto, E. D., & Fokin, V. M. (2005). Pressure dependence of viscosity. *The Journal of chemical physics*, *122*(7).

Sippel, J., Fuchs, S., Cacace, M., Braatz, A., Kastner, O., Huenges, E., & Scheck-Wenderoth, M. (2013). Deep 3D thermal modelling for the city of Berlin (Germany). *Environmental Earth Sciences*, *70*, 3545-3566.

Sliwa, T., Gonet, A., Sapinska-Sliwa, A., Knez, D., & Jezuit, Z. (2015, April). Applicability of Borehole R-1 as BHE for Heating of a Gas Well. In *Proceedings World Geothermal Congress* (Vol. 2015).

Templeton, J. D., Ghoreishi-Madiseh, S. A., Hassani, F., & Al-Khawaja, M. J. (2014). Abandoned petroleum wells as sustainable sources of geothermal energy. *Energy*, *70*, 366-373.

Trautwein, U., Huenges, E. (2005). Poroelastic behaviour of physical properties in Rotliegend Sandstones under uniaxial strain, Internat. J Rock Mech Min Sci. 42(7–8):924–32.

Urbistat. (n.d.). (2024). *City population*. Accessed [November, 2024], https://ugeo.urbistat.com.

van Wees, J.-D., Stephenson, R.A., Ziegler, P.A., Bayer, U., McCann. T., Dadlez, R., Gaupp, R., Narkiewicz, M., Bitzer, F., and Scheck, M. (2000). On the origin of the Southern Permian Basin, Central Europe. Mar Pet Geol.17: 43–59.

Wolfgramm, M., Seibt, A., Hurter, S., Zimmermann, G. (2003). Origin of geothermal fluids of Permo-Carboniferous rocks in the NE German Basin (NE Germany). *Journal of Geochemical Exploration*, 78-79, p. 127-131.

Wormbs, H., Diener, I., Rusitzka, I., Pasternak, G., Toleikis, R., Tessin, R., Trottner, D., and Wunderlich, H. (1989). Abschlußbericht Geothermische Ressourcen im Nordteil der DDR (2) - Blatt Neubrandeburg/Torgelow: Berlin, ZGI Berlin.

Younglove, B., Ely, J.F. (1987). Thermophysical properties of fluids. II. Methane, ethane, propane, isobutane, and normal butane. *Journal of Physical and Chemical Reference Data* 16, 577–798.

Zimmermann, G., Moeck, I., Blöcher, G. (2010). Cyclic waterfrac stimulation to develop an enhanced geothermal system (EGS): Conceptual design and experimental results. *Geothermics*, 39, 1, pp. 59-69.

Zimmermann, G., Reinike, A., Blöcher, G., Milsch, H., Gehrke, D., Holl, H.-G., Moeck, I., Brandt, W., Saadat, A., and Huenges, E. (2007). Well path design and stimulation treatments at the geothermal research well GT GRSK 4/05 in Groß Schönebeck. *Proc. 32nd Workshop on Geothermal Reservoir Engineering*, Stanford University, Stanford, Calif., 22–24 January 2007, SGP-TR-183.